REGULATION OF OSTEOBLAST ACTIVITY BY PYK2-TARGETED APPROACHES

Sumana Posritong

Submitted to the faculty of the University Graduate School
in partial fulfillment of the requirements
for the degree of
Doctor of Philosophy
in the School of Dentistry,
Indiana University

February 2017

Accepted by the Graduate Faculty, Indiana University, in partial fulfillment of the requirements for the degree of Doctor of Philosophy.

_____
Angela Bruzzaniti, Ph.D., Chair

_____
Tien-Min G. Chu, D.D.S., Ph.D.

Doctoral Committee

_____
Marco C. Bottino, D.D.S., M.S., Ph.D.

_____
Jiliang Li, Ph.D.

November 15, 2016

_____
Russell P. Main, Ph.D.

DEDICATION

I dedicate this dissertation to my beloved parents, who made all of this possible, for their unconditional love, support and encouragement.

ACKNOWLEDGEMENTS

Undertaking this Ph.D. has been a truly life-changing experience for me and it would not be possible without the support and guidance from many people. First of all, I would like to express my sincere gratitude to my mentor, Dr. Angela Bruzzaniti, for trusting in me for this challenging project and for all of her valuable help, advice, encouragement, and support in the Ph.D. study and dissertation. I feel extremely fortunate to have had an opportunity to work with such a dedicated individual and gained expertise from her. This Ph.D. would not have been achievable without her guidance and constant feedback. As well, my sincere gratitude goes to my other mentor, Dr. Tien-Min G. Chu, for giving me an opportunity to study and work in his lab, and for all of his guidance and suggestions.

Aside from my mentors, I would like to thank Dr. Marco C. Bottino, Dr. Jiliang Li, and Dr. Russell P. Main for serving as my committee members and for their comments and suggestions to fulfill my dissertation.

My appreciation is also expressed to Dr. Melissa Kacena and her lab members for helping me to prepare osteoblasts used in this project, and to Dr. Chien-Chi Lin and Tanja Greene for their assistance with the rheometry experiments.

I also appreciate the assistance of Dr. Pierre Eleniste, who is a good friend that always gives his best suggestions. My sincere thanks also go to Dr. Jung min Hong, Vruti Patel, and all lab members in Dr.Bruzzaniti's lab for their assistance that allowed me to complete my dissertation. It would have been a lonely lab without them.

In addition, I am grateful to my friends and colleagues especially Joy Wayakanon, Jun Palasuk, Nui Supornpun, and Beth Nida for all of their support and encouragement throughout this long journey.

I would like to acknowledge the Royal Thai Government Scholarship who fully sponsored me throughout my M.S.D and Ph.D. studies at Indiana University School of Dentistry.

Most importantly, I wish to express my heartfelt gratitude to my beloved family especially my parents and my sister for their endless love, care, and understanding. Their constant moral support, motivation, and confidence in me have enhanced my ability to get through this long journey.

Sumana Posritong

REGULATION OF OSTEOBLAST ACTIVITY BY PYK2-TARGETED APPROACHES

The hormonal and cellular mechanisms controlling bone formation are not completely understood. The proline-rich tyrosine kinase 2 (Pyk2) is important for osteoblast (OB) activity and bone formation. However, female mice lacking Pyk2 (Pyk2-KO) exhibit elevated bone volume/total volume. Previously, our laboratory found ovariectomized Pyk2-KO mice supplemented with 17β-estradiol (E2) exhibited a greater increase in bone volume than WT mice treated with E2. The overall hypotheses of our studies are that Pyk2 regulates OB activity by modulating the E2-signaling cascade and that a Pyk2-inhibitor will promote OB activity and be suitable for bone regeneration applications. In Aim1, we determined the mechanism of action of Pyk2 and E2 in OBs. Pyk2-KO OBs showed significantly higher proliferation, matrix formation, and mineralization than WT OBs. In the presence of E2 or raloxifene, a selective estrogen receptor (ER) modulator, both matrix formation and mineralization were further increased in Pyk2-KO OBs, but not WT OBs. Consistent with a role of Pyk2 in E2 signaling, Pyk2-depletion led to the proteasome-mediated degradation of ERα, but not ERβ. Finally, we found Pyk2-depletion and E2 have an additive effect on ERK phosphorylation, known to increase cell differentiation and survival. In Aim2, we developed a Pyk2-inhibitor loaded hydrogel and evaluated its viscosity, gelation time, swelling, degradation, and release behavior. We found that a hydrogel composed of PEGDA1000 plus 10% gelatin exhibited viscosity and shear-thinning behavior suitable for use as an injectable-carrier. Importantly, the Pyk2-inhibitor-hydrogel was cytocompatible, retained its inhibitory activity against Pyk2 leading to an increase in OB activity. In conclusion, therapeutic strategies targeting Pyk2 may improve systemic bone formation, while Pyk2-inhibitor loaded hydrogels may be suitable for targeted bone regeneration in craniofacial and/or the other skeletal defects.

Angela Bruzzaniti, Ph.D., Chair

TABLE OF CONTENTS

LIST OF TABLES

LIST OF FIGURES

LIST OF ABBREVIATIONS

3D	three-dimensional
AA	ascorbic acid
AF-1	activation function site 1
AF-2	activation function site 2
AKT	protein kinase B or a serine/threonine protein kinase
ALP	alkaline phosphatase
AP1	activator protein 1
BCA	bicinchoninic acid
BMD	bone mineral density
BMP	bone morphogenic protein
BMU	basic multicellular unit
BSP	bone sialoprotein
BV/TV	bone volume/total volume
Ca^{2+}	calcium
cDNA	complementary deoxyribonucleic acid
CO_2	carbon dioxide
CPC	cetyl pyridinium chloride
Cre	Cre recombinase
Ct	threshold cycle
Da	dalton
DBD	DNA-binding domain
dH_2O	deionized water
DMP1	dentin matrix protein 1
DNA	deoxyribonucleic acid
DPN	diarylpropionitrile
DTT	dithiothreitol
E2	17β-estradiol
ECL	enhanced chemiluminescence
ECM	extracellular matrix
EDTA	ethylenediaminetetraacetic acid

ER	estrogen receptor
ERE	estrogen response element
ERK	extracellular signal-regulated kinase
ERRα	the orphan nuclear ER–related receptor α
ERα	estrogen receptor alpha
ERβ	estrogen receptor beta
FAK	focal adhesion kinase
FasL	Fas ligand
FAT	focal adhesion targeting
FBS	Fetal Bovine Serum
FDA	Food and Drug Administration
FGF 23	fibroblast growth factor 23
G′	storage modulus
G″	loss modulus
GH	growth hormone
HCl	hydrochloric acid
HRP	horseradish peroxidase
IC_{50}	inhibitory concentration of 50%
IGF-1	insulin growth factor-1
IGFBP-4	insulin-like growth factor binding protein 4
IL	interleukin
IP	immunoprecipitation
KO	knockout
LAP	lithium phenyl-2,4,6-trimethylbenzoylphosphinate
LB	Luria-Bertani
LBD	ligand binding domain
LED	light-emitting diode
LRP	lipoprotein receptor-related proteins
MAPK	mitogen-activated protein kinase
MCSF	macrophage colony stimulating factor
MEPE	matrix extracellular phosphoglycoprotein

MG-132	proteasome inhibitor Z-Leu-Leu-Leu-al
$MgCl_2$	magnesium dichloride
MMP	matrix metalloproteinase
mRIPA	modified radio-immunoprecipitation assay
mRNA	messenger ribonucleic acid
MSC	mesenchymal stem cell
MTS	3-(4,5-dimethylthiazol-2-yl)-5-(3-carboxymethoxyphenyl)-2-(4-sulfophenyl)-2H-tetrazolium)
NaCl	sodium chloride
NaF	sodium fluoride
NaOH	sodium hydroxide
OB	osteoblast
OC	osteoclast
OCN	osteocalcin
OPG	osteoprotegerin
OPN	osteopontin
Osx	osterix
OVX	ovariectomized
p-NPP	p-nitrophenyl phosphate
P/S	Penicillin/Streptomycin
P1000	25% PEGDA1000
P1000:G10	25% PEGDA1000 and 10% gelatin
P600	25% PEGDA600
P600:G5	25% PEGDA600 and 5% gelatin
pAKT	phosphorylated protein kinase B
PBS	phosphate buffer saline
PCR	polymerase chain reaction
PEG	Poly (ethylene glycol)
PEGDA	PEG-diacrylate
PEGDM	PEG-dimethacrylate
pERK	phosphorylated extracellular signal-regulated kinase

PF-43	PF-431396
PF-46	PF-4618433
PGE_2	prostaglandin E2
Pi	inorganic phosphate
PMS	phenazine methosulfate
PMSF	phenylmethanesulfonyl fluoride
PPi	pyrophosphate
PPT	propyl-pyrazoletriol
PRD	proline rich domain
Prx1	paired-related homeobox 1
PTH	parathyroid hormone
Pyk2	proline-rich tyrosine kinase 2
QPCR	quantitative polymerase chain reaction
RANKL	receptor activator of nuclear factor-κB ligand
RGD	Arg-Gly-Asp
rhBMP-2	recombinant human BMP-2
RT-PCR	reverse transcription-polymerase chain reaction
Runx2	Runt-related transcription factor 2
SERM	selective estrogen receptor modulator
SIBLING	Small Integrin-binding Ligand N-linked Glycoprotein
sIPN	semi-interpenetrating network
SLRPs	small leucine-rich proteoglycans
TBS	tris-buffered saline
TBST	tris-buffered saline-tween
TGF-β	transforming growth factor-beta
TIEG	TGF-β-inducible gene that inhibits DNA synthesis
Tm	melting temperature
TNF-α	tumor necrosis factor alpha
uv	ultra violet
v/v	volume/volume
vs.	versus

w/v	weight/volume
Wnt	Wingless-type MMTV integration site family member
WT	wild type
α-MEM	alpha-minimum essential medium
β-GP	beta-glycerophosphate
μ-CT	micro-computed tomography

CHAPTER 1

INTRODUCTION

1.1 Bone Cells and Bone Remodeling

Bone is a highly specialized connective tissue that provides protective, mechanical, and metabolic functions. Bone tissue consists of three different bone cell types; osteoclasts (OC) which degrade bone, osteoblasts (OB) which build bone, and osteocytes which mediate signaling to other osteocytes and to OCs and OBs on the bone surface in response to mechanical strain and hormonal cues (Burr and Allen 2013). Through the coordinated actions of the bone cell types, new bone is formed, grows in length and width, and is repaired throughout life through the processes of bone modeling and remodeling. However, during aging or as a result of certain metabolic diseases, drug usage, or trauma, bone quality and quantity is compromised, which can lead to an increase in bone fracture and breakage (Burr and Allen 2013; Henriksen et al. 2009; Nakahama 2010).

1.1.1 Osteoclasts

OCs are multinucleated cells derived from the hematopoietic stem cell lineage and function in bone resorption (Vaananen and Laitala-Leinonen 2008). Osteoclastogenesis is regulated by OBs and osteocytes via secretion of receptor activator of nuclear factor-κB ligand (RANKL), macrophage colony stimulating factor (MCSF), and osteoprotegerin (OPG) among other cytokines (Burr and Allen 2013; Datta et al. 2008). MCSF induces the proliferation and commitment of OC precursors, which, under the control of RANKL, differentiate and fuse to form multinucleated OCs. OBs and osteocytes also secrete OPG which acts as a decoy receptor for RANKL to prevent osteoclastogenesis. Thus, the ratio of RANKL and OPG is a key determinant of OC numbers *in vivo* (Boyce and Xing 2008; Boyle et al. 2003; Burr and Allen 2013).

1.1.2 Osteoblasts

OBs are derived from mesenchymal stem cells (MSCs) and are responsible for new bone production (Aubin et al. 1995; Datta et al. 2008). OB formation or osteoblastogenesis involves multiple steps: proliferation, extracellular matrix (ECM) formation and maturation, mineralization, and subsequently apoptosis. Each step is controlled by different cytokines, growth factors, hormones, ECM

proteins, and transcription factors. Schemas of osteoblastogenesis and the osteoblastic genes expressed during this process are shown in Figures 1 and 2, respectively.

MSCs proliferate and become committed to the OB lineage as osteoprogenitor cells, which requires the canonical Wnt pathway and associated proteins that stimulate osteoblast formation but inhibit adipogenesis of MSCs. In addition, the canonical Wnt pathway regulates the expression of transcription factors, such as Runt-related transcription factor 2 (Runx2) and osterix (Osx) (Kokabu et al. 2016). Transcription factors of the activator protein 1 complex (AP1) such as c-fos are also highly expressed during OB proliferation and in the initial stages of differentiation (Machwate et al. 1995; Wagner 2002). MSC pre-OBs begin to produce the ECM and enter into their differentiation phase (Aubin 1998). Mature OBs that are localized along active matrix production sites stain intensely for alkaline phosphatase (ALP) (Aubin 1998). Unlike pre-OBs, mature OBs are cuboidal in shape, and have a large nucleus, enlarged Golgi apparatus and extensive endoplasmic reticulum, which are characteristics of cells highly engaged in protein production. Following OB proliferation, mature OBs secrete osteoid which then is mineralized. The transition from pre-OBs to mature and mineralizing OBs is controlled by the specific expression pattern of key genes and proteins (Figure 2).

Collagen type I, ALP, bone sialoprotein (BSP), osteocalcin (OCN), and osteopontin (OPN) (Burr and Allen 2013; Datta et al. 2008; Soares et al. 2008) are OB markers expressed during the matrix development. Collagen type I is the main component of the ECM in bone, constituting approximately 90% of the total organic matrix in bone. The combination of collagen type I and minerals determines the mechanical property and functional integrity of bone tissues. Collagen type I provides the flexibility of bone, while the mineral in bone is responsible for bone strength (Viguet-Carrin et al. 2006). Thus, collagen type I is an early indicator of OB differentiation (Liu et al. 1994). Although collagen type I is the most abundant organic matrix in bone, other ECM molecules, such as osteonectin and

thrombospondin-2, also promote collagen fiber assembly and modulate OB lineage progression (Alford et al. 2015).

Bone-specific ALP is the most commonly used marker to evaluate OB activity (Rodan and Noda 1991). The up-regulation of ALP occurs after collagen type I production but is detected before the expression of non-collagenous matrix markers and prior to mineralization (Long 2001). The main role of ALP in bone is to mediate mineralization, hence its expression is correlated with increased collagen type I synthesis. *In vitro* studies found that ALP generates inorganic phosphate (P_i) from substrates such as β-glycerophosphate (β-GP) to facilitate mineralization (Fallon et al. 1980). *In vivo* studies have revealed that mineralization is facilitated by ALP-mediated elimination of pyrophosphate (PP_i), which is a potent mineralization inhibitor (Hessle et al. 2002). BSP, a member of the Small Integrin-binding Ligand N-linked Glycoprotein (SIBLING) family, is also present within the bone matrix. BSP contains the Arg-Gly-Asp (RGD) amino acid motifs which mediate cell integrin to ECM attachment (Roach 1994). Moreover, BSP can bind to hydroxyapatite via polyglutamic acid sequences (Ganss et al. 1999). The presence of BSP in bone matrix, combined with a nucleation factor for hydroxyapatite formation and deposition, suggests that BSP has a potential role in the early mineralization of OBs (Hunter and Goldberg 1993).

Once the organic matrix or osteoid is deposited OBs secrete ECM vesicles which contain calcium apatite crystals and are highly enriched in ALP (Stein et al. 2004). The alignment of collagen fibrils in osteoid controls the direction of growth of the calcium apatite crystals (Anderson et al. 2005; Nudelman et al. 2010). In addition to collagen fibrils, non-collagenous ECM proteins, including OCN also contribute to mineral crystal nucleation and propagation (Alford et al. 2015). OCN, or bone gamma-carboxyglutamic acid, is the most abundant non-collagenous protein in bone, and is expressed in mature OBs and osteocytes, and is therefore considered to be a marker of late OB differentiation. In addition, OCN serum levels are used as a marker for bone turnover in clinical settings (Seibel 2005; Szulc and Delmas 2008; Vasikaran et al. 2011). *In vitro* studies indicate that OCN plays a role in regulating mineralization through calcium and hydroxyapatite binding, which

may allow OCN deposition within the mineralized matrix (Hauschka et al. 1989; Nefussi et al. 1997; Patti et al. 2013; Razzaque 2011). However, it is worth noting that the physiological role of OCN *in vivo* is still unclear and some studies suggest it may be involved in the interaction of OBs with OCs and in bone resorption to enhance bone loss. Consistent with this, it has been reported that OCs resorb bone poorly in the absence of OCN (Hauschka et al. 1989; Patti et al. 2013; Villafan-Bernal et al. 2011).

Another important non-collagenous protein found in mineralized tissue is the glycoprotein osteopontin (OPN), which is secreted in both mineralized and non-mineralized tissues. Within bone tissue, OPN plays key functions including cell adhesion, migration and survival (Standal et al. 2004). In addition, OPN can serve as a cell-matrix/matrix-mineral mediator due to its intrinsic RGD sequence (McKee and Nanci 1996). Further, OPN may also play a mineralization role in non-skeletal tissue such as in teeth and epithelial lining tissues. (McKee and Nanci 1996).

As our knowledge broadens, new markers of mineralization are being identified. Recent studies have led to the identification of two novel small leucine-rich proteoglycans (SLRPs), asporin and keratocan, which also interact with collagen and minerals, and are known to promote mineralization (Igwe et al. 2011; Kalamajski et al. 2009). However, their mechanism of action is currently unclear.

At the completion of bone formation, most OBs undergo programmed cell death or apoptosis. However, some mature OBs become entrapped in the mineralized matrix and differentiate into osteocytes. Alternatively, remaining OBs become flat, quiescent bone lining cells, which are mostly found on the non-remodeling bone surfaces (Aubin et al. 1995; Datta et al. 2008; Harada and Rodan 2003). The bone lining cells have the potential to be reactivated to form active OBs when required for bone repair or in response to physiological changes in hormone or mineral levels (Dobnig and Turner 1995).

1.1.3 Osteocytes

Osteocytes are the most abundant cells in mineralized bone and are important in bone structure maintenance. Osteocytes are terminally differentiated cells derived from OBs that have become embedded in the secreted bone matrix

(Burr and Allen 2013). Osteocytes are morphologically distinct to OBs and are stellate in shape due to the presence of membrane extensions known as dendrites. Within bone, osteocytes are enclosed within lacunae, and their dendritic processes run along narrow canaliculi within the mineralized matrix to communicate with other osteocytes as well as with OCs and OBs on bone surfaces (Burr and Allen 2013; Noble 2008). Concomitant with changes in their cell morphology, osteocytes exhibit significant decreases in the expression of several OBs-related proteins including: collagen type I, ALP, BSP, and OCN. However, osteocytes exhibit higher levels of proteins related to bone mineralization, such as dentin matrix protein 1 (DMP1), matrix extracellular phosphoglycoprotein (MEPE) and fibroblast growth factor 23 (FGF 23) (Burr and Allen 2013; Zhu et al. 2001). In addition, osteocytes secrete sclerostin, the product of the *SOST* gene, which is important for controlling bone formation by OBs.

Osteocytes function as mechanosensory cells and coordinate the time and location of bone remodeling units (Noble 2008). The osteocyte lacunar-canalicular network is present within the entire volume of bone which allows osteocytes to detect circulating factors i.e., hormones and ions, as well as mechanical signals such as fluid flow and mechanical strain (Noble 2008; van Oers et al. 2008). Osteocytes also produce MCSF, RANKL, and OPG and also stimulate OBs to secrete these factors, which controls osteoclastogenesis and therefore OC number (Simonet et al. 1997; Tatsumi et al. 2007). Furthermore, osteocytes secrete sclerostin, which is an antagonist of several members of bone morphogenic proteins (BMPs) (Krause et al. 2010) and low-density lipoprotein receptor-related proteins (LRP) 5/6 on OBs to counteract Wnt signaling (Li et al. 2005). Both BMPs and Wnts are important for OB formation and activity. Thus, the inhibition of BMPs and Wnts by sclerostin can lead to the disruption of osteoblastic bone formation.

Mechanical loading affects osteocytes by altering fluid flow along the lacuna-canalicular system, which leads to the activation of several intracellular signaling pathways (van Oers et al. 2008). Mechanical loading results in decreased sclerostin levels in bone, allowing activation of Wnt/β-catenin

signaling in OBs, which subsequently leads to increased bone formation. Conversely, in the absence of mechanical loading, such as when astronauts are exposed to weightlessness, and in skeletal unloading during extended bed rest, sclerostin expression in bone is increased, which antagonizes Wnt/β-catenin signaling in OBs leading to decreased bone formation (Moustafa et al. 2012; Tian et al. 2011; van Oers et al. 2011). Osteocytes also respond to mechanical forces by releasing prostaglandin E_2 (PGE_2), which stimulates OB recruitment from the bone marrow and activates the Wnt/β-catenin signaling pathway (Liu et al. 2010). Furthermore, mechanical loading increases nitric oxide secretion to stimulate bone formation. In addition, skeletal unloading decreases the secretion of OC-inhibitory signals (such as OPG) while pro-osteoclastogenesis signals (such as RANKL) are increased leading to an increase in OC numbers, favoring overall bone resorption (You et al. 2008). Thus, bone formation is the physiological response to mechanical stress, while bone resorption is the reaction to skeletal unloading or skeletal disuse (Tan et al. 2007).

1.1.4 The bone remodeling process

Bone tissue dynamically changes through the processes of bone modeling and bone remodeling. Bone modeling occurs on the periosteal surface during skeletal growth to achieve the optimal bone geometry and strength, while bone remodeling occurs throughout life and is a bone renewal process that helps to retain bone strength. This complex process is carried out by a coordinated balance between OC bone resorption, OB bone formation, and osteocyte-mediated mechano-signaling (Xiong and O'Brien 2012).

Bone remodeling occurs predominantly on the endosteal surfaces within basic multicellular units (BMUs) (Figure 3) (Burr and Allen 2013; Orwoll 2003; Parfitt 2001; Proff and Romer 2009). BMUs are located on bone surfaces and is covered by a canopy of bone lining cells and nearby marrow capillaries (Sims and Martin 2014). Within BMUs, bone remodeling begins with the resorptive phase, when OCs are stimulated by MCSF and RANKL and degrade bone. Next, the reversal phase begins which is characterized by the cessation of osteoclastic bone resorption due to OC apoptosis and the initiation of osteoblastic bone formation.

OBs are recruited to resorbed areas of bone by a process that is not yet clear, and begin the bone formation phase, which includes OB proliferation and differentiation, osteoid formation, and mineralization of bone. During the last phase in the bone remodeling cycle, the so-called “resting” phase, selected mature OBs become trapped in the mineralized matrix and differentiate into osteocytes, or they flatten on the bone surface to form bone lining cells. Matrix mineralization within the BMU continues over time until mineralization is complete and the bone surface is reestablished and maintained until the next bone remodeling episode (Burr and Allen 2013).

1.2 Regulators of Osteoblast Activity

1.2.1 The role of estrogen and SERMs in bone tissue

Estrogen, a sex steroid hormone, plays a significant role in bone metabolism and provides an osteoprotective action in both males and females. The consequence of estrogen deficiency is increased bone turnover due to an increase in osteoclast activity, which can lead to osteoporosis, especially in post-menopausal women (Compston 2001; Imai et al. 2010; Krum 2011). Published studies suggest that estrogen therapy, including selective estrogen receptor modulators (SERMs), can prevent bone loss and increase bone mineral density (BMD) in post-menopausal women (Riggs and Hartmann 2003). Furthermore, the fracture risk of hip, spine, and wrist in post-menopausal women can be decreased by estrogen therapy (Compston 2001).

SERMs are a group of natural or synthetic non-steroidal substances that act as either tissue specific agonists or antagonists of the estrogen receptors (ERs). Structurally, SERMs adopt a conformational structure that is similar to estrogen which allows them bind to the ligand-binding domain of the ER (Riggs and Hartmann 2003) (Figure 4). Ideally, a SERM should have positive effects on the cardiovascular system and bone, without having adverse effects on the breast and endometrium and without causing an increase in cancer risks. To date, there are two SERMS approved for osteoporosis treatment, raloxifene and

bazedoxifene, both of which have estrogen activity in the bone and prevent bone loss, improve bone BMD, and are associated with a decrease in the risk of vertebral fracture (Russell 2015). Raloxifene exerts its estrogenic effects on bone by decreasing the remodeling rate, reducing OC activity, and maintaining OB activity (Hegde et al. 2015). Furthermore, raloxifene acts as a complete estrogen antagonist on the uterus. Unlike hormone replacement therapy, raloxifene does not cause an increase in vaginal bleeding, endometrial thickening, or uterine volume in human studies. Thus, raloxifene has not been associated with an increase in the risk of endometrial cancer in postmenopausal women (Cohen et al. 2000; Goldstein et al. 2000). In addition, raloxifene has been shown to substantially decrease the risk of invasive breast cancer (Barrett-Connor et al. 2006).

1.2.2 Effects of estrogen on OB activity

The effects of estrogen on its target tissues are not fully understood. Published studies suggest that the actions of estrogen can be mediated either by genomic or non-genomic pathways (Imai et al. 2010; Krum and Brown 2008). The genomic pathway of estrogen occurs through its binding to nuclear ERs either by direct interaction of estrogen-ER complex with the estrogen response element (ERE) in transcription promoter regions or indirect binding of estrogen-bound ER to ERE via other transcription factors. In contrast, the non-genomic actions of estrogen or rapid estrogen responses occur via interaction of estrogen with ERs present at the cell membrane or in the cytoplasm, resulting in the activation of signal transduction pathways including calcium flux and kinase activation within target cells (Figure 5). It is to be noted that kinase activation does not only cause post-translational changes in proteins, but also leads to transcriptional changes mediated by kinase-activated transcription factors (Burr and Allen 2013; Carroll et al. 2006; Heldring et al. 2007; Hewitt et al. 2016; Imai et al. 2010; Marino et al. 2006; Simoncini and Genazzani 2003).

Published studies demonstrate that 17β-estradiol (E2), the most potent form of estrogen, increases OB proliferation and activity. Some studies have shown that 17β-estradiol affects gene expression in OBs, including the induction of insulin growth factor-1 (IGF-1), transforming growth factor-beta (TGF-β), TIEG (a TGF-β-

inducible gene that inhibits DNA synthesis) and BMP-6 (Compston 2001; Ernst and Rodan 1991; Oursler et al. 1991; Rickard et al. 1998; Tau et al. 1998). Estradiol also increases the effect of parathyroid hormone (PTH) on collagen synthesis and ALP mRNA expression in osteoblastic SaOS-2 cells (Nasu et al. 2000), and enhances the expression of insulin-like growth factor binding protein 4 (IGFBP-4), which regulates osteoblastogenesis and OB activity (Krum 2011). Furthermore, 17β-estradiol increases the expression of receptors for growth hormone, 1α,25-dihydroxy vitamin D3 ($1,25(OH)_2D_3$), and progesterone (Ishibe et al. 1995; Slootweg et al. 1997). ALP is also up regulated by 17β-estradiol (Krum et al. 2008b; Plant and Tobias 2001). Likewise, BMP-2 is increased with estrogen treatment (Zhou et al. 2003). However, the effects of 17β-estradiol on the expression of OB activity markers, ALP, OCN, and collagen type I, is still controversial. Some studies reported 17β-estradiol treatment increased ALP, OCN, and collagen type I mRNA, whereas other results showed no changes or decreased expression of these markers after 17β-estradiol treatment (Keeting et al. 1991; Majeska et al. 1994; Robinson et al. 1997).

Several studies demonstrated that 17β-estradiol increases Fas ligand (FasL) secretion by primary OBs and MC3T3-E1 osteoblastic cells, which subsequently binds to the pro-apoptotic Fas receptor on OCs to promote OC apoptosis (Krum et al. 2008a; Wang et al. 2015). Estradiol treatment also increases the level of OPG, a decoy receptor for RANKL (Bord et al. 2003) as well as decreasing RANKL in human OBs (Eghbali-Fatourechi et al. 2003). Together, the increase in the OPG/RANKL ratio in response to 17β-estradiol reduces osteoclastogenesis.

1.2.3 The role of estrogen receptors in bone formation

ERs are members of the steroid hormone receptor family regulated transcription factors. The ERs contain several domains, which include the activation function sites 1 and 2 (AF-1 and AF-2). The AF-1 domain, a ligand-independent site, is responsible for promotor-specific activation which can phosphorylate and activate the ERs, whereas AF-2 is a ligand-specific activation site. The C region consists of the DNA-binding domain (DBD). The D domain is a

hinge region and contributes to the specificity of DNA binding and nuclear localization of ERs. The ligand binding domain (LBD) is in the E region. The ERs consist of at least 2 subtypes, ER-alpha (ERα) and ER-beta (ERβ). ERα and ERβ exhibit close structural homology particularly in the DBD (>95% amino acid identity), and to a lesser extent in the LBD (~60% amino acid identity) (Figure 6.) (Compston 2001; Hewitt et al. 2016; Marino et al. 2006). Estrogen has similar binding affinities for both ERα and ERβ. Compared to estrogen, raloxifene shows lower binding affinities for both ERα and ERβ, and preferentially binds ERα (approximately 3.5 fold higher affinity for ERα than ERβ) (Zhu et al. 2006).

ERs are expressed in many tissues such as the central nervous system, cardiovascular system, reproductive organs, bladder, kidney, intestine, and bone (Compston 2001; Kuiper et al. 1997). In skeletal tissue, both ERα and ERβ are detected in OBs, OCs, and osteocytes. In human cortical bone, immunohistochemistry revealed intense staining for ERα in OBs and osteocytes next to the periosteal surface, and OCs on the resorbing surface. It was reported that ERα expression is high in newly incorporated cortical bone osteocytes, but older osteocytes in the cortical mineralized matrix exhibit lower ERα levels (Bord et al. 2001; Braidman et al. 2001). In cancellous bone, OBs, OCs, and osteocytes strongly express ERβ, while ERα is present but at reduced levels compared to ERβ. The distinct pattern of expression of the ERs, with ERα predominantly expressed in the cortical bone, whereas ERβ is predominantly found in the trabecular bone, suggests they may exhibit unique cellular functions and be responsible for differential regulation of cortical and cancellous bone tissues directly by estradiol and less specifically through non-genomic actions in the cells.

Although OBs express both ER subtypes, ERα and ERβ are differentially expressed during OB differentiation. In SV-HFO cells, a human OB cell line, it was shown that ERα mRNA levels slightly increase until day 10 of culture, and then remain constant. In contrast, ERβ mRNA levels increase steadily throughout the 10 day culture (Arts et al. 1997). In another study using MG-63 human osteosarcoma cells cultured for up to 25 days, ERβ mRNA expression remained at a constant high level whereas ERα mRNA was barely identified. However, ERα

mRNA expression in human primary OBs was much greater than ERβ mRNA levels during the same culture duration (Chen et al. 2004). In rat calvarial OBs, ERα mRNA expression was increased during matrix maturation and then decreased during mineralization phase, while ERβ mRNA levels were relatively constant throughout differentiation and revealed more constitutive expression (Bord et al. 2003; Onoe et al. 1997; Wiren et al. 2002). ERs are also regulated by estrogen, and one study reported that ERα mRNA is increased after estradiol treatment of human primary OBs for 24 hours, but no data regarding the effect of estradiol on ERβ mRNA levels was shown (Bord et al. 2003).

An additional mode of regulation of the ERs is by intracellular degradation. Several studies suggest that ERα undergoes ubiquitin-proteasome mediated degradation (Chai et al. 2015; Lu et al. 2010; Petrel and Brueggemeier 2003; Zhou and Slingerland 2014). The ubiquitin-proteasome pathway is a major pathway of selective protein degradation. Cytosolic and nuclear proteins are first labeled for degradation by the attachment of ubiquitin, an amino acid that is highly conserved in all eukaryotes. Polyubiquinated proteins are then recognized and degraded by the proteasome, a large and multi-subunit protease complex. Lu et al. (Lu et al. 2010) found that a decrease in ERα after docosahexaenoic acid treatment of MCF-7 breast cancer cells was reversed in the presence of MG-132, a proteasome inhibitor. Another study reported that ERα protein levels in an adenocarcinoma breast cell line (BT474) were reduced after treated with TGF-β1 for 6 hours. MG-132 abolished all effects on ERα protein by TGF-β1, which suggests ERα protein degradation occurs through a proteasome-dependent pathway (Petrel and Brueggemeier 2003). A recent study found that REGγ, a member of proteasome coactivator family, plays a role in ERα protein degradation in MCF-7 and BT474 cell lines via the ubiquitin–proteasome pathway (Chai et al. 2015). Evidence suggests that ERα-binding ligands such as 17β-estradiol and fulvestrant (ER antagonist) also affect ERα degradation through the proteasome pathway (Callige and Richard-Foy 2006). There is also evidence that ERβ protein in MCF-7 cells undergoes ubiquitin-proteasome degradation through the activation of the AKT pathway (Sanchez et al. 2013). In addition, it was found that ERβ ubiquitination

and degradation in MDA-MB231 breast cancer cells occurs in an estrogen dependent manner (Tateishi et al. 2006). Collectively, these studies suggest ERα and ERβ can in part be regulated through the proteasome pathway, although if this occurs in all cells is unclear.

1.2.4 Effect of genetic deletion ERα and/or ERβ on the murine skeleton

Genetic mouse models have been used to examine the role of the ERs in skeletal bone. Female and male mice with global knockout (KO) of ERα (ERα-KO) exhibit an increase in trabecular BMD and bone volume/total volume (BV/TV) when compared to WT mice. In contrast, deletion of ERβ leads to different responses in male and female mice. ERβ-KO female mice exhibit an increase in trabecular BMD and BV/TV, whereas trabecular bone of male mice is unaffected (Lindberg et al. 2001; Sims et al. 2002). Although several labs have investigated the skeletal effects of deletion of both ERα and ERβ, differences in phenotype were found; one study reported that ERαβ-double KO female mice showed an increase in cancellous BMD (Lindberg et al. 2001), while another study showed a profound decrease in trabecular BV/TV, with a decrease in bone turnover in females. On the other hand, trabecular BMD was found to be unaffected in ERαβ-double KO male mice (Sims et al. 2002). This suggests that bone remodeling in male mice involves predominantly ERα, whereas in female mice, ERα and ERβ may play a compensatory effect to influence bone remodeling (Sims et al. 2002).

In contrast to the reduced bone mass observed in post-menopausal women and ovariectomized (OVX) rodents, an impairment of bone development or low bone mass was not reported in female ERα-KO or ERβ- KO mice, which have high bone mass, while global ERαβ double KO mice have normal bone mass. A possible explanation may be differences in the levels of estradiol, the most important form of circulating estrogen. OVX rodents and post-menopausal women have circulating estradiol deficiency, while ERα-KO female mice exhibit high levels of circulating estradiol, which may be able to interact with ERβ, leading to higher bone mass (Harada and Rodan 2003; Imai et al. 2010; Sims et al. 2002; Zaidi 2007). Similarly, the elevation of circulating estradiol and testosterone in these mice may increase the activation of other receptors such as the androgen receptor

(Imai et al. 2010; Lindberg et al. 2001; Sims et al. 2002) and prevent loss of trabecular BMD in ERα-KO and/or ERβ-KO mice. An alternative explanation is that the osteoprotective actions of estrogen occur through endocrine or paracrine factors that may be secreted from bone marrow or other extra-skeletal tissues and cells. For example, hepatic IGF-1 is known to stimulate osteoblastogenesis; IGF-1 modulates the action of growth hormone (GH) in bone development. Thus, the elevated estradiol in global ERα-KO and/or ERβ-KO mice may stimulate hepatic IGF-1 production, which can promote bone formation. Nevertheless, the molecular basis behind this mechanism remains unclear (Imai et al. 2010; Sims et al. 2000).

Recently, cell-specific mouse models of ERα-KO and ERβ-KO were generated to better understand the bone-specific effects of estrogen signaling without the confounding physiological changes that likely affect global ERα and/or ERβ mice. However, no change in bone mass was observed either in cortical or cancellous bone in OB-specific ERα knockout mice in which Cre-mediated deletion was driven by the collagen type 1α promoter. However, when ERα was deleted in OB progenitors by crossing with osterix1 (*Osx-Cre*) or paired-related homeobox 1 (*Prx1-Cre*) mice, BMD and cortical thickness in the femur were decreased in female mice, but no change in cancellous bone was observed (Almeida et al. 2013). In contrast, ERβ deletion in osteoprogenitors (*Prx1-Cre*) enhanced cancellous bone mass in female mice, but had no effect on cortical bone (Nicks et al. 2015). In mice in which ERα deletion was driven by the OCN-Cre promoter, cortical and cancellous BV/TV were reduced in young female mice (Maatta et al. 2013; Melville et al. 2014). However, this phenotype disappeared in adult mice (Maatta et al. 2013). Furthermore, in mice with osteocyte-specific deletion (*Dmp1-Cre*) of ERα, a decrease in cancellous bone was observed only in male mice, and cortical bone was unaltered in both males and females (Windahl et al. 2013). On the contrary, another study found that osteocyte ERα deletion (*Dmp1-Cre*) female mice exhibited a significant decrease in trabecular BMD, but not in male mice (Kondoh et al. 2014). The discrepancies between these 2 studies maybe from the differences in genetic background of ERα-floxed mice.

1.2.5 Pyk2 and its effects on bone cells and bone remodeling

To understand the actions of the ERs and the function of bone cells in the bone remodeling process, it is important to understand the role of key signaling proteins. Our laboratory has focused on elucidating the role of the proline-rich tyrosine kinase 2 (Pyk2). Pyk2 is homologous to the focal adhesion kinase, FAK (Eleniste and Bruzzaniti 2012; Lipinski and Loftus 2010) and is expressed in OBs and OCs (Buckbinder et al. 2007; Eleniste et al. 2015; Gil-Henn et al. 2007; Kacena et al. 2012). Pyk2 consists of multiple protein domains: the FERM domain (N-terminal), a catalytic kinase domain, several proline rich domains (PRD), and a focal adhesion targeting (FAT) domain at the C-terminus (Eleniste et al. 2012; Gil-Henn et al. 2007). Pyk2 is stimulated by multiple extracellular cues including inflammatory cytokines, stress signals, intracellular calcium, and integrin-mediated cell adhesion (Gil-Henn et al. 2007). Pyk2 responds to integrin activation and intracellular calcium by autophosphorylation at tyrosine residue Y402 which is important for Pyk2 kinase activity. Phosphorylated Y402 also provides a binding site for SH2 domains of Src kinases (Eleniste et al. 2012; Kimble et al. 1996), thus acting as a protein scaffolding domain. Pyk2 is linked to a variety of cellular activities including proliferation and migration (Boutahar et al. 2004; Buckbinder et al. 2007; Gil-Henn et al. 2007; Kacena et al. 2012). Recently, it was reported that Pyk2 facilitates cell proliferation and survival by degrading p53, the tumor suppressor protein (Lim et al. 2008; Lim et al. 2010).

Pyk2 has two isoforms, the full-length Pyk2 (118 kDa) and a mRNA spliced shorter form, Pyk2-S (106 kDa), which lacks a 42-amino acid motif compared to the full-length Pyk2 (Figure 7A). In addition, differences in the expression of Pyk2 and Pyk2-S were observed during OB differentiation (Kacena et al. 2012) (Figure 7B). We found that the ratio of Pyk2 to Pyk2-S decreases during OB differentiation, with Pyk2-S expression exceeding Pyk2 by day 14 and day 21. These findings suggest the transition from Pyk2 to Pyk2-S may control the transition from immature proliferating OBs to mature matrix mineralizing OBs, although this remains to be confirmed.

Recent studies have reported the importance of Pyk2 in the regulation of bone mass and in the function of OCs and OBs (Bruzzaniti et al. 2009; Buckbinder et al. 2007; Eleniste and Bruzzaniti 2012; Gil-Henn et al. 2007; Wang et al. 2003). Pyk2 has been shown to be a positive regulator of OC maturation and bone resorption *in vitro*. Pyk2 is localized to OC podosomes, which are actin-rich structures that facilitate cell attachment and migration (Buckbinder et al. 2007; Eleniste and Bruzzaniti 2012; Gil-Henn et al. 2007; Kacena et al. 2012). Pyk2-deletion leads to OC impairment in part due to a disruption in the organization of podosomes and the formation of the actin ring (sealing zone) necessary for bone resorption (Bruzzaniti et al. 2009; Gil-Henn et al. 2007). Pyk2 is also expressed in OBs, and the deletion of Pyk2 affects the differentiation and migration of OBs. Deletion of Pyk2 in OBs also affects actin remodeling, which impacts the turnover of focal adhesion structures necessary for OB attachment to ECM proteins (Eleniste and Bruzzaniti 2012). Our studies and others demonstrated that OB differentiation and bone formation are enhanced in the absence of Pyk2 (Buckbinder et al. 2007; Cheng et al. 2013; Eleniste et al. 2015; Kacena et al. 2012). Furthermore, it has been reported that bone marrow cells of Pyk2-KO mice cultured in an osteogenic medium exhibit increasing levels of OB activity markers: ALP, OCN, and calcium deposition (Allen et al. 2009; Cheng et al. 2013). Pyk2-KO mice exhibit an osteopetrotic phenotype, which is in part due to increased osteoblastic bone formation as well as decreased osteoclastic bone resorbing activity (Buckbinder et al. 2007; Gil-Henn et al. 2007). Pyk2-KO mice exhibit a 139% increase in bone formation rate in the tibia compared to wild type (WT) mice. This increase was the result of both increased mineralizing surface per bone surface and increased mineral apposition rate (Gil-Henn et al. 2007).

Unpublished observations from Dr. Bruzzaniti's laboratory have revealed that global Pyk2-deletion in mice leads to an increase in bone mass in female mice, but not in male mice (Figure 8). Since the high bone mass of Pyk2-KO mice is sex-specific, this suggests that Pyk2 may interact with estrogen, the major female sex hormone important for maintaining bone mass through the regulation of OC and OB numbers. To examine the potential role of estrogen in the regulation of bone

mass in Pyk2-KO mice, Dr. Bruzzaniti's laboratory performed OVX surgery on female WT and Pyk2-KO mice, followed by 17β-estradiol supplementation. The bone morphometrics of estrogen-depleted (OVX) and estrogen-replete female mice (OVX + E2) was compared after 4 weeks. The results showed that female OVX Pyk2-KO mice exhibited a much greater increase in bone mass following estrogen supplementation than OVX WT + E2 mice (Figure 9). These findings indicate that Pyk2-KO mice may be more responsive to estrogen than WT mice, and therefore that Pyk2 may regulate bone mass in part by modulating estrogen signaling cascades. However, the molecular mechanism for the role of Pyk2 in estrogen signaling remains unknown.

1.3 Osteoporosis and Systemic Bone Loss

The bone remodeling process is regulated by many factors at both the systemic and local levels, which include hormones, growth factors, mechanical stimuli and transcription factors (Compston 2001). These factors affect the coupling between bone formation and bone resorption. The disruption in the coupling process can lead to high or low bone mass diseases such as osteopetrosis or osteoporosis, respectively.

Osteoporosis is a systemic skeletal disease characterized by low BMD and bone architecture deterioration, which compromises bone strength and increases the risk of bone fractures. Risk factors for osteoporosis include genetic, behavioral, and nutritional in nature. The female sex, individuals with a petite skeletal structure, and being of Caucasian or Asian descent are all considered to be genetic factors. Aging, a sedentary lifestyle, smoking, and low body weight are also risk factors. Nutritional factors include low calcium or vitamin D intake, and alcohol abuse (Downey and Siegel 2006). Common metabolic diseases such as diabetes and certain drugs such as glucocorticoid therapy also lead to compromised bone mass and quality (Pisani et al. 2016; Rosen and Bouxsein 2006; Whittier and Saag 2016). Osteoporosis is most commonly seen in post-menopausal women due to declining levels of the osteoprotective hormone, estrogen. Estrogen deficiency

promotes OC differentiation and survival, increasing OC numbers and bone resorption, which subsequently leads to decreases in bone mass and bone strength (Nakamura et al. 2007; Novack 2007). Long-term estrogen depletion is also associated with the induction of OB apoptosis, leading to a decrease in OB number and a subsequent disruption in bone formation (Almeida et al. 2007; Khosla et al. 2012). Recent studies have demonstrated that post-menopausal women show significantly higher serum levels of sclerostin, a key inhibitor of Wnt signaling in OBs, than pre-menopausal women, which can lead to inhibition of osteoblastic bone formation (Mirza et al. 2010).

1.4 Periodontal Bone Loss: Correlation with Osteoporosis

Bone remodeling in the oral cavity proceeds via the same series of osteoblastic and osteoclastic activity events as found in the rest of the skeleton. This process is considered essential in controlling tooth eruption, orthodontic tooth movement, tooth socket healing, alveolar bone healing after periodontal treatment or other surgical procedures, and osseointregation of dental implants. The uncoupled sequence of alveolar bone resorption and formation resulting in alveolar bone loss may occur from many causes including: infection, trauma, systemic or local alterations of the host response, pathological diseases, or multifactorial causes (Jeffcoat 1993).

Periodontal disease is an inflammatory disease that leads to periodontium destruction; this disease can be classified into gingivitis and periodontitis. Periodontitis is characterized by loss of connective tissue and alveolar bone mass, and can eventually leads to tooth loss or loss of alveolar ridge height. Periodontitis is considered as the result of the interaction between pathogenic bacteria and the immune response of host. The primary etiology of periodontitis is dental plaque biofilm, which is formed by bacteria and toxins (Kinane and Marshall 2001; Varela-Lopez et al. 2016). The host response to infection is another important factor to determine the extent and severity of periodontitis. Evidence suggests that systemic factors can modify the periodontitis through their effects on the immune and

inflammatory mechanisms. Systemic factors that enhance the extent and severity of periodontitis include a decrease in number or function of polymorphonuclear leukocytes, immuno-suppressive diseases such as HIV infection, smoking, and diabetes (Kinane and Marshall 2001; Loe 1993; Oliver and Tervonen 1994).

Like osteoporosis, periodontitis is a bone-resorptive, host-dependent, and multifactorial disease. A correlation between skeletal BMD and the number of remaining teeth in post-menopausal women was observed in a 7-year longitudinal clinical study of Caucasian post-menopausal women (Krall et al. 1996). It was reported that in post-menopausal women experiencing a decrease in BMD of 1% per year, a significantly increase in the relative risks (4.83) of tooth loss was observed this indicating a link between systemic BMD and tooth loss. Recent studies also reported that post-menopausal women with osteoporosis had a greater chance of developing periodontitis and tooth loss when compared to those without osteoporosis (Gomes-Filho et al. 2007; Moedano et al. 2011; Pereira et al. 2015). Patients with low systemic BMD also showed higher alveolar attachment loss than individuals with normal BMD (Iwasaki et al. 2013). Although the mechanisms are unknown, these findings suggest a link between osteoporosis and localized chronic bone destruction in the oral cavity.

1.5 Pharmaceutical Approaches to Increase Bone Mass

Current pharmaceuticals for the treatment of osteoporosis are classified into 2 groups: anti-resorptive and anabolic medications. The examples of anti-resorptive or anti-catabolic agents are bisphosphonates, calcitonin, hormone replacement therapy (estrogen), SERMs, and Denosumab, a RANKL antibody. Bisphosphonates and calcitonin directly inhibit OC activity and induce OC apoptosis (Bellido and Plotkin 2011). Published clinical studies reported that bisphosphonates and calcitonin treatment stabilized or improved spine BMD in post-menopausal women, resulting in a decrease in vertebral fracture in post-menopausal women who received these two drugs compared to the non-treated group (Chesnut et al. 2000; Drake et al. 2008; Mehta et al. 2003). The FDA-

approved anti-RANKL antibody, Denosumab, prevents RANKL from binding to the RANK receptor on OC precursors and as such inhibits osteoclastogenesis (Das and Crockett 2013). Thus Denosumab leads to an increase in bone mass, with a positive effect on cortical bone, and prevents fractures in post-menopausal osteoporosis patients (Cummings et al. 2009; Gifre et al. 2016; McClung et al. 2006). As described in section 1.2.1, estrogen and SERMs can prevent bone loss and increase BMD in post-menopausal women, and lead to a decrease in fracture risk (Compston 2001; Riggs and Hartmann 2003). Estrogen and SERMs stimulate estrogen receptors leading to decrease in OC number, and consequently a decrease in the rate of bone loss (Pineda et al. 2012). Unlike estrogen, raloxifene does not cause negative effects on reproductive organs because it acts as a complete estrogen antagonist on these organs (Barrett-Connor et al. 2006; Cohen et al. 2000; Goldstein et al. 2000).

In contrast to anti-resorptives, anabolic drugs induce bone formation by stimulating OB differentiation and restraining OB apoptosis (Jilka et al. 1999). Recombinant PTH (teriparatide) is the only FDA-approved bone anabolic medication (Riancho and Hernandez 2012), and it was found that teriparatide increased bone formation, bone volume, and BMD in post-menopausal women and anorexia nervosa patients (Eriksen et al. 2014; Fazeli et al. 2014). However, recombinant PTH still has some limitations, including parenteral administration and risk of osteosarcoma (Pazianas and Abrahamsen 2016). Currently in development is an anti-sclerostin antibody which is in clinical trials and is showing positive effects on bone anabolism (MacNabb et al. 2016).

1.6 Pyk2 Inhibitors Increase Bone Mass in Mice

Evidence has shown that Pyk2 plays a key role in the regulation of bone formation, so the chemical inhibitors of this kinase might have potential therapeutic effects on bone tissue regeneration. A combined Pyk2/FAK inhibitor, PF-431396 (PF-43) or $C_{22}H_{21}F_3N_6O_3S \cdot xH_2O$ was developed by Pfizer, Groton, CT, having IC_{50} values of 11-32 nM of Pyk2 and 1.5 nM of FAK (Figure 10). The PF-43 has

been investigated for its effects on bone mass in OVX female rats, an animal model of post-menopausal osteoporosis (Buckbinder et al. 2007). It was reported that PF-43 (10 and 30 mg/kg) administration for 21 days increased cancellous bone formation rate, and increased the mineralizing surface and mineral apposition rates in the proximal tibia of OVX rats. This suggests that PF-43 promotes OB activity (Allen et al. 2010; Allen et al. 2009; Buckbinder et al. 2007). In other studies, PF-562-271, another dual FAK/Pyk2 inhibitor, inhibited tumor growth on lytic bone metastasis by decreasing bone resorption as well as increasing bone formation (Bagi et al. 2008; Roberts et al. 2008). Taken together, these findings suggest that Pyk2 inhibitors may be alternatives for bone disease treatment and bone regeneration without increasing cancer risk.

Another inhibitor which is specific to Pyk2, is PF-4618433 (PF-46) or $C_{24}H_{27}N_7O_2$ (Figure 10). PF-46 has IC_{50} values of 100 nM for Pyk2 and 10,000 nM for FAK. One study revealed that PF-46 also enhances ALP activity and mineralization in human MSCs *in vitro*, but no data was reported for the in vivo effects of PF-46 (Han et al. 2009).

1.7 Use of Hydrogels for Bone Regeneration

1.7.1 The bone regeneration process

Bone regeneration is a complex and well-orchestrated process of bone formation and bone resorption, which can be seen during normal fracture healing, and it is involved in bone remodeling process throughout life. Bone fracture healing is a unique biological process which can restore both anatomy and function of bone to the normal condition. Bone fracture healing can be divided into primary healing and secondary healing. Primary or direct fracture healing occurs through intracortical remodeling without callus formation, and it occurs only in fractures that have been stabilized by rigid fixation. It normally requires a few months to a few years for complete primary healing. Secondary or indirect fracture healing involves a response of the periosteum and soft tissues at the fracture site. Normally, it occurs when some micro-movement still exists, and typically it is enhanced by

movement and inhibited by rigid fixation. We can see both intramembranous and endochondral ossification in this type of bone fracture healing. The new bone formed by intramembranous ossification is usually seen at the peripheral of the fracture site, and it does not contribute to bridging the fracture. Endochondral bone formation, which forms a callus, occurs at the fracture site and responds directly for fracture bridging (Aubin et al. 1995; Oryan et al. 2015).

Bone fracture healing and regeneration consist of 4 stages; Inflammatory, soft callus, hard callus and bone remodeling. 1) The inflammatory stage usually happens within 24 hours and can last for a week. In this stage, the vessels will be disrupted and the hematoma will be formed. 2) In the soft callus formation stage, granulation tissues will be formed and replaced with fibrocartilage after hematoma formation; this usually takes about 7-10 days post fracture in a rodent model. 3) The hard callus or endochondral ossification stage usually occurs about 14 days post fracture in rodents. This stage includes the cartilaginous matrix formation by chondrocytes, and later the cartilage will be degraded by OCs then it will be replaced by the disorganized bone structure or woven bone produced by OBs. 4) During the bone remodeling stage, woven bone will be replaced by a more definitive bone tissue or lamellar bone by a coordinated balance between osteoclastic bone resorption and osteoblastic bone formation. This stage occurs around 3-4 weeks after fracture and may take years to be completed (Burr and Allen 2013; Marzona and Pavolini 2009; Oryan et al. 2015).

Bone can spontaneously heal when minor bone defects occur. However, the large bony defects and cases of compromised bone regeneration such as avascular necrosis and in osteoporosis patients require large scale of bone regeneration (Dimitriou et al. 2011; Zomorodian and Baghaban Eslaminejad 2012). Nowadays, standard approaches widely used in clinical setting to augment bone regeneration in extensive bone defects including distraction osteogenesis and bone grafting techniques. Autologous bone graft is considered the current gold standard because it has all required properties of a bone-graft material include: osteogenesis, osteoinduction, and osteoconduction. Furthermore, it is histocompatible and non-immunogenic, which decreasing immunogenic reactions

and transmission of diseases. Nonetheless, autologous bone graft requires an additional surgical procedure for graft harvesting that cause discomfort for patients and may increase complications. In addition, there is a limitation of graft quantity and grafts frequently associated with donor site morbidity. Alternative treatments are allogenic and xenogenic bone graftings, which exclude the problems of graft harvesting and the limitation of graft quantity. However, they possess a decrease in osteoinduction and no osteogenesis component. The addition disadvantages are immunogenicity, rejection reactions, and possibility of increasing the risk of infection and disease transmission (Amini et al. 2012; Dimitriou et al. 2011; Oryan et al. 2014).

1.7.2 General principles of tissue engineering

Bone tissue engineering has been extensively investigated to overcome the limitation of bone grafting and enhance bone healing (Mourino and Boccaccini 2010; Romagnoli et al. 2013). Tissue engineering for bone regeneration requires: 1) scaffolds with good biocompatibililty, biodegradation and mechanical properties, 2) an appropriate cell source, and 3) biological factors (Amini et al. 2012; Li et al. 2008; McCullen et al. 2009; Tollemar et al. 2016; Yoshimoto et al. 2003). The desirable physical and biological characteristics of bone tissue scaffolds include: 1) be osteoinductive (the ability to recruit MSCs and stimulate them into pre-OBs) and osteoconductive (the ability to allow bone to grow on the surface of materials), 2) promote osseointegration (the ability to stable anchorage of an implant to bone), 3) provide adequate temporary mechanical support (10-1500 MPa), 4) demonstrate interconnected porous structures that allow vascularization, cell migration and adhesion, and mass transport, 5) exhibit controlled degradation, 6) create non-toxic degradation products, 7) allow sterilization without bioactivity loss, and 8) be capable of delivering bioactive molecules (Bose and Tarafder 2012; Janicki and Schmidmaier 2011; Li et al. 2014; Romagnoli et al. 2013). Currently, there is no all-inclusive material that meets the above requirements.

1.7.3 Biomolecules for bone regeneration

Several studies have focused on loading biomolecules such as growth factors, proteins or drugs into scaffolds to enhance their function (Mourino and

Boccaccini 2010; Romagnoli et al. 2013). The bone morphogenic proteins (BMP), especially BMP-2, have been the most extensively used due to their potent osteoinductive ability to recruit MSCs and stimulate pre-OB formation (Li et al. 2014; Romagnoli et al. 2013). The osteoinductive effect of BMP-2 is well established for the regeneration of segmental bone defects, fractures, spinal fusion, aseptic bone necrosis, critical bone defects, and tooth socket healing (Chu et al. 2007; de Oliveira et al. 2013; Mont et al. 2004; Romagnoli et al. 2013). Recombinant human BMP-2 (rhBMP-2) is the form of BMP-2 that has been approved for limited clinical use. However, rhBMP-2 has been revealed to increase the risk of radicular pain, ectopic bone formation, osteolysis, premature epiphyseal fusion and poor global outcomes (Fu et al. 2013; Lewandrowski et al. 2007; Mesfin et al. 2013; Rodgers et al. 2013; Simmonds et al. 2013). Other published literature indicates that antiresorptive agents such as bisphosphonates and Denosumab cause a delay in bone remodeling process, but still enhance bone quality and quantity in the fracture repair site (Hegde et al. 2016). Although to date there are no reports on the effect of Pyk2 inhibitors for bone regeneration, the finding that genetic Pyk2-deletion increases OB activity and bone mass, and rats treated with the Pyk2-inhibitor (PF-43) showed an increase in bone formation rate and bone volume suggests that Pyk2 inhibitors may be an effective therapeutic agent for bone regeneration as well as for the treatment of systemic bone loss.

1.7.4 Hydrogels in tissue engineering

Hydrogels are three-dimensional (3D) biopolymeric networks that exhibit the ability to absorb large amounts of water. The 3D networks occur through the polymeric crosslinking, which can arise from physical interactions, covalent bonding, hydrogen bonding or van der Waals interactions (Lin et al. 2015). Hydrogels can be fabricated using both natural and synthetic polymers that do not cause adverse biological responses, and they can be fabricated in various forms such as microparticles, nanoparticles, films, and slabs. In addition, hydrogels are able to encapsulate biomolecules, drugs or cells, and allow control of the release behavior by changing physical or chemical structure of gels (Lin and Anseth 2009). Consequently, hydrogels are widely used in biomedical applications including

regenerative medicine and tissue engineering. In bone tissue engineering, natural or synthetic hydrogels combined with biomolecules such as biotin, growth factors and BMP-2 have shown positive bone healing effects in various animal models (Park 2011; Shi et al. 2012).

The controlled release behavior of hydrogels combines with their biocompatibility, biodegradability, and ability to mimic ECM structures ensue hydrogels are attractive materials for the carrier in drug delivery systems (Tronci et al. 2014). A crucial factor in the drug delivery system is the carrier must have the capacity to incorporate a drug, carry the drug to the specific target site and maintain an adequate drug concentration level for a desired period of time. In addition, a drug carrier should be gradually degraded without any toxicity in order to control drug release, deliver a drug at constant rates, and subsequently be replaced by tissue growth (Peppas et al. 2000). All these characteristics are well provided by hydrogels. Drugs or biomolecules can be incorporated into the gel networks by post-fabrication equilibrium partitioning or *in situ* encapsulation. Although the post-fabrication equilibrium partitioning method, which concentrated drug solutions are loaded through incubated gels, helps to preserve drug stability, it does not permit accurate control in the amount of drug loading. On the other hand, *in situ* encapsulation, which is a process to encapsulate drugs at the same time as network crosslinking, can be used to rapidly prepare hydrogels loaded with a more accurate amount of drugs. However, the drawback of *in situ* loading is the possibility that polymerization may cause undesired reactions with fragile biomolecules. The bioactivity of a drug released from hydrogels depends on numerous factors such as the drug loading technique, the molecular characteristics and size of the drug, the release profile of drugs, and the cellular/in vivo environment. The molecule release mechanisms from hydrogels are different from hydrophobic polymers due to their hydrophilicity, and they can be classified into 3 models; diffusion-controlled, swelling-controlled, and chemically controlled release (Lin and Anseth 2009). Many studies of drug release from hydrogels usually use only one mechanism to explain the release mechanism, which is not a realistic phenomenon. The coupled effects of diffusion and chemical matrix

degradation of hydrogels are more applicable and realistic to explain drug release from hydrogels (Lin and Metters 2006).

1.7.5 Poly (ethylene glycol) (PEG) hydrogels

PEG, one of the non-ionic hydrophilic synthetic polymers, has been extensively used for several decades for controlled drug delivery and cell delivery in tissue engineering applications due to the controllable material properties that enable hydrogels to be fabricated with the desired functions and properties. For example, the molecular weight of the polymer and crosslink density can be adjusted to obtain the desired degradation rate and release profile (Lin and Anseth 2009; Lin et al. 2015). PEG-based macromers with reactive termini have been increasingly developed for hydrogel fabrication. Among these macromers, PEG-di (meth) acrylate (PEGDA or PEGDM) (Figure 11) is highly used in hydrogel fabrication because of the simplicity of synthesis and its availability from commercial sources (Hao and Lin 2014).

PEG hydrogels can be formed by various methods including: physical, ionic and covalent interactions. Among these gelation methods, covalent or chemical crosslinking can produce stable hydrogels with tunable physicochemical properties such as permeability, diffusivity, and degradation rate. Covalently crosslinked PEG hydrogels can be synthesized through chain-growth, step-growth, or mixed-mode polymerization. Normally, chain-growth mechanism is developed from functional PEG molecules, such as PEGDA. The initiators for polymerization are free radicals, which propagate via unsaturated vinyl bonds on the PEG macromers. Then, chain-growth mechanism occurs and results in high molecular weight chains. One of the disadvantages of chain-growth polymerization is that non-ideal network hydrogels usually occur, and they may unfavorably affect drug release behavior and properties of materials (Lin and Anseth 2009). Step-growth polymerization occurs when at least two multifunctional monomers with reactive chemical groups are reacted together without free radical initiators. This mechanism creates fewer network defects, which allows accurate control of crosslink density and properties of hydrogels (Malkoch et al. 2006). This advantage is important in the drug delivery system because it allows precisely determined

drug dosing and release kinetics. Lastly, PEG hydrogels are also formed through mixed-mode polymerization, which presents both chain and step-growth polymerization characteristics (Lin and Anseth 2009). PEGDA hydrogels have also been used in bone regeneration as a carrier of biomolecules such as BMP-2. Evidence found that PEGDA hydrogel tethered with BMP-2 exhibits rapid bone healing in *in vivo* studies (Chen et al. 2011; Sonnet et al. 2013).

1.7.6 Gelatin hydrogels

Gelatin is a hydrocolloid protein derived from partial hydrolysis of collagen, usually from collagen type I, or denaturation at above 40°C. Gelatin has been widely used in biomedical applications because of its biocompatibility, biodegradability, and hydrogel characteristics, as well as its cost efficiency (Li et al. 2008). Furthermore, the presence of cell-recognition motifs such as the RGD sequence in gelatin structures improves its final biological characteristics over synthetic polymers. In drug delivery systems, gelatin has proven to be a versatile drug carrier because of its isoelectric point that enables charged biomolecule loading. In addition, release kinetics from gelatin can be tuned by the modification of its degradation (Santoro et al. 2014). Gelatin exhibits thermo-responsiveness, it forms gel at temperature below 35°C and becomes an aqueous solution at physiological temperature (37°C) (Bigi et al. 2004). Rapid degradation of gelatin is the factor limiting its applications in tissue engineering. However, this limitation has been improved by using covalent chemical crosslinking with various crosslinkers (Bigi et al. 2001; Chang et al. 2003).

1.7.8 PEG and gelatin hydrogels

Recently, the combination of PEG and gelatin has been investigated in order to overcome the limitations of PEG and gelatin hydrogels. PEGylation, the modification of gelatin with PEG for drug carriers has been developed to create slower drug clearance from the body and extended circulatory time (Santoro et al. 2014). One study found that nano-encapsulation of ibuprofen within PEGylated gelatin nano-vehicle revealed a slow and sustained release of ibuprofen along with increased pharmacokinetics and bioavailability of drug, thereby increasing the duration of action, which could lead to prolonged pharmacological effects. This

helps reduce the dosage and frequency of drug administration, which minimizes the side effects of ibuprofen and enhances therapeutic drug benefits (Narayanan et al. 2013). A semi-interpenetrating network (sIPN), which contains of photocrosslinked PEG matrices and physically entrapped gelatin, has been developed as an effective drug delivery and tissue engineering scaffold (Fu et al. 2012). sIPN of PEG matrices improve protein resistance and mechanical stability. The mesh size of sIPN depends on the amount of PEG in the system, which may impact the transportation of biomolecules out of the sIPN. Incorporating gelatin in matrices enhances elasticity and biodegradability of the system. Clearly, drug molecules can be directly added into the polymer solution prior to polymerization which allows for more accuracy in the amount of drug loaded rather than relying on equilibrium partitioning; thereby preventing drug overloading (Fu and Kao 2009).

1.8 Project Rationale, Hypotheses and Specific Aims

As described above, bone mass is controlled by the coordinated actions of the bone cells. The mechanisms that control bone mass are still not completely understood. An imbalance in the bone cell coupling process can lead to systemic bone loss as in osteoporosis as well as localized bone loss associated with periodontitis or osteoarthritis. To date, many therapeutic approaches have been developed to improve these low bone mass conditions, but most of them have some clinical concerns; bisphosphonates can causes bisphosphonate-related osteonecrosis of the jaw (Ruggiero et al. 2004), and PTH has several limitations include, parenteral administration, and risk of osteosarcoma (Pazianas and Abrahamsen 2016). Likewise, bone tissue engineering as an alternative therapy for targeted bone regeneration still has limitations in term of biomaterial properties and the efficacy of biomolecules being used. For example, collagen sponges exhibit an initial uncontrolled burst release of a loaded biomolecule, which can cause adverse effects to surrounding tissues (Fu et al. 2013; Simmonds et al. 2013). In addition, BMP-2, which is a well-established enhancer of bone

regeneration, is associated with increased risk of radicular pain, ectopic bone formation, and osteolysis (Fu et al. 2013; Mesfin et al. 2013; Rodgers et al. 2013; Simmonds et al. 2013). Therefore, a need for improved biomolecules and biomaterials for bone regeneration remains.

Pyk2 is important for OB activity and bone formation as well as OC activity (Buckbinder et al. 2007; Eleniste et al. 2015; Gil-Henn et al. 2007; Kacena et al. 2012). Pyk2-deletion and small molecule inhibitors of Pyk2 have been shown to increase OB activity and bone formation in vitro and in vivo. In addition, studies in Dr. Bruzzaniti's laboratory showed that estrogen supplementation after OVX results in a greater increase in BV/TV in Pyk2-KO OVX mice than WT OVX mice. Furthermore, the Pyk2 inhibitor, PF-43, also increased bone mass and protected rats from OVX-induced bone loss (Buckbinder et al. 2007; Han et al. 2009). Together, these findings suggest that Pyk2-KO mice are more responsive to estrogen than WT mice. Although the molecular mechanism for the role of Pyk2 in estrogen signaling is still unknown, these findings suggest that Pyk2 and estrogen may be part of a common mechanism to regulate OB activity. Finally, therapeutic strategies that target Pyk2 activity may be effective for bone regeneration.

The studies described in this thesis were undertaken with two overall goals; (1) To understand the actions of the tyrosine kinase Pyk2 as well as estrogen signaling through its cognate receptors to increase bone formation, and (2) to develop of a Pyk2-inhibitor loaded hydrogel which may be suitable for bone regeneration applications. The achievement of these aims required the integration of knowledge and skills related to both bone biology and biomaterial research. Experiments and results described in Chapters 3 and 4 are based on Specific Aims 1 and 2, respectively.

Specific Aim 1: *To determine the mechanism of action of Pyk2 and estrogen in osteoblastic bone formation in vitro (Chapter 3).* The effects of Pyk2 in combination with E2 on the expression of key OB markers were examined. In addition, the effects of Pyk2 with and without E2 or raloxifene on cell proliferation, ALP activity, and mineralization were determined. The reciprocal effects of E2 and Pyk2 on OB

activity were also investigated. Furthermore, the functional roles of the Pyk2 and Pyk2-S isoforms on OB differentiation were investigated.

Hypothesis 1): Pyk2-deletion enhances OB differentiation and mineralization through modulation of the estrogen signaling cascade.

.

Specific Aim 2: *To develop a Pyk2-inihbitor loaded hydrogel for bone regeneration applications (Chapter 4).* Small peptide inhibitors of Pyk2 were examined for their efficacy in increasing OB proliferation, ALP activity, and mineralization *in vitro*, with minimal cytotoxicity. Next, we developed and tested different hydrogels composed of PEGDA and gelatin. Once the optimal properties of PEGDA-gelatin hydrogel combination were identified including viscosity, gelation time and the release profile, then the efficacy of released Pyk2 inhibitors on OB activity was evaluated *in vitro*.

Hypothesis 2): A Pyk2-inhibitor loaded hydrogel will exhibit suitable properties for use as an injectable-carrier, and will retain its bioactivity against Pyk2 to promote osteoblastic activity.

CHAPTER 2

MATERIALS AND METHODS

2.1 Materials and Methods for Studies Described in Chapter 3

2.1.1 Media

α-MEM with L-glutamine (HyClone Laboratories, Inc., South Logan, UT, USA), phenol red free α-MEM with L-glutamine (Life Technologies, Carlsbad, CA, USA)

2.1.2 Chemicals, Solutions and Kits

Collagenase type IA (Sigma-Aldrich Co. LLC, St. Louis, MO, USA), Fetal Bovine Serum (FBS, Biowest, Kansas city, MO, USA), L-ascorbic acid and β-glycerophosphate (Sigma-Aldrich), 0.25%Trypsin with 0.02% EDTA (Quality Biological, Gaithersburg, MD, USA), phosphate buffer saline (PBS, HyClone Laboratories, Inc.), SYBR® Green PCR Master Mix (Applied Biosystems, Warringtons, UK), Taq DNA Polymerase (Thermo Fisher Scientific, Grand Island, NY, USA), agarose gel (Alkali Scientific, Pompano beach, FL, USA), ethidium bromide (Sigma-Aldrich), Tris-Chloride (Tris-Cl, Sigma-Aldrich) , sodium chloride (NaCl, Sigma-Aldrich), Igepal CA 630 (NP-40,Sigma-Aldrich), sodium deoxycholate (Sigma-Aldrich), leupeptin hydrochloride (Thermo Fisher Scientific), aprotinin (Thermo Fisher Scientific), pepstatin (Thermo Fisher Scientific), Phenylmethanesulfonyl fluoride (PMSF, Sigma-Aldrich) sodium fluoride (NaF, Sigma-Aldrich), sodium orthovanate (Thermo Fisher Scientific), p-nitrophenol phosphate and alkaline buffer (Sigma-Aldrich), Alizarin Red-S (Sigma-Aldrich), acetylpyridinium chloride (Sigma-Aldrich), X-tremeGENE HP DNA Transfection Reagent (Roche Applied Science), Nupage® Gels (Novex, Thermo Fisher Scientific), Nitrocellulose membranes (Protran®, Sigma-Aldrich), the enhanced chemiluminescence reagent (SuperSignal West Pico Chemiluminescent Substrate, Thermo Fisher Scientific), Oneshot Top10® (Life Technologies, Carlsbad, CA, USA), and Luria-Bertani (LB) (DOT Scientific Inc., Burton, MI, USA), EDTA (Thermo Fisher Scientific). 17β-estradiol (E2, Sigma-Aldrich), raloxifene hydrochloride (Sigma-Aldrich), Penicillin/Streptomycin (P/S, Lonza, Allendale, NJ, USA, Z-Leu-Leu-Leu-al (MG-132, Sigma-Aldrich), propyl-pyrazoletriol (PPT, Sigma-Aldrich), diarylpropionitrile (DPN, Sigma-Aldrich), RNeasy® Mini Kit

(Qiagen, Valencia, CA, USA), DNase I enzyme (Fisher Scientific, Pittsburgh, PA, USA), Transcriptor First Strand cDNA Synthesis Kit (Roche Applied Science, Indianapolis, IN, USA), MTS assay kit (CellTiter 96® AQueous Non-Radioactive Cell Proliferation Assay kit, Promega Life Science), Pierce™ BCA protein assay kit (Thermo Fisher Scientific), QIAGEN plasmid maxi kit (QIAGEN).

2.1.3 Antibodies

Anti-Pyk2 polyclonal antibody (Upstate™, Thermo Fisher Scientific), anti-ERα polyclonal antibody (MC20) and anti-ERβ monoclonal antibody (1531) (Santa cruz biotechnology, Dallas, TX), anti-p-Y402 monoclonal antibody (Alexis, Farmingdale, NY), anti-p-ERK, anti-p-AKT, and AKT rabbit monoclonal antibodies (Cell signaling, Beverly, MA), anti-V5 monoclonal antibody (Promega Life Science, Madison, WI, USA), anti-actin monoclonal antibody (Millipore, Bellerica, MA, USA), an anti-mouse antibody conjugated with horseradish peroxidase (HRP) and anti-rabbit HRP (Promega Life Science).

2.1.4 Preparation of calvarial-derived OBs from WT and Pyk2-KO mice

C57BL/6 mice (WT) were obtained from Jackson Laboratories. Pyk2-KO mice were provided by Pfizer, Groton, CT. Pyk2-KO mice were generated by creating a mutation into the murine *Pyk2* gene as described previously (Buckbinder et al. 2007; Okigaki et al. 2003). Pyk2-KO mice have been back-crossed for more than 10 generations and maintained on a C57BL/6 background. Mice were bred as heterozygotes and crossed to generate Pyk2-KO mice and WT littermates (Cheng et al. 2013; Kacena et al. 2012). WT littermate mice were used as controls. All mice used in this project were handled according to the guidelines of the American Association for Laboratory Animal Science using Institutional Animal Care and Use Committee (IACUC) approved protocols (IACUC approval: DS000885R) and in according with the NIH (Guide for the Care and Use of Laboratory Animals, 1996).

Murine calvarial cells were prepared using the previously described protocol (Cheng et al. 2013; Kacena et al. 2012). Briefly, calvaria from neonatal mice 2-3 days old were pretreated with 10 mM EDTA in PBS for 30 minutes. Next, the calvaria were subjected to sequential collagenase digestions with 0.1%

collagenase type IA from *Clostridium histolyticum* in serum-free α-MEM media with 1% (v/v) P/S for 30 minutes in each digestion at 37°C under shaking conditions (200 rpm). Cells were collected following incubation in collagenase from fractions 3–5, which consist of about 95% OBs or OB precursors (Kacena et al. 2012). Calvarial OBs were passaged twice and expanded prior to use. For passage 1, calvarial WT and Pyk2-KO OBs were seeded at 3×10^6 cells in a 10 cm^2 petri-dish in α-MEM with L-glutamine supplemented with 10% (v/v) FBS and 1% (v/v) P/S in an incubator at 37ºC with 5% CO_2. OBs were grown for 2 days and then were passaged a second time and 5×10^6 cells were expanded into a T175 cm^2 flask for 2 additional days. All experiments used OBs from the second passage.

2.1.5 Culturing of MC3T3-E1 osteoblastic cells

The MC3T3-E1 mouse osteoblastic cell line was originally purchased from the American Type Culture Collection (ATCC). Frozen cells were thawed and grown in α-MEM with L-glutamine supplemented with 10% (v/v) FBS and 1% (v/v) P/S in an incubator at 37ºC with 5% CO_2. Aliquots of MC3T3-E1 cells were stored frozen in liquid nitrogen. Cells were thawed and passaged once before being used for experiments.

2.1.6 Estrogen and raloxifene treatment of cells

WT and Pyk2-KO calvarial OBs were seeded in culture plates. The numbers of cells per well were as follows: 1) 2×10^3 cells/well in a 96-well culture plate, 2) 5×10^4 cells/well in a 12-well culture plate, and 3) 2×10^5 cells/well in a 6-well culture plate. After 24 hours of calvarial OBs seeding and MC3T3-E1 transfected with Pyk2 and Pyk2-S, cells were treated from 12 hours – 28 days with either 17β-estradiol (E2) or raloxifene in osteogenic medium, which contained 50 μM of ascorbic acid (AA) and 5 mM of β-GP in phenol red free α-MEM with L-glutamine supplemented with 2% (v/v) FBS and 1% (v/v) P/S. We used phenol red free media and low serum concentration in order to eliminate the estrogenic actions of phenol red and serum (Berthois et al. 1986). The medium was replaced every 2 days. The concentration 100 nM of E2 was used in all experiments based on our preliminary studies and literature that primary OBs and osteoblastic cell lines show the highest response at this concentration (Cheng et al. 2002; Taranta et al. 2002; Zhou et al.

2001). The vehicle control for E2 was 100% ethanol. For raloxifene, the concentration from 0.1 -10 nM was used and the vehicle control was DMSO. The vehicle controls were used to determine whether the vehicles alone cause any effects to cells (Johnson and Besselsen 2002). The number of cells seeded, the duration of each drug treatment, and subsequent analyses are shown in Table 1.

2.1.7 Transient expression of Pyk2 and Pyk2-S cDNA in MC3T3-E1 cells

MC3T3-E1 cells 6.7×10^4 were plated per well in a 24-well culture plate for 24 hours before transfection. Two micrograms of Pyk2 or Pyk2-S cDNA were used for one reaction and diluted in a 200-µL serum free α-MEM media and completely mixed by pipetting. Next, 6 µL of X-tremeGENE HP DNA Transfection Reagent was added into the diluent cDNA mixture (3:1 reagent to cDNA ratio) and then pipetted to mix thoroughly. The mixture of cDNA and transfection reagent was incubated for 20 minutes at room temperature to allow complex formation. After this, the complexes of cDNA and transfection reagent were added to the cells in a dropwise manner, and the culture plate was gently swirled and shaken to ensure the even distribution of the cDNA and transfection complexes. Following transfection, cells were incubated for 24 hours prior to the subsequent treatment and assays.

2.1.8 Plasmid purification

Pyk2 and Pyk2-S cDNA expression constructs were previously generated in Dr. Bruzzaniti's laboratory by PCR cloning (Figure 12). Briefly, the pEF6/V5-His-TOPO® vector was used. The pEF6/V5-His-TOPO® construct contains 5840 nucleotides including a EF-1α promoter, a T7 promoter/priming site, a TOPO® cloning site, a V5 epitope, a C-terminal polyhistidine (6xHis) tag, a bovine growth hormone (BGH) reverse priming site, a BGH polyadenylation signal, an f1 origin, an SV40 promoter and origin, an EM-7 promoter, a blasticidin resistance gene, an SV40 early polyadenylation signal, a pUC origin, a bla promoter, and an ampicillin resistance gene. The primers used for cloning are as follow: 5'-GATATG TCT GGG GTG TCC GAG CCC CTG AGC CGA GTA A, and 5'- CTC TGC AGG TGG GTG GGC CAG ATT GGC CAG AAC. Pyk2 and Pyk2-S cDNA was generated by

RT-PCR using human Pyk2 cDNA. The PCR product was then cloned into the pEF6/V5-His-TOPO® vector, amplified and purified.

In the current study, we started with amplifying plasmid cDNA expressing Pyk2 or Pyk2-S. Each plasmid cDNA (5 µL) was added into a tube of Oneshot Top10®, which is commercial *Escherichia coli* with high efficiency cloning and plasmid propagation. The mixture was incubated for 30 minutes on ice, then heat shocked in a 42°C water bath for 30 seconds and immediately placed on ice for 2 minutes. Next, 250 µL of Super Optimal broth with Catabolite repression (S.O.C) was added into the mixture and incubated at 37°C for 1 hour under shaking conditions at 225 rpm. The 200 µL of cultured mixture was spread on Luria-Bertani (LB) agar plates containing the 100 µg/mL ampicillin and incubated overnight at 37°C. A single colony was selected and inoculated into 10 mL LB broth with ampicillin (100 µg/mL) and incubated overnight at 37°C at 200 rpm in the shaker incubator. All 10 mL of the culture was transferred into a 250 mL fresh LB broth and cultured under the same conditions. Bacteria were then harvested by centrifugation (6000x g) at 4°C for 15 minutes, and all of the supernatant were removed.

Plasmids were purified using a QIAGEN plasmid maxi kit. The pellet was thoroughly re-suspended into 10 mL of re-suspension buffer. Cells were lysed in 10 mL of lysis buffer, mixed gently by inverting the tube 4-6 times, and then were incubated at room temperature for 5 minutes. Next, the mixture was mixed vigorously with 10 mL chilled neutralization buffer and incubated on ice for 30 minutes to promote the precipitation of the genomic DNA, proteins, and cell debris. Then the solution was centrifuged at 20,000x g for 30 minutes at 4°C, and the supernatant containing plasmid DNA was transferred to a new tube. The columns were prepared by adding 10 mL equilibration buffer through the column to reduce surface tension. The filter sheets were placed on top of the column, then the supernatant was loaded into the column and filtrated, then all contaminants were washed out with 60 mL wash buffer. The DNA was eluted using 15 mL elution buffer, and the precipitation of DNA was achieved by adding 10.5 mL isopropanol at room temperature to the eluted DNA and mixed vigorously, then centrifuged at

15000x g for 30 minutes at 4°C. The DNA pellet was washed with 5 mL room temperature 70% ethanol and centrifuged at 15000x g for 10 minutes. Lastly, the pellet was dissolved using Tris-EDTA (TE) buffer (10 mM Tris base, 1mM EDTA, pH 8.0) at 4°C overnight and kept at -20°C.

2.1.9 RNA isolation

Cell pellets of OBs were disrupted and homogenized in 350 µL of buffer RLT in RNeasy® Mini Kit. The lysate was centrifuged at 13000x g for 3 minutes at 4°C. The supernatants were transferred into new Eppendorf tubes, and 350 µL of 70% ethanol was added and mixed well by pipetting. All of the sample (700 µL) was transferred to an RNeasy Mini spin column placed in a 2 mL collection tube and centrifuged at 10,000 rpm for 15 seconds at 4°C, and the flow-through was discarded. Next, 700 µL of buffer RW1 was added to the column and centrifuged at 10,000 rpm for 15 seconds at 4°C, and the flow-through was discarded. Then, 500 µL of buffer RPE was added to the column twice and centrifuged at 10,000 rpm at 4°C for 15 s and 2 minutes, respectively. All of the flow-through was discarded. The column was placed in a new 2 mL collection tube and centrifuged at the maximum speed in order to dry the spin column membrane. After this, the column was placed in a new 1.5 mL collection tube and 30-50 µL of RNase-free water was added directly to the column membrane, and then centrifuged at 10,000 rpm for one minute at 4°C to elute RNA. The purity and quantification of RNA were measured using a nanodrop spectrophotometer. The purity of RNA is evaluated using the ratio of the absorbance at 260 and 280 nm ($A_{260/280}$), and the $A_{260/280}$ of pure RNA is approximately two. The remnant genomic DNA in RNA samples were removed by digestion with DNase I enzyme. One unit of DNase I enzyme and 10x DNase buffer were used to clean up remnant DNA from RNA up to 1 µg. The reaction of DNase I enzyme was activated by incubation at 37°C for 30 minutes, and then the reaction was inactivated with 50 mM EDTA at 65°C for 10 minutes.

2.1.10 Synthesis of cDNA by reverse transcription reaction

Complementary DNA (cDNA) was synthesized using the Transcriptor First Strand cDNA Synthesis Kit, which used the reverse transcriptase and random hexamer ($pd(N)_6$) primers to convert mRNA to cDNA. One µg of RNA was used

for each reaction. The RNA mixture with random hexamer primers was incubated at 65°C for 10 minutes in order to denature the RNA secondary structure. Next, the reverse transcriptase reaction with dNTPs was activated by incubating at 25°C for 10 minutes followed by 60 minutes at 50°C. The reaction was stopped by heating at 85°C for 5 minutes and at 4°C continually until the cDNA was stored at -20°C.

2.1.11 Reverse Transcription-Polymerase Chain Reaction (RT-PCR)

The RT-PCR was done using the two-step technique. The first step was cDNA generation by reverse transcription reaction as previously described. The second step was a standard PCR that amplified a region of the interested cDNA. The PCR mixture was set up by mixing nuclease-free water, 10x Taq buffer, 2mM dNTPs, 25mM $MgCl_2$, forward and reverse primers, Taq DNA Polymerase and template cDNA. β-Actin and GAPDH were used as the internal controls for RT-PCR experiments. A list of the primers examined is shown in Table 2. PCR was performed using thermocycling conditions as follows: 1) initial denaturation at 95°C for 3 minutes, 2) denaturation at 95°C for 30 seconds, annealing at melting temperature (Tm) – 5°C for 30 seconds, and extension at 72°C for 1 minute, all repeating for 30-45 cycles, 3) final extension at 72°C for 5 minutes. The PCR products were separated using 2% agarose gel electrophoresis with ethidium bromide and then imaged with a Bio-Rad Gel Doc XR system.

2.1.12 Primers for QPCR and RT- PCR

Details are in Table 2.

2.1.13 Quantitative Real-time Polymerase Chain Reaction (QPCR)

QPCR was used to quantify mRNA expression from WT and Pyk2-KO OBs. In order to complete QPCR, SYBR® green PCR Master Mix was used. A list of the genes examined is shown in Table 1. The *18S* RNA housekeeping gene was used as an endogenous control. In each QPCR reaction, 100 ng of cDNA was used. All samples were run in the ABI Prism® 7000 sequence detection system using STEP1 Software Solutions in duplicate with the temperature profile as follows: 1) 50°C for 2 minutes, 2) 95°C for 10 minutes, 3) 40 repeating cycles of 95°C for 15 seconds and 56°C or 60 °C for 1 minute, and 4) dissociation stage included: 95°C

for 15 seconds, 56°C or 60°C for 20 seconds, and 95°C for 15 seconds. The threshold cycle (Ct) for each test gene was normalized against 18S. QPCR was analyzed as absolute mRNA quantification of Pyk2-KO and WT OBs with or without E2 supplement.

2.1.14 Cell proliferation assay

The cell proliferation assay was performed by examining the proliferation activity of OBs and also counting cell number in each treatment. For proliferation activity assay, the CellTiter 96® AQeous Non-Radioactive Cell Proliferation Assay kit, a colorimetric method for determining the number of viable cells, was used. This kit consists of a tetrazolium compound, which is called MTS, and an electron-coupling reagent that is phenazine methosulfate (PMS). MTS was reduced into a soluble formazan product by cellular activity, and the amount of formazan product can be measured directly from the culture plate using a Thermomax spectrophotometer recording the absorbance at 490 nm. For each proliferation assay, one hundred µL of PMS solution was added to 2 mL of MTS and completely mixed with pipetting, then 20 µL of the combined MTS/PMS was pipetted into each well of the 96-well culture plate that contained the culture of WT and Pyk2-KO OBs in the presence or absence of E2 for 12 hours at 37°C in a humidified, 5% CO_2 atmosphere. After addition of the MTS solution (time 0), absorbance at 490 nm was read every hour from 1-6 hours.

To determine changes in OB cell number, an equal number of WT and Pyk2-KO OBs were cultured in the same condition as in the MTS metabolic activity assay. OBs from each group were harvested on day 1 and day 4 by incubating with 0.05% trypsin and EDTA for 5 minutes at 37°C in a humidified, 5% CO_2 atmosphere. Cell number per well was counted using a hemocytometer under the light microscope.

2.1.15 Western blot analysis

OBs and MC3T3-E1 cells were lysed in a modified radio-immunoprecipitation assay (mRIPA) buffer (50 mM Tris-Cl pH 7.5, 150 mM NaCl, 1% NP-40, 0.25% Sodium deoxycholate) supplemented with 10 µg/mL leupeptin hydrochloride, 10 µg/mL aprotinin, 10 µg/mL pepstatin, 1 mM PMSF, 1mM sodium

fluoride, and 1mM sodium orthovanate, and then sonicated for 5 minutes. The lysates were centrifuged at maximum speed for 5 minutes, and the supernatants were collected. The protein amount was quantified using the Pierce™ BCA protein assay kit, and 30 µg of protein was resolved by SDS-PAGE electrophoresis. The loading buffer (62.5 mM Tris HCl pH 6.8, 2% w/v SDS, 25% glycerol, and 0.01% bromophenol blue) was added to protein samples, and then boiled at 100°C for 5 minutes to denature protein. The samples were loaded onto gradient (4%-12%) Nupage® Bis-Tris gels along with the molecular weight protein markers and subjected to electrophoresis. Proteins were resolved at 120 volts for approximately 2.5 hours. The proteins from the gel were transferred to the nitrocellulose membrane in Nupage® transfer buffer with 20% methanol at 100 volts for 1 hour at 4°C.

The non-specific proteins on the membrane were blocked with 5% skim milk in a TBST solution (0.2 M Tris Base and 0.6 M NaCl at pH 7.4 containing 0.1% Tween-20) for 1 hour under shaking condition at room temperature. The membrane was incubated with the primary antibody (section 2.1.3), which was diluted in the TBST buffer (1:1000) overnight at 4°C. Next, the membrane was washed with the TBST buffer for 15 minutes 3 times to remove unbound primary antibody. An anti-mouse antibody conjugated with horseradish peroxidase (HRP) and anti-rabbit HRP were used as secondary antibodies. The anti-mouse antibody HRP was diluted 1:20000, while anti-rabbit HRP was diluted 1:10000 in the TBST buffer and incubated with the membrane for 1 hour at room temperature with agitation. The membrane was washed 3 times for 15 minutes in the TBST buffer, and then proteins were detected using the enhanced chemiluminescence (ECL) reagent (SuperSignal™ West Pico Chemiluminescence Substrate, Sigma-Aldrich) for 5 minutes according to the manufacturer's recommendations. A radiographic film was used to record the emitted signal from the membrane.

2.1.16 Quantitative ALP activity assay

OB and MC3T3-E1 cells were lysed in 100 µL of the mRIPA buffer supplemented with protease/kinase inhibitors as previously described. The lysate was sonicated for 5 minutes, and then centrifuged at maximum speed for 5 minutes

and the supernatant were collected. Five µL of the cell lysates was pipetted into each well of a 96-well plate. Then 100 µL of ALP substrate (40 mg of p-nitrophenyl phosphate (p-NPP), 10 mL of alkaline buffer, and 10 mL of dH_2O) were added to each well, and the assay plate was incubated for 50 minutes at 37°C in a dark atmosphere. The reaction was stopped by adding 95 µL of 20 mM NaOH. ALP activity was determined by the colorimetric conversion of p-NPP to nitrophenol. Optical absorbance at 405 nm was recorded using a Thermomax spectrophotometer. ALP activity was normalized by total protein using a Pierce™ BCA protein assay kit.

2.1.17 Quantitative analysis of Alizarin Red S staining

OB and MC3T3-E1 cells were washed with PBS and fixed with cold 70% ethanol for 1 hour at -20°C. The fixed cells were allowed to warm up to room temperature and washed twice with deionized water (dH_2O). One mL of 40 mM Alizarin Red S (pH 4.2) was used to stain calcium in each well for 10 minutes with agitation. The Alizarin Red S stained samples were washed 5 times with dH_2O, followed by 15 minutes of PBS washing on the shaker. Next, the bound Alizarin Red S was extracted with 750 µL of 1% cetyl pyridinium chloride (CPC) in 10 mM sodium phosphate (pH 7.0) for 15 minutes on the shaker at room temperature. The extracted solution was collected and mixed thoroughly and then 150 µL were pipetted into a 96-well plate, and calcium deposition was measured by recording the absorption of extracted Alizarin Red S at 562 nm using a Spectramax 190 spectrophotometer.

2.2 Materials and Methods for Studies Described In Chapter 4

2.2.1 Media

α-MEM with L-glutamine (HyClone Laboratories, Inc.), phenol red free α-MEM with L-glutamine (Life Technologies).

2.2.2 Chemicals and solutions

FBS (Biowest, Kansas city, MO, USA), AA and β-GP (Sigma-Aldrich), 0.25%Trypsin with 0.02% EDTA (Quality Biological), PBS (HyClone Laboratories,

Inc.), p-nitrophenol phosphate and alkaline buffer (Sigma-Aldrich), collagen sponges (RCF, Surgical Supplies Co. Brockton, MA, USA), PEGDA 1000 Da and 600 Da (Polysciences Inc, Warrington, PA, USA), dithiothreitol (DTT, Thermo Fisher), type B gelatin from bovine skin (Sigma-Aldrich), 7-amino-4-methylcoumarin (Sigma-Aldrich), Penicillin/Streptomycin (P/S, Lonza). PF-43 (Sigma-Aldrich), PF-46 (Adipogen, San Diego, CA, USA), Pierce^{TM} BCA protein assay kit (Thermo Fisher Scientific), Universal Tyrosine Kinase Assay Kit (Takara Bio, Mountain View, CA, USA).

2.2.3 Antibodies

Details are in section 2.1.3.

2.2.4 Preparation and culturing of murine MSCs

Murine MSCs were obtained from tibias and femurs of 10-14-weeks old C57BL/6 mice. Both proximal and distal ends of tibias and femurs were cut away from epiphysis, and the marrow was flushed out with PBS. The released cells were collected and cultured in a 35 mm^2 petri-dish in α-MEM with L-glutamine supplemented with 10% (v/v) FBS and 1% (v/v) P/S in an incubator at 37ºC with 5% CO_2. The medium was changed after 24 hours in order to remove non-adherent cells. Sub confluent MSCs were passaged and expanded into T75 cm^2. All experiments used OBs from the second passage.

2.2.5 MC3T3-E1 osteoblast cell line and human embryonic kidney 293 cells (293VnR) culturing

MC3T3-E1 and 293VnR cells were grown in α-MEM with L-glutamine supplemented with 10% (v/v) FBS and 1% (v/v) P/S in an incubator at 37ºC with 5% CO_2. MC3T3-E1 and 293VnR cells were used for experiments after the first passage.

2.2.6 Pyk2 inhibitors treatment

WT MSCs were seeded in culture plates, and the number of cells per well was as follows: 1) 2×10^3 cells/well in a 96-well culture plate and 2) 4×10^4 cells/well in a 12-well culture plate. After 24 hours of MSCs seeding, cells were treated from 1-28 days with PF-43, PF-46 or DMSO (vehicle control) in osteogenic medium. The medium was replaced every 2 days. The doses of PF-43 and PF-46

were 0.0125, 0.025, 0.05, 0.1 and 0.3 μM (Buckbinder et al. 2007; Han et al. 2009). The number of seeding cells, the duration for treatment of each drug, and subsequent analyses are shown in Table 3.

2.2.7 Cell proliferation assay

The cell proliferation assay of mouse MSCs treated with and without PF-43 or PF-46 was performed using the CellTiter 96® AQeous Non-Radioactive Cell Proliferation Assay kit as described in section 2.1.14

2.2.8 Quantitative ALP activity assay

The quantitative ALP activity of mouse MSCs treated with and without PF-43 or PF-46 was performed by the technique described in section 2.1.16.

2.2.9 Quantitative analysis of Alizarin Red S staining

The quantitative calcium deposition of mouse MSCs treated with and without PF-43 or PF-46 was performed by the technique described in section 2.1.17.

2.2.10 Preparation of Scaffolds

1. Collagen sponge preparation

Collagen sponges, RCF, were purchased from Surgical Supplies Co, and then were cut into disks of 5 mm in diameter and 3 mm in thickness by using a hole-puncher and ready to be used.

2. PEGDA-gelatin hydrogels fabrication

PEGDA 600 Da or 1000 Da was dissolved in α-MEM at 37°C under stirring to form a 50% w/v solution overnight, and the other required components, which are 2% lithium phenyl-2,4,6-trimethylbenzoylphosphinate (LAP) photoinitiator, and 0.1 mM DTT, were added and stirred for 8 hours. Type B gelatin was also dissolved in α-MEM at 37 °C under stirring to form 10% or 20% v/v solution overnight. Next, PEGDA solution was mixed with gelatin solution at ratio 1:1 by volume under stirring to get gel formulations as follows: 1) 25% PEGDA1000 and 10% gelatin (P1000:G10), 2) 25% PEGDA600 and 5% gelatin (P600:G5), 3) 25% PEGDA1000 (P1000), and 4) 25% PEGDA600 (P600). All the concentrations indicated were the final concentration in the prepolymer solution. The prepolymer solution 150 μL was pipetted into the disk-shaped silicone mold of 5 mm in diameter and 3 mm in

thickness and exposed under LED light 450-470 nm and 1000 J/cm^2 for 2-6 minutes in order to get complete photopolymerization.

2.2.11 Dynamic viscosity test

P600, P600:G5, P1000, and P1000:G10 prepolymer solutions were prepared as previously described in section 2.2.10. Dynamic viscosity of the prepolymer solutions (1 mL) from every group was measured on a Bohlin CVO 100 digital rheometer (viscometry mode) using 4° cone/plate geometry in controlled continuous shear rate from 100 to 600 s^{-1} with a gap size of 150 μm at room temperature (Lin et al. 2011).

2.2.12 Measurement of gelation time

P600, P600:G5, P1000, and P1000:G10 prepolymer solutions were prepared as previously described in section 2.2.10. We determined the gelation time of hydrogels by using 2 techniques as follows:

1. Probing technique

Gelation times of all groups were determined using a technique as described previously (Lemon et al. 2003; Murata et al. 2004). Briefly, the prepolymer solution 150 μL was pipetted into the disk-shaped silicone mold of 5 mm in diameter and 3 mm in thickness and exposed under visible LED light 450-470 nm and 1000 J/cm^2 for 20 seconds; then a periodontal probe was used to contact the surface. This contact was repeated at 20-second intervals after light exposure. Gelation time was defined as the time when the surface of the material hardened and the material did not adhere to the tip of the periodontal probe. This experiment was carried out at the room temperature (N=5/group).

2. In situ photorheometry test

To monitor gelation kinetics, in situ photorheometry by shear oscillation measurements were performed using a Bohlin CVO 100 digital rheometer with a light cure attachment. Four groups of prepolymer solutions were prepared as previously described in section 2.2.10. A hundred μL of each prepolymer solution was pipetted on a quartz plate in the light cure cell and irradiated with light through a flexible light guide using Omnicure S1000 system (1000J/cm^2). Light was turned on at 10 s after starting time-sweep mode, using 25 mm parallel plate geometry

with 10% strain, 1 Hz frequency, and a gap size of 90 μm. Gel points or gelation times were defined as the time when storage modulus (G′) crossed over loss modulus (G″) (Greene and Lin 2015).

2.2.13 Swelling and degradation of PEGDA-gelatin hydrogels

P1000:G10 and P600:G5 gels were prepared as previously described in section 2.2.10 (N=5/group), and were dried under the vacuum for 48 hours to completely remove remaining water. The initial dry weight of hydrogel was measured. Hydrogels were immersed in 1 mL of pH 7.4 PBS in Eppendorff tubes and stored at 37°C. Hydrogels were removed from the tubes and dried with Whatman paper to remove excess water from hydrogel surfaces and then weighed every 30 minutes for the first four hours, and then at 24, 48, 72, 120, 240, 360, 480, and 600 hours. One mL of PBS was replaced at every time point to keep the volume constant. The percentage of swelling ratio (*Q*) was calculated as:

$$Q = \frac{Wt}{Wd} \times 100\%$$

where *Wt* is wet weight at time t, and *Wd* is dried weight of hydrogels.

For degradation, we performed hydrolytic degradation by using the same method as swelling experiment. The extent of degradation (D) was calculated on day 1, 2, 3, 5, 10, 15, and 25 as following equation:

$$D = \left[1 - \frac{mt}{mi}\right] \times 100\%$$

where *mt* is the gel mass at a particular time point and *mi* is the original gel mass.

2.2.14 *In vitro* release behavior of the PEGDA-gelatin hydrogel

7-amino-4-methylcoumarin was used as a representative of PF-46 for the study of release behavior of hydrogel due to its easily detectable by using simple equipment. P1000:G10, P600:G5, and collagen sponge disks were fabricated as previously described in section 2.2.10 (N=5/group), and 50 μg of 7-amino-4-methylcoumarin were added to collagen sponge and the prepolymer solution before photopolymerization. The loading efficacy was evaluated to determine the amount of 7-amino-4-methylcoumarin that was successfully loaded into the scaffolds. Samples from each group were soaked in 1 mL of PBS and stored in an incubator at 37ºC for 24 hours, and samples from all groups were sonicated. The

total amount of 7-amino-4-methylcoumarin in the samples was measured by using a Biotek Synergy HTX multi-mode reader. Fluorescence was measured using 370 nm excitation and 460 nm emission wavelengths. The loading efficacy will be calculated as follows:

$$\% \text{ loading efficacy} = \frac{amount\ of\ drug\ in\ the\ scaffold}{drug\ added} \times 100$$

For the release profile of 7-amino-4-methylcoumarin, the samples were also soaked in 1 mL of PBS at 37°C, and the soaking solution was collected 500 µL on day 0, 1, 2, 3, 5, 10, 15, 20 and 25 to measure the 7-amino-4-methylcoumarin amount using a Biotek Synergy HTX multi-mode reader (n=5/group). The samples were replaced with fresh 500 µL of PBS at every time point in order to keep a constant volume of medium. We have chosen to perform a release profile using this time frame based on rhBMP-2 studies, in which a drug vehicle with sustained rhBMP-2 of at least 10% of the initial dose after 5 weeks has been shown to be sufficient for inducing callus formation in rabbit bone defects (Seeherman et al. 2003). The concentration of release 7-amino-4-methylcoumarin was calculated from a standard curve of 7-amino-4-methylcoumarin.

2.2.15 *In vitro* cytotoxicity test

P600:G5, P1000:G10, and collagen sponge gel disks (N = 5/group) were prepared as previously described in section 2.2.10. All samples were sterilized by UV light for 30 minutes per each side. Each sample was immersed in 1 mL of α-MEM with L-glutamine supplemented with 10% (v/v) FBS and 1% (v/v) P/S in an incubator at 37ºC for 24 hours. P600:G5, P1000:G10, and collagen sponge eluates were then collected.

The cytotoxicity of eluates was evaluated on MC3T3-E1 cells using the CellTiter 96® AQeous Non-Radioactive Cell Proliferation Assay kit. MC3T3-E1 were seeded at 1.5 × 10^3 cells per well in a-96-well culture plate and incubated overnight at 37°C with 5% CO_2. Thereafter, the medium was replaced with 150 µL of P600:G5, P1000:G10, or collagen sponge eluates. For the control group, a fresh medium was replaced. After incubation for 24 hours, the CellTiter 96®AQeous Non-Radioactive Cell Proliferation Assay kit was used as described in the section 2.1.14.

2.2.16 *In vitro* tyrosine kinase activity assay

P1000:G10 gels were prepared as previously described in section 2.2.10, and 20 μg of PF-46 were added to the prepolymer solution before photopolymerization. The representative dosage 20 μg of PF-46 was used in the *in vitro* experiment based on the effective ratio of rhBMP-2 using *in vitro* and local approach *in vivo* studies (30 ng/mL: 10 μg) (Chu et al. 2007; Jikko et al. 1999).

All samples were sterilized by UV light for 30 minutes per each side. Each sample was immersed in 1 mL of α-MEM with L-glutamine supplemented with 10% (v/v) FBS and 1% (v/v) P/S under shaking conditions (50 rpm) at 37ºC for 24 hours.

Pyk2 catalytic activity depends on its autophosphorylation on tyrosine residues (Bruzzaniti et al. 2009; Eleniste and Bruzzaniti 2012; Eleniste et al. 2012). 293VnR cells (Bruzzaniti et al. 2005) were cultured and then transiently transfected with Pyk2 cDNA for 72 hours, and incubated with or without fresh PF-46 or the released PF-46 at the concentration of 0.1, and 0.3 μM (N=5/group) for 45-120 minutes (Tse et al. 2009). Changes in Pyk2 kinase activity were evaluated using the Universal Tyrosine Kinase Assay Kit (Takara Bio). Cells were washed with PBS, 1 mL of extraction buffer was added to the culture plate, and cells were scraped. The samples were spun at 10,000x g for 10 minutes at 4°C. The supernatant which contains the total protein extract was transferred to a new tube. Next, the specific protein tyrosine kinase activity assay was performed using immunoprecipitation (IP). The Protein G agarose (50 μL) (Roche Applied Science) was added into 1 mL of total protein extracts. Non-specific binding proteins in the Protein G agarose were removed by shaking gently for 20 minutes, and then spun at 10,000x g for 10 minutes at 4°C. The supernatant was transferred to a new tube, and 3 μg of Pyk2 antibody (polyclonal antibody) were added into the supernatant and incubated at 4°C overnight. Protein G agarose (40 μL) was added again into the supernatant and incubated for 1 hour at room temperature, then spun for one minute at 10,000x g and the supernatant was discarded. The precipitate was washed 3 times with 1 mL of PBS on the shaker for 10 minutes and spun at 10,000x g for 1 minute at 4°C, and the supernatant was removed. The kinase reacting solution (150 μL) with 2-mercaptoethanol was added to the precipitate,

and then the sample was diluted 2 times with the kinase reacting buffer. Forty µL of the diluent was added into each well of a 96-well plate with 10 µL of 40 mM ATP-2Na, and the sample was incubated for 30 minutes at 37°C. The sample was washed with the washing buffer 4 times, and blocked with 100 µL of the blocking solution and incubated for 30 minutes at 37°C. The blocking solution was removed, and 50 µL of anti-phosphotyrosine (PY20)-HRP was added into each well and incubated for 30 minutes at 37°C. The content in each well was washed 4 times with the washing buffer, and 100 µL of HRP substrate solution was added into each well and incubated at 37°C for 15 minutes. The reaction was stopped by adding 100 µL of the stop solution. The absorbance at 450 nm was measured.

2.2.17 Quantitative ALP activity assay of mouse MSCs treated with the released PF-46

PF-46 loaded P1000:G10 were prepared, sterilized, and extracted the released PF-46 as described in section 2.2.16. Mouse MSCs 4×10^4 were cultured for 7 days under osteogenic conditions with and without fresh PF-46 or the released PF-46 at the concentration of 0.1 and 0.3 µM (N=5/group). After this, quantitative ALP activity assay was performed as described in section 2.1.16.

2.3 Statistical Analyses for All Studies in Chapter 3 and Chapter 4

All data from specific aim 1 and 2 were analyzed by one-way analysis of variance (ANOVA) and/or two-way ANOVA or multifactorial ANOVA followed by post hoc multiple comparisons where appropriate. Data was analyzed by using SPSS 24 software (IBM Corporation, Armonk, NY, USA). Data is presented as means ± standard error of means (SEM), and a significant difference was determined at $p \leq 0.05$.

CHAPTER 3

MECHANISM OF ACTION OF PYK2 AND ESTROGEN IN OSTEOBLAST BONE FORMATION *IN VITRO*

3.1 Introduction

The bone remodeling occurs throughout life to maintain bone mass. This process involves a coordinated balance between osteoclastic bone resorption and osteoblastic bone formation, which are regulated by many factors at both the systemic and local levels. These factors include hormones, growth factors, transcription factors, and mechanical stimuli (Compston 2001). When an imbalance occurs in this process, excessive osteoclastic bone resorption and/or decreased osteoblast function leads to low bone mass diseases such as osteoporosis. The risk of osteoporosis increases with age, and it is common in post-menopausal women due to declining levels of the osteoprotective hormone estrogen. Evidence suggests that estrogen therapy, including SERMs, can prevent bone loss and increase BMD in post-menopausal women (Riggs and Hartmann 2003). Moreover, the risk of fracture of the hip, spine, and wrist in post-menopausal women is decreased by estrogen therapy (Compston 2001).

The actions of estrogen on target tissues are mediated by genomic and non-genomic mechanisms (Imai et al. 2010; Krum and Brown 2008). The ERs consist of at least 2 subtypes, ERα and ERβ, which exhibit close structural homology (Compston 2001; Hewitt et al. 2016). Estrogen has high binding affinity for both ERα and ERβ, and its binding affinities for these two ERs are quite similar. However, the SERM raloxifene shows lower binding affinity for the ERs than estrogen, and it preferentially binds ERα with an approximately 3.5-fold higher affinity for ERα than ERβ (Zhu et al. 2006).

The proline-rich tyrosine kinase, Pyk2, is important for the regulation of bone mass and for the function of OBs and OCs (Bruzzaniti et al. 2005; Buckbinder et al. 2007; Eleniste and Bruzzaniti 2012; Gil-Henn et al. 2007). Our studies and others demonstrated that OB differentiation and bone formation are enhanced in the absence of Pyk2 (Buckbinder et al. 2007; Cheng et al. 2013; Eleniste et al. 2015; Kacena et al. 2012). Pyk2-KO mice exhibit an osteopetrotic phenotype, which is in part due to increased osteoblastic bone formation as well as decreased osteoclastic bone resorption (Buckbinder et al. 2007; Gil-Henn et al. 2007).

Unpublished observations from Bruzzaniti et al. reveal that the high bone mass is predominantly seen in female Pyk2-KO mice. Notably, OVX Pyk2-KO mice exhibited a much greater increase in bone density with 17β-estradiol supplementation than OVX WT mice. Together these data suggest that Pyk2 may regulate bone mass through estrogen signaling in bone cells.

The aim of studies described in this thesis was to understand the mechanism of action of Pyk2 and estrogen in osteoblastic bone formation *in vitro*. First, the effects of Pyk2 and 17β-estradiol (E2) or the SERM, raloxifene, on OB activity were determined by examining the expression of key osteoblast markers, OB proliferation activity, ALP activity, and mineral deposition levels. Next, the reciprocal effects of E2 and Pyk2 signaling cascades in OBs were investigated using Western blot analysis. Finally, we examined the effect of the Pyk2 and Pyk2-S isoforms on the proliferation, ALP activity, and mineralizing activity of MC3T3-E1, a preosteoblastic cell line.

3.2 Results

3.2.1 Estrogen increases the proliferation of Pyk2-KO and WT OBs.

First, we determined the culture conditions for our *in vitro* OB studies. Standard culture media is supplemented with 10% FBS and contains phenol red as a pH indicator, both of which have estrogenic effects (Berthois et al. 1986; Ganguly et al. 2008). Therefore, we compared the effects of α-MEM and phenol red free α-MEM media containing either 10% or 2% FBS on WT and Pyk2-KO OBs. Cells were plated at the same cell density and the total number of viable cells (excluding Trypan blue) were counted after 4 days (Figure 13). When cultured in α-MEM or phenol red free α-MEM with 10% FBS, no difference was found between the number of Pyk2-KO OBs and WT OBs. However, when cells were cultured in 2% FBS in either α-MEM or phenol red free α-MEM, Pyk2-KO OB numbers were significantly higher than WT OB numbers. These findings indicate that type of media does not affect OB number, but the concentration of serum is important for distinguishing differences between Pyk2-KO and WT OBs. There was

a significant interaction between genotype and serum concentration (p=0.04). Furthermore, these findings suggest that WT OBs seem to be more sensitive to reduced serum than Pyk2-KO OBs.

Based on these findings, we examined the effects of estrogen on WT and Pyk2-KO cell number. WT and Pyk2-KO calvarial OBs were cultured in phenol red free α-MEM with 2% FBS in the presence or absence of 100 nM E2 for 1 or 4 days and then counted. E2 at 100 nM was used which was based on published literature showing that human primary OBs, mouse MSCs, calvarial OBs and osteoblastic cell lines show a peak response to E2 at this concentration (Cheng et al. 2002; Taranta et al. 2002; Zhou et al. 2001). As expected, Pyk2-KO OBs showed significantly higher numbers than WT OBs on both days (p<0.05) (Figure 14A). After 4 days of E2 supplementation, a significant increase in the number of WT OBs was observed, compared to untreated WT OBs (p<0.05). In contrast, E2 had no effect on the number of Pyk2-KO OBs.

We also examined the effect of short-term E2 on OB proliferation using an MTS cell proliferation activity assay. An equal number of WT and Pyk2-KO OBs were cultured in the presence or absence of 100 nM E2 for 12 hours prior to MTS assay. As shown in Figure 14B, Pyk2-KO OBs had a significantly higher level of proliferation activity compared to WT OBs (p<0.05), indicating that OB proliferation was increased in the absence of Pyk2. However, WT or Pyk2-KO OBs cultured with E2 showed no significant increases in proliferation activity.

To further examine proliferation, we examined the expression level of c-fos, which is a transcription factor highly expressed during cell proliferation (Figure 15A). WT and Pyk2-KO OBs were cultured for 4 days in the presence or absence of E2. QPCR analysis revealed significantly higher c-fos mRNA levels in Pyk2-KO OBs, compared to WT OBs (2.5 fold, p=0.01). However, E2 supplementation of either Pyk2-KO or WT OBs did not lead to a statistical significant change in c-fos mRNA. Together with Figure 13, these findings suggest that Pyk2-deletion increases OB proliferation and that E2 does not significantly alter the proliferation of Pyk2-KO OBs.

3.2.2 Estrogen treatment of Pyk2-KO OBs increases ALP activity and mineralization.

To examine the effect of Pyk2-deletion and E2 on OB differentiation, WT and Pyk2-KO calvarial OBs were cultured under osteogenic conditions containing 50 μM ascorbic acid and 5 mM β-GP in the presence or absence of 100 nM E2 for 4 and 28 days. Several genes involved in matrix formation and maturation, and mineralization of OB, including ALP, collagen type 1, and OCN were examined using QPCR. In addition, quantitative ALP activity and Alizarin Red S staining, which stains bound calcium on the collagen matrix were determined.

After 4 days of treatment, Pyk2-KO OBs exhibited significantly higher collagen type 1 mRNA expression than WTs (1.9 fold, p=0.03) (Figure 15B). Notably, E2 supplementation significantly increased collagen type 1 mRNA expression in Pyk2-KO (p=0.04), but not WT OBs. However, ALP and OCN mRNA expressions in Pyk2-KO were not significantly different from WT OBs (Figure 15C and 15D). Moreover, E2 had no effect on the expression of ALP or OCN mRNA in 4-day E2-treated WT or Pyk2-KO OBs.

Next, we examined whether mature OBs cultured for 28 days in the absence or presence of E2 showed differences in ALP or OCN expression. Similar to our findings after 4 days, ALP mRNA levels in 28-day cultures were not significantly different between WT and Pyk2-KO OBs. Further, E2 treatment for 28 days had no effect on ALP expression in either WT or Pyk2-KO OBs (Figure 15E). In contrast, Pyk2-KO OBs showed increased expression of OCN mRNA more than WT OBs, (8.75 fold, p=0.007), although E2 supplementation did not increase OCN mRNA levels in either genotype (Figure 15F).

Since Pyk2-deletion and E2 did not appear to affect ALP mRNA expression, we next examined if ALP enzymatic activity was altered in these OBs. WT and Pyk2-KO OBs were cultured in osteogenic media with or without E2 supplementation for 4, 14, 21 or 28 days, and ALP activity was assayed using a quantitative biochemical assay and normalized for total protein as a measure of cell number (Section 2.1.16). Although ALP activity was not significantly changed in either WT or Pyk2-KO OBs cultured for 4 and 14 days (Figures 16A and 16B),

a robust increase in ALP activity was seen in Pyk2-KO OBs cultured for 21 days (12.1±1.52 nM/mL/μg) and 28 days (13.8±1.7 nM/mL/μg) compared to WT OBs (5.4±0.31 and 6.8±0.7 nM/mL/μg, respectively) (p<0.05). Furthermore, ALP activity in Pyk2-KO OBs was additionally increased when cells were cultured in the presence of E2 for 21 (1.5 fold, p=0.009) and 28 days (2 fold, p=0.005). WT OBs did not show an increase in ALP activity at any of the time points tested in the presence of E2. Our results suggest that Pyk2 deletion and E2 affect ALP activity but not ALP mRNA expression in mature differentiated OBs.

Similarly, calcium deposition, which is one of the markers of mature OB activity, was evaluated by culturing WT and Pyk2-KO OBs with ascorbic acid and β-glycerolphosphate in 2% FBS with phenol red free α-MEM. In the presence or absence of E2 supplementation for 14, 21 or 28 days, and quantitative Alizarin Red S staining was assayed (section 2.1.17). We found that calcium deposition levels in Pyk2-KO OBs were markedly higher than WT OBs at every time point tested (p <0.05, Figure 17). In addition, calcium deposition levels in Pyk2-KO OBs were significantly increased when cells were supplemented E2 for 14, 21, and 28 days (1.35 fold, 1.37 fold, and 1.62 fold, respectively, p<0.05). WT OBs did not show an increase in mineralization in the presence E2 at any of the time points tested. This suggests that calcium deposition levels in OBs were affected by Pyk2 deletion and E2 supplementation.

3.2.3 Raloxifene increases ALP activity and mineral deposition in Pyk2-KO OBs.

Raloxifene is an FDA-approved SERM for the treatment of post-menopausal osteoporosis. We examined if raloxifene affects the activity of WT and Pyk2-KO OBs, in a similar manner to E2. We cultured WT and Pyk2-KO OBs in osteogenic media with or without raloxifene (0.1, 1 and 10 nM) for 28 days. The time of treatment was based on the most robust effects observed for E2. The raloxifene concentration used was determined based on the literature (Lin et al. 2004; Matsumori et al. 2009) and our pilot studies (data not shown). After 28 days, we performed quantitative ALP activity and calcium deposition (mineralization) assays. As shown in Figure 18A, Pyk2-KO OBs exhibited significantly higher ALP

activity than WT OBs in the absence or presence of raloxifene (p<0.05). Notably, 1 nM and 10 nM raloxifene further increased ALP activity only in Pyk2-KO OBs (1.4 fold and 1.7 fold, respectively) (p<0.05); ALP activity in WT OBs was not changed by raloxifene, similar to our findings with E2. Interestingly, raloxifene (0.1, 1 and 10 nM) enhanced calcium deposition in Pyk2-KO OBs (p<0.05) compared to vehicle controls. Although raloxifene increased mineral deposition by WT OBs, this was not observed with the lowest concentration of raloxifene (0.1 nM) (Figure 18B). Moreover, the overall percentage increase in calcium deposition by raloxifene was greater in Pyk2-KO OBs than WT OBs (116% vs 44%, respectively, at 1 nM, p<0.05). Together, these findings suggest that both E2 and raloxifene exert a significant osteogenic effect on Pyk2 OBs. In contrast, E2 has no effect on and raloxifene exerts only a minimal effect on calcium deposition in WT OBs.

3.2.4 Pyk2-deletion regulates ERα protein levels.

To begin to determine the mechanism of action of Pyk2 in the estrogen signaling cascade, we first determined if Pyk2 regulates the expression of the estrogen receptors, ERα and ERβ, in early and mature OBs. WT and Pyk2-KO calvarial OBs were grown under osteogenic conditions in the presence or absence of 100 nM E2 for 4 and 28 days. QPCR analysis revealed that ERα and ERβ mRNA expression was similar in Pyk2-KO OBs and WT OBs, and that ERα or ERβ mRNA expression was unchanged in cells treated with E2 for 4 or 28 days (Figure 19A-19D).

Next, we examined if Pyk2-deletion affects ERα and ERβ protein levels. Total cell lysates were resolved by SDS-PAGE and Western blotting was performed using antibodies specific to ERα or ERβ (section 2.1.3). Protein loading in all wells was confirmed by blotting with antibody to β-actin. ERα and ERβ protein levels, normalized to β-actin, were quantified by densitometry using ImageJ software. Of interest, we found a decrease in ERα protein levels in Pyk2-KO OBs when compared to WT OBs after 4 and 28 days of culture (Figure 20A and 20C). In contrast, we found that ERβ protein levels in Pyk2-KO OBs were not different from WT OBs (Figure 20B and 20D). Moreover, the addition of E2 for 4 or 28 days had no further effect on ERα or ERβ protein levels in either Pyk2-KO or WT OBs.

Together, these findings suggested that Pyk2 regulates the expression ERα in early (day 4) and late (day 28) stages of OB differentiation, whereas E2 stimulation has no effect on ERα or ERβ in either WT or Pyk2-KO. In addition, the data suggest that Pyk2 may regulate OB activity in part by regulating ERα protein levels.

3.2.5 Pyk2-KO OBs promote ERα protein degradation through the ubiquitin-proteasome pathway.

Several studies suggest that ERα can undergo proteasome-mediated degradation (Chai et al., 2015; Zhou and Slingerland, 2014;(Levi-Montalcini et al. 1996; Petrel and Brueggemeier 2003). Therefore, the decreased ERα in Pyk2-KO OBs could potentially be due to degradation of ERα. To demonstrate this, we examined the effect of the proteasome inhibitor, MG-132, on the distribution of ERα protein levels in cytosol and the plasma membrane. WT and Pyk2-KO OBs were cultured for 4 days and then treated with or without MG-132 (20 μM) for the final 3 hours of culture. Cells were lysed with mRIPA lysis buffer and pelleted by centrifugation. The soluble fraction, which contains the cytosolic proteins, was separated from the insoluble pellet fraction that contains proteins associated with the plasma membrane, nucleus, and cytoskeleton (pellet fraction). We found that ERα (after normalization with β-actin control) in WT OBs was more abundant in the pellet fraction than in the soluble fraction. However, in Pyk2-KO OBs, ERα was more abundant in the soluble fraction when compared to the pellet fraction. Consistent with section 3.2.4, we found that Pyk2-KO OBs exhibited a decrease in ERα protein when compared to WT OBs, and this occurred in the pellet fraction (Figure 21). In WT OBs, MG-132 surprisingly enhanced ERα protein degradation in both fractions. This may suggest that MG-132 stabilizes an unknown protein which can promote the degradation of ERα in WT OBs under certain cellular condition. Conversely, we found that OBs may be regulated by E2 via a non-genomic pathway through translocation of ERα protein to the cytosol (Levi-Montalcini et al. 1996; Petrel and Brueggemeier 2003). Therefore, the decreased ERα in Pyk2-KO after MG-132 showed an increase in ERα protein in soluble fraction compared to non-treated Pyk2-KO OBs. Our findings suggest that MG-

132 prevents ubiquitin-proteasome mediated ERα protein degradation in Pyk2-KO OBs, leading to an accumulation of ERα in the cytosol.

3.2.6 An ERβ agonist promotes mineralization in Pyk2-KO OBs.

As we found a decrease in ERα protein in Pyk2-KO OBs, we examined whether decreasing ERα protein expression was related to changes in OB activity. WT and Pyk2-KO calvarial OBs were cultured under osteogenic conditions for 21 days. In addition, an ERα-specific agonist (propyl-pyrazoletriol (PPT)) at the concentrations of 0.04, 0.1, and 0.4 μM was added for the whole time of culture. The time of treatment was based on our previous experiments and PPT concentration was determined based on the literature (Galea et al. 2013; Somjen et al. 2011). Quantitative Alizarin Red S staining was then performed as described in section 2.1.17. We found that PPT had no effect on the mineralization or either WT or Pyk2-KO OBs, although in Pyk2-KO OBs there was a trend towards increasing mineralization at 0.1 μM PPT (Figure 22A). This finding was not unexpected given that WT OBs did not show an increase in mineralization with E2, and Pyk2-KO have reduced levels of ERα and potentially do not respond efficiently to PPT. Alternatively, it is possible, we did not achieve the optimal PPT concentration to observe a statistically significant increase in mineralization, as we observed with raloxifene (Figure 18).

Pyk2-deletion did not result in a change in ERβ protein levels, suggesting that ERβ was likely to be active in Pyk2-KO OBs. We used an ERβ-specific agonist (diarylpropionitrile (DPN)) to examine if WT and Pyk2-KO OBs were cultured with 0.1 μM and 0.4 μM DPN for 21 days. WT OB treated with DPN showed no change in mineralization, whereas DPN (0.4 μM) increased mineralization in Pyk2-KO OBs (Figure 22B). This finding suggests that ERβ signaling could potentially contribute to the increase in ALP activity and mineralizing activity observed in Pyk2-KO OBs.

3.2.7 Pyk2-deletion and E2 activate the ERK pathway.

OB proliferation and differentiation are controlled by signaling pathways such as mitogen-activated protein kinases/extracellular signal-regulated kinases (MAPKs/ERKs) (Ge et al. 2012; Lai et al. 2001) and protein kinase B (AKT) (Ayala-Pena et al. 2013; Burr and Allen 2013; Ge et al. 2012; Lai et al. 2001; Mandal et

al. 2016). ERK1 (44 KDa) and ERK2 (42 KDa) are expressed in OBs and have relevant functions in bone metabolism. ERK activation was reported to increase ALP activity (Jaiswal et al. 2000), OCN mRNA levels and mineralization during OB differentiation (Ge et al. 2007; Matsushita et al. 2009). The activation of AKT is also associated with cell growth, proliferation and survival. AKT in concert with BMP-2 can mediate OB differentiation from MSCs (Ghosh-Choudhury et al. 2002). It was also found that the OBs with disrupted AKT1, a major AKT in OBs and OCs, showed increased susceptibility to apoptosis and decreased the expression of Runx2, an early OB differentiation regulator (Kawamura et al. 2007). In addition, E2 binding to ER promotes the rapid interaction of ER with the SRC kinase leading to ERK and AKT activation (Marino et al. 2006).

Our results indicate that Pyk2-KO OBs have significant increases in proliferative activity, matrix maturation and mineralization, which were further increased with E2 or raloxifene. Therefore, we investigated if Pyk2-deletion and/or stimulation with E2 affected downstream signaling of ERK or AKT. WT and Pyk2-KO calvarial OBs were cultured alone or in the presence of 100 nM E2 for 4 days. Cell pellets were lysed with mRIPA lysis buffer. Proteins were resolved by SDS-PAGE, then blotted with anti-phospho-ERK (p-ERK) and anti-phospho-AKT (p-AKT) antibodies and subsequently re-blotted with ERK and AKT antibodies, respectively.

As shown in Figure 23A, Pyk2-KO OBs enhanced ERK phosphorylation when compared to WT OBs. Moreover, E2 further increased ERK phosphorylation in Pyk2-KO and WT OBs, suggesting an additive effect of E2 in both genotypes. However, total ERK phosphorylation in E2-treated Pyk2-KO OBs was still higher than in E2-treated WT OBs. A non-specific band approximating the molecular weight of p38 and p-p38 was also detected as indicated. These findings suggest that Pyk2-deletion combined with E2, activates the ERK pathway to promote OB activity. We did not detect a difference in AKT phosphorylation or total AKT between WT and Pyk2-KO OBs, either with or without E2 treatment (Figure 23B).

Since we found increases in ERK phosphorylation in Pyk2-KO OBs, we further investigated if Pyk2-deletion and/or E2 stimulation affected ERK signaling

in mature OBs, after 21 days of culture. We cultured WT and Pyk2-KO calvarial OBs in the presence or absence of 100 nM E2 for 21 days, and then performed Western blot analysis as described above. Our results revealed no differences in ERK phosphorylation or total ERK protein levels between WT and Pyk2-KO OBs (Figure 24). E2 stimulation also had no effect on ERK phosphorylation or total ERK after 21 days of treatment. These results suggest that Pyk2-deletion and E2 increase the mitogenic activity of early OB through ERK, whereas ERK activation does not appear to be required for mature OBs function. Whether other signaling pathways may be involved requires further investigation.

3.2.8 Pyk2 and Pyk2-S inhibit ALP and mineralization.

We previously identified two isoforms of Pyk2, which represent full length Pyk2 and the shorter mRNA splice variant, Pyk2-S; Pyk2-S lacks a 42-amino acid insert compared to Pyk2 (Figure 25A). Furthermore, differences in the ratio of Pyk2 and Pyk2-S expression were observed during OB differentiation (Figure 7B and 25B) (Kacena et al. 2012). This suggests that Pyk2/Pyk2-S may have different roles in OB activity. To examine the roles of Pyk2 or Pyk2-S in OB activity we chose to transiently express each isoform in pre-osteoblastic cell line, MC3T3-E1, since primary OBs are difficult to transfect. We had previously determined and confirmed herein (Figure 25B) that MC3T3-E1 cells do not express Pyk2/Pyk2-S, making them a suitable Pyk2-deficient cell model. MC3T3-E1 cells were transiently transfected with cDNA expression constructs for Pyk2, Pyk2-S or a vector cDNA control (Figure 26A) and were incubated for 24 hours. Consistent with our finding that primary Pyk2-KO OBs exhibit increased proliferation (Figure 14B), expression of Pyk2 or Pyk2-S decreased the proliferation of MC3T3-E1 cells to a similar extent, compared to the vector control. (Figure 26B).

We next examined if Pyk2 or Pyk2-S affect ALP activity and mineral deposition of MC3T3-E1 cells. Expression of either Pyk2 or Pyk2-S decreased ALP activity to a similar extent (Figure 26C). We also examined the effect of Pyk2 versus Pyk2-S on mineral deposition in MC3T3-E1 cells. We found that Pyk2 and Pyk2-S expressing cells decreased to a similar extent mineral deposition after 3 days, compared control MC3T3-E1 cells (Figure 26D). Our findings suggest that

Pyk2 and Pyk2-S appear to have redundant activities in OBs since both decrease OB activity in pre-OB MC3T3-E1 cells, differentiated for 3 days. However, given that the ratio of Pyk2 to Pyk2-S varies during OB differentiation, it is likely that the actions of Pyk2 and Pyk2-S are temporally separated and/or that they play distinct roles in other unidentified signaling effects in OB.

3.2.9 Estrogen regulates Pyk2 and Pyk2-S protein expression and phosphorylation.

The use of transiently transfected MC3T3-E1 cells precluded our ability to examine long-term effects of E2 of Pyk2 and Pyk2-S. Therefore, as an alternative approach, we compared undifferentiated OBs (predominately express Pyk2) and calvarial OBs differentiated for 14 days (predominately express Pyk2-S). Pyk2 Y402 phosphorylation is critical for Pyk2 activity and downstream signaling (Eleniste et al. 2012) as discussed in Section 1.1.8. Therefore, we examined if E2 altered the Y402 phosphorylation of Pyk2 or Pyk2-S in undifferentiated and mature primary OBs, respectively. WT calvarial OBs were grown without (day 0) or with osteogenic media for 14 days and stimulated with 100 nM E2 or vehicle (ethanol) for the 6 hours prior to harvesting. As expected, we observed a shift in the molecular weight of Pyk2 from full length (118 KDa) on day 0 to the shorter Pyk2-S isoform (106 KDa) after 14 days of culture (Figure 27), which is consistent with our previous publication (Kacena et al. 2012) and Figure 7B. In undifferentiated OBs, which primarily express full-length Pyk2, E2 treatment for 6 hours had no effect on Pyk2 Y402 phosphorylation. Similarly, differentiated OB which primarily express Pyk2-S showed no change in Y402 phosphorylation after 6 hours of E2 treatment.

Next, we examined whether longer E2 treatment times might alter Pyk2 or Pyk2-S phosphorylation. We cultured WT calvarial OBs alone or in the presence of 100 nM E2 for 4 or 28 days. We confirmed that after 4 and 28 day cultures, OBs predominately express Pyk2 and Pyk2-S, respectively (Figure 28A and 28B). After 4 days treatment with E2, the ratio of pY402/Pyk2 was decreased when compared to non-treated OBs and the total level of Pyk2 (relative to actin) was increased (Figure 28A). The converse was seen in day 28 cultures. That is, E2 treatment for

28 days led to an increase in the ratio of pY402/total Pyk2-S which was correlated with a decrease in Pyk2-S levels (relative to actin) (Figure 28B). Together, our findings suggest that in early and mature OBs, E2 has differential effects on Pyk2 and Pyk2-S protein levels, respectively, as well as on the Y402 phosphorylation of these isoforms.

3.3 Discussion

Osteoblastic bone formation is essential for bone remodeling as well as fracture repair. Our studies and others have shown that Pyk2-KO mice have higher bone mass compared to WT mice and that OBs from these mice show increased bone formation activity (Buckbinder et al. 2007; Gil-Henn et al. 2007). In this study, we focused on the role of Pyk2 and estrogen on OB activity. We found that Pyk2-KO OBs exhibited higher proliferation and differentiation than WT OBs as determined by an increase in proliferation, cell number and c-fos mRNA levels in Pyk2-KO OBs compared to WT OBs in low serum conditions. These results are different from our previously publication (Cheng et al. 2013), in which it was reported that Pyk2-KO OB proliferation was not different between Pyk2-KO and WT OBs. The reason for this discrepancy was found to be the percentage of serum present during the cultures; 10% FBS versus 2% FBS. In the current study, we found a decrease in total cell number for both WT and Pyk2-KO OBs in 2% FBS, compared to 10% FBS. Nevertheless, Pyk2-KO OBs showed higher proliferation compared to WT OBs. These findings suggest that WT OB proliferation is more affected by reduced serum levels than Pyk2-KO OBs.

During the early stage of differentiation, collagen type I mRNA expression levels, an early indicator of OB differentiation, was higher in Pyk2-KO OBs than WT OBs. At later stages of the OB differentiation process, Pyk2-KO OBs exhibited higher OCN mRNA expression, which is a marker of mature OBs. In addition, ALP activity and calcium deposition in Pyk2-KO OBs were greater than WT OBs. These findings reproduced our previously published studies (Cheng et al. 2013; Eleniste et al. 2015) which were performed in 10% FBS, confirming that our current findings

were not simply the result of reduced serum levels. Generally, matrix formation precedes mineralization in OBs (Anderson et al. 2005; Nudelman et al. 2010; Stein et al. 2004). Interestingly, in Pyk2-KO OBs we found that the matrix formation, maturation and mineralization phases appeared to be overlapping. Specifically, we found an increase in ALP activity in Pyk2-KO OBs when cultured for 21 and 28 days compared to WT OBs. However, the calcium deposition levels in Pyk2-KO OBs were markedly higher than WT OBs started from day 14 to day 28. These findings suggest that the matrix formation and mineralization phases may be maintained for longer periods in Pyk2-KO OBs than in WT OBs. Overall, our results confirm that Pyk2 is a negative regulator of OB activity, which is consistent with our previous data as well as other published studies (Buckbinder et al. 2007; Cheng et al. 2013; Eleniste et al. 2015; Kacena et al. 2012).

We examined the role of Pyk2 and estrogen in OB proliferation and differentiation, and found that E2 had no effect on OB proliferation on day 1 of treatment, either in WT or Pyk2-KO OBs. However, we demonstrated that 4 days of E2 supplementation significantly increased the number of WT OBs, but did not show a corresponding increase in proliferation assessed using the MTS assay. The explanation for the different results may be from the duration of E2 supplementation. In the cell counting experiment, OBs were treated with E2 for 1 and 4 days, while for the MTS assay, cells were cultured in E2 for only 12 hours. Although E2 did not affect Pyk2-KO OBs number, E2-treated Pyk2-KO OBs still exhibited higher cell number than E2-treated WT OBs due to the high basal OB number compared to WT OBs, which was likely due to the decreased sensitivity of Pyk2-KO OBs to low serum. Thus, our data indicates that E2 maintained WT OBs in a proliferative state, most likely in the G1 phase of the cell cycle (Bonnelye et al. 2001; Wakeling et al. 1991), whereas Pyk2-KO OBs likely enter the differentiation phase at a faster rate than WT cells. The increase in the ratio of mineralizing to proliferating Pyk2-KO OBs, compared to WT OBs may also explain the increase in ALP activity and mineralization in E2-treated Pyk2-KO OBs compared to E2-treated WT OBs (Figure 16 and 17). In support of this, in differentiated Pyk2-KO OBs but not in WT OBs, we found that E2 augmented collagen type I mRNA

expression levels, and collagen is known to be necessary for mineralization. Moreover, we observed an additive effect of Pyk2-deletion and E2 on ALP activity and calcium deposition levels. Interestingly, there was a strong trend for decreased ALP mRNA expression with 28 days of E2 treatment in both WT and Pyk2-KO OBs. This suggests that long term E2 treatment may accelerate OBs enter to mineralization phase faster than non-treated group. These findings suggest that differentiated Pyk2-KO OBs are influenced by E2 to a greater extent than WT OBs, resulting in increased osteogenesis. This finding may also in part explain our unpublished in vivo data in which we observed a greater increase in trabecular BV/TV in E2-supplemented OVX Pyk2-KO mice than in E2-treated OVX WT mice (Figure 9).

We investigated the mechanism of action of Pyk2 in the estrogen-signaling cascade and found that ERα protein levels were reduced in Pyk2-KO OBs, compared to WT OBs, whereas ERβ protein levels were similar for the two genotypes. Our studies suggested that the decrease in ERα in Pyk2-KO OBs was likely to be the result of ubiquitin-proteasome mediated degradation of ERα in the cytosol compartment, although other mechanisms for protein degradation (such as lysosomal) cannot yet be ruled out. However, the percentage of ERα in cytosolic compartment versus membrane/nucleus compartments were not so skewed that significant genomic regulation could still occur. In addition, it is known that regulation by ERs in OBs occurs through translocation from cytosol to nucleus in response to certain stimuli such as strain. The evidencealso showed that estrdiol had little effect upon β-catenin location in the cell (Armstrong et al. 2007). Furthermore, it is known that ERα mRNA is highly expressed during matrix maturation and then decreases during mineralization, while ERβ mRNA levels remain relatively constant throughout differentiation (Bord et al. 2003; Onoe et al. 1997; Wiren et al. 2002). Therefore, the increased degradation of ERα in Pyk2-KO OBs may also reflect the increased differentiation state of these cells, compared to WT OBs. Unexpectedly, MG-132 treatment enhanced ERα protein degradation in WT OBs, and although the mechanism is still unclear, the evidence has shown that ER degradation depends on ubiquitin-activating E1 enzyme (UBA) and

ubiquitin-conjugating E2 enzymes (UBCs), as well as other co-activators/repressors and MG132 may also block their protein degradation *in vitro* (Ismail and Nawaz 2005; Nawaz et al. 1999).

Our studies demonstrated decreased ERα levels in Pyk2-KO OBs, suggesting that the *in vitro* phenotype may be related to the reduction in ERα. It has been reported that ERα-KO calvarial OBs exhibit normal mineralization when compared to WT OBs (McCauley et al. 2003). On the contrary, Almeida et al. showed that OBs from mice with Prx-targeted or osterix-targeted deletion of ERα showed significantly decreased differentiation when compared to controls (Almeida et al. 2013). This effect may be from the reduced ability of MSC to enter the OB lineage. Unexpectedly, it has been shown that 17β-estradiol can stimulate osteogenic differentiation of bone marrow cells derived from ERα-KO mice, which was demonstrated by an increase in collagen type I synthesis, ALP activity, and mineralization. Interestingly, the increased ALP activity in 17β-estradiol -treated ERα-KO OBs was even higher than 17β-estradiol -treated WT OBs (Parikka et al. 2005), similar to our findings in 17β-estradiol-treated Pyk2-KO OBs (Figure 16). In another study, it was reported that 17β-estradiol treatment significantly enhanced ALP activity and collagen type I mRNA expression in MG-63 osteosarcoma cells with reduced levels of ERα, but not ERβ (Cao et al. 2003). These findings suggest that the additive effect of 17β-estradiol on ALP and mineralization in our Pyk2-KO OBs, compared to WT OBs, may be mechanistically linked with the decrease in ERα in Pyk2-KO OBs. However, our studies do not rule out the possibility that E2 signaling via ERβ may also contribute to the increase in mineralization of Pyk2-KO OBs. Indeed, we found that DPN, which is an ERβ agonist increased the mineralization of Pyk2-KO OBs (Figure 22B), suggesting that the ERβ signaling pathway can be activated in these cells.

Together, our findings suggest that Pyk2 may regulate OB activity in part by modulating ERα and/or ERβ signaling. It is also possible that Pyk2-KO OBs respond to E2 by mechanisms other than ERα and/or ERβ, such as through the N-terminal truncated ERα isoform, or the orphan nuclear ER–related receptor α (ERRα) which was reported to affect bone formation and is differentially expressed

relative to ERα and ERβ in OBs (Bonnelye and Aubin 2002; Bonnelye et al. 2001; Parikka et al. 2005). In addition, Pyk2 may play a role in the regulation of male sex steroid hormone receptors, androgen receptor. In support of this, a recent study found that Pyk2 promoted the expression and phosphorylation of the androgen receptor (Hsiao et al. 2016). Further studies are needed to investigate the role of Pyk2 and these receptors in OB activity.

To examine if Pyk2-deletion potentially affects signaling cascades that are common to ERα and/or ERβ, we examined ERK and AKT phosphorylation, which are important of mitogenesis and anti-apoptotic activity, respectively. Although AKT levels were similar in WT and Pyk2-KO OBs, Pyk2-KO OBs exhibited enhanced ERK phosphorylation compared to WT OBs.

It is well-established that MAPKs are activated by phosphorylation of tyrosine/threonine residues in signal transduction cascades, which include ERK, leading to the activation of nuclear transcription factors such c-jun, which is highly expressed during early OB differentiation (Marie 2008). Consistent with this, ERK activation was also reported to increase ALP activity (Jaiswal et al. 2000), OCN mRNA and OB mineralization (Ge et al. 2007; Matsushita et al. 2009). Similarly, mice lacking ERK1/ERK2 exhibited substantially reduced bone mineralization when compared to WT mice (Matsushita et al. 2009). Given the increased proliferation and differentiation of Pyk2-KO OBs, we speculate that Pyk2-deletion leads to an increase in ERK phosphorylation, and subsequently leads to increases in collagen type I and OCN mRNA levels, ALP activity and mineralization. We also found that E2 had an additive effect on ERK phosphorylation in both WT and Pyk2-KO OBs. This finding is consistent with published evidence that 17β-estradiol supplementation enhances ERK phosphorylation via ERα in MC3T3-E1 cells, and leads to inhibition of OB apoptosis (Yang et al. 2013). Thus, estrogen stimulation augment ERK phosphorylation signaling in Pyk2-KO OBs, which already exhibit high basal ERK phosphorylation, resulting in an overall increase in OB differentiation and possibly survival as seen by the marked increase in matrix formation and mineralization in 17β-estradiol treated Pyk2-KO OBs. In addition, it will be interesting to see whether an increase in OB activity with Pyk2 deletion

involves other signaling pathways such as p38 pathway, which is part of the MAPK subfamily, similar to ERK and is involved in cell proliferation. Published evidence shows that the activation of p38 plays important roles in differentiation of calvarial OBs, bone marrow cells, and some OB cell lines (Hu et al. 2003; Rodriguez-Carballo et al. 2016; Wang et al. 2007).

Similar to our findings with E2, we found that raloxifene, which is an activator of ERα and ERβ, had a significant osteogenic effect on both WT and Pyk2-KO OBs. However, the osteogenic effect on Pyk2-KO OBs was markedly greater than on WT OBs. The mechanism of action of raloxifene on target tissue is not well understood, but it is believed that its actions are mediated by genomic and non-genomic pathways through ERα and ERβ (Jordan et al. 2001; Tee et al. 2004). It has been shown that raloxifene exerts its estrogenic effects on bone by decreasing the remodeling rate, reducing OC activity, and maintaining OB activity (Hegde et al. 2015). In addition to its antiresorptive activity, several studies suggest that raloxifene may act as an anabolic agent by increasing proliferation activity, and Runx2 and collagen type I mRNA expression in primary human OBs and this effect was found to be partly mediated via ERK1 and ERK2 activation (Noda-Seino et al. 2013; Taranta et al. 2002). This suggests that raloxifene may promote Pyk2-KO OB activity via a similar mechanism as E2.

The Pyk2 and Pyk2-S isoforms were previously identified (Kacena et al. 2012) and shown to be differentially expressed during OB differentiation, with Pyk2 levels decreasing during differentiation while Pyk2-S levels progressively increase (Figure 25B). This suggests that Pyk2 and Pyk2-S isoforms potentially exert unique roles in OB activity. Contrary to our expectations, we found that Pyk2 and Pyk2-S exert similar effects in MC3T3-E1 cells, and reduce OB proliferation, ALP activity, and mineralization levels to the same extent (Figure 26). These results indicate that both Pyk2 and Pyk2-S are negative regulators of OB activity, which is consistent with our results that Pyk2-KO OBs have enhanced activity. However, it is possible that Pyk2 and Pyk2-S may affect OBs at different stage of differentiation due to their differential expression; Pyk2 may inhibit OB activity in

the early stage of OB differentiation, while Pyk2-S may affect later stages of OB differentiation or be active in mature OBs.

The phosphorylation of residue Y402 in Pyk2, and presumably Pyk2-S, is critical for its tyrosine kinase activity and the recruitment of other signaling proteins, such as c-Src (Eleniste et al. 2012; Kimble et al. 1996). Therefore, we examined if E2 affects the phosphorylation of Pyk2 or Pyk2-S in early or mature OBs, respectively. In OBs treated with E2 for 4 days, which primarily express full-length Pyk2, E2 led to a small decrease in the ratio of phosphorylated Y402 to total Pyk2, as well as a significant increase in total Pyk2 levels (Figure 28A). Conversely, in OBs cultured for 28 days, which primarily express Pyk2-S, E2 significantly increased the ratio of phosphorylated Y402 to total Pyk2-S, and decreased total Pyk2-S levels (Figure 28B). Thus, we speculate that E2 likely increases downstream signaling in early OBs via Pyk2 through proteins other than Y402-mediated recruitment of Src. In contrast, E2 is likely to promote the recruitment of Src to Pyk2-S in mature OBs. Currently, only one published study has reported an increase in Pyk2 protein levels in MCF-7 cells, a human breast cancer cell line, when stimulating with E2 for 30 minutes at the concentration of 0.4, 40, and 400 nM. Although the mechanism of regulation of Pyk2 or Pyk2-S protein levels is unknown, one possibility is through the regulation of microRNA species. miRNAs are a class of short, non-protein coding RNAs that serve to post-transcriptionally regulate gene expression through either translational repression or mRNA degradation. In addition, miRNAs also play important roles in cell proliferation, differentiation, apoptosis, and tumorigenesis (Cai et al. 2009; Loftus et al. 2012; Maillot et al. 2009). It was reported that a set of miRNAs, which include miR-23b, are down regulated by E2 in a number of human breast cancer cell lines (Maillot et al. 2009). In addition, it was shown that decreased miR-23b expression in glioma cells enhanced Pyk2 expression, which was correlated with an increase in glioma cell migration *in vitro* (Loftus et al. 2012). Therefore, it is possible that E2 stimulation of early OBs may increase miR-23b which leads to the increase in Pyk2. In contrast in mature OBs, perhaps miR-23b levels are upregulated, leading

to a decrease in Pyk2-S. Whether miR-23b levels are temporally altered during OB differentiation and by E2 remains to be determined.

3.4 Summary and conclusions

We examined the effect of E2 on Pyk2-KO OBs.. We found a decrease in ERα protein levels in Pyk2-KO OBs compared to WT OBs which was due to ERα degradation in the cytosol through the ubiquitin proteasome pathway. In contrast, ERβ protein levels in Pyk2-KO OBs were similar to WT OBs. For OB activity, our results indicated that during early differentiation (4 days) Pyk2-KO OBs exhibit significant increases in c-fos and collagen type I mRNA expression levels, and up-regulated basal ERK phosphorylation compared to WT OBs. Moreover, we found an additive effect of estrogen on collagen type I mRNA in Pyk2-KO OBs, and on ERK phosphorylation in both WT and Pyk2-KO OBs. Mature Pyk2-KO OBs (14-28 days) also showed higher OCN mRNA levels, ALP activity, and calcium deposition levels compared to WT OBs. Estrogen stimulation led to a further increase in both ALP activity and calcium deposition in Pyk2-KO OBs, but not in WT OBs. Likewise, raloxifene supplementation markedly enhanced ALP activity and calcium deposition levels in Pyk2-KO OBs, whereas a minimal effect on mineral deposition was observed in WT OBs. Although both Pyk2 and PyK2-S isoforms were found to negatively regulate OB activity, we found that the Y402 phosphorylation of Pyk2 or Pyk2-S, which is necessary for tyrosine kinase activation, is differentially regulated by E2 in early and mature OBs, respectively, suggesting that functional differences between these isoforms in OBs may exist. Whether the actions of Pyk2 or Pyk2-S in early or mature OBs, respectively, are interchangeable, or whether our observed differences reflect the different stages of the OB differentiation process is currently unknown.

In conclusion, our results indicate that Pyk2 (and Pyk2-S) is a negative regulator of OBs. Furthermore, Pyk2 stabilizes ERα protein levels by preventing its proteasome-mediated degradation. Pyk2-deletion and E2 have an additive stimulatory effect on ERK signaling suggesting that Pyk2 is integrated into the E2-

ERα/ERβ signaling cascade via ERK, which leads to inhibition of OB differentiation and mineralization. Thus, we speculate that Pyk2-deletion promotes bone formation and potentiates the effects of estrogen (and raloxifene) on OB matrix formation and mineralization, resulting in an increase in bone mass. Figure 29 describes our current working model for the action of Pyk2 and E2 signaling in OBs.

CHAPTER 4

DEVELOPMENT OF PYK2-INHIBITOR LOADED HYDROGEL

4.1 Introduction

Bone can regenerate in response to injury or pathological diseases, as well as during the remodeling process that occurs throughout life. Bone regeneration is a well-orchestrated process of bone formation and bone resorption, involving a number of biological events in an effort to repair bone damage and eventually restore skeletal function. Bone can spontaneously repair in cases of minor bone damage. However, clinical intervention for large scale bone regeneration such as reconstructive surgery and bone transplantation are required in cases of extensive bone damage including large bony defects resulting from trauma, infection, tumor, and skeletal abnormalities, or cases of compromised bone regeneration such as avascular necrosis and in osteoporosis patients, which result in a decrease in bone quality (Dimitriou et al. 2011; Zomorodian and Baghaban Eslaminejad 2012). The current gold standard clinical therapy for the regeneration of large bone defects is the use of autologous grafts because they possess inherent osteoconductivity, osteoinductivity, and osteogenicity. However, there is a limited supply of grafts and grafts frequently associated with donor site morbidity. An alternative treatment incorporates the use of allogenic or xenogenic bone grafts, which exhibit no donor site morbidity and supply limitations. Even though advantageous, they still have drawbacks associated with increasing the risk of infection and disease transmission (Amini et al. 2012; Oryan et al. 2014).

Bone tissue engineering has been extensively investigated as an alternative therapy for bone grafting (Chu et al. 2007; Li et al. 2014; Romagnoli et al. 2013). In order to enhance bone healing, a tissue engineering technique using biomolecules or drugs incorporated into scaffolds have been investigated (Mourino and Boccaccini 2010; Romagnoli et al. 2013). Among these biomolecules, BMP-2 is a well-established enhancer used in bone regeneration for orthopedic and maxillofacial applications (Chu et al. 2007; de Oliveira et al. 2013; Mont et al. 2004; Romagnoli et al. 2013). Nevertheless, BMP-2 still has some clinical concerns that should not be overlooked which include: increasing risk of radicular pain, ectopic bone formation, osteolysis, and poor global outcomes. These suggest that a need

for alternative biomolecules for bone regeneration and bone tissue engineering remains (Fu et al. 2013; Mesfin et al. 2013; Rodgers et al. 2013; Simmonds et al. 2013).

Our studies and others suggest that Pyk2 deletion increases OB differentiation and enhances bone formation, resulting in a high bone mass phenotype in global Pyk2-KO mice (Buckbinder et al. 2007; Cheng et al. 2013; Gil-Henn et al. 2007; Kacena et al. 2012). Importantly, Buckbinder et al. reported that PF-431396 (PF-43), which is a dual FAK/Pyk2 inhibitor, increased bone mass and protected rats against OVX-induced bone loss (Buckbinder et al. 2007). In addition, PF- 461-8433 (PF-46), which is more specific to Pyk2, has been shown to enhance ALP activity and mineralization in human MSCs, but has not been investigated for *in vivo* studies (Han et al. 2009). These findings suggested that a Pyk2-inhibitor loaded scaffold may promote OB activity, and may therefore be useful for future studies to regenerate bone defects.

Bone healing and regeneration consist of several phases including inflammatory phase, soft callus formation phase, hard callus or endochondral ossification phase, and bone remodeling phase (Burr and Allen 2013; Marzona and Pavolini 2009; Oryan et al. 2015). Drug delivery systems for bone regeneration usually target osteoblastic bone formation, and the systems that increase the availability of proteins, growth factors, or drugs have been proven for safety and efficiency for bone regeneration such as rhBMP-2 and collagen sponge (Ratko et al. 2010). Nevertheless, the collagen sponges loaded with rhBMP-2 often exhibits an initial uncontrolled burst release of rhBMP-2, which can cause side effects to surrounding tissues such as osteolysis around the bone graft (Fu et al. 2013; Simmonds et al. 2013). Therefore, the need for a drug carrier system that allows for local sustained release of biomolecules is still required to achieve a therapeutic efficacy. Nowadays, hydrogels are widely used in biomedical applications including bone tissue engineering due to their biocompatibility, biodegradability, and ability to mimic ECM structures. In addition, the controlled release behavior ensures hydrogels may be good carrier materials for drug delivery systems (Park 2011; Shi et al. 2012; Tronci et al. 2014).

Poly (ethylene glycol) (PEG), a non-ionic hydrophilic synthetic polymer, has been extensively used for several decades for controlled drug delivery and cell delivery in tissue engineering applications due to the controllable material properties that enable hydrogels to be fabricated with the desired functions and properties (Lin and Anseth 2009; Lin et al. 2015). PEG-diacrylate (PEGDA), a PEG-based macromers with reactive termini, is highly used in hydrogel fabrication because of the simplicity of synthesis and its availability from commercial sources (Hao and Lin 2014). PEGDA hydrogels have also been used in bone regeneration as carriers of biomolecules such as BMP-2. It has been reported that PEGDA hydrogel tethered with BMP-2 promotes bone healing *in vivo* (Chen et al. 2011; Sonnet et al. 2013).

A semi-interpenetrating network (sIPN), which contains photocrosslinked PEG matrices and physically entrapped gelatin, has been developed as an effective drug delivery and tissue engineering scaffold (Fu et al. 2012). sIPN of PEG matrices improves protein resistance and mechanical stability. The mesh size of sIPN depends on the amount of PEG in the system, which may impact the transportation of biomolecules out from the sIPN. Incorporated gelatin in matrices enhances biological characteristics because gelatin contains cell-recognition motifs such as the RGD sequence, and gelatin can be cleaved by various proteases such as matrix metalloproteinase 2 (MMP-2) and MMP-9, which can improve the biodegradability of the system. Furthermore, drug molecules can be directly added into the polymer solution prior to polymerization, which can prevent drug overloading (Fu and Kao 2009; Santoro et al. 2014).

In the current study, we hypothesized that PEGDA-gelatin hydrogel would be an effective candidate carrier for Pyk2 inhibitors to increase osteoblastic activity in terms of material handling, release behavior, retained bioactivity of inhibitors, and hydrogel biodegradability. This chapter describes the development of a Pyk2-inhibitor loaded hydrogel suitable for promoting OB activity.

4.2 Results

4.2.1 A Pyk2-targeted inhibitor (PF-46) enhances matrix formation and mineralization of OBs.

First, we examined the effects of the Pyk2 inhibitors, PF-43 and PF-46, on the proliferation of OB precursors and on the activity of differentiated mature OBs. For these studies, we mostly used bone marrow derived MSC as these cells more closely replicate an *in vivo* bone healing environment in which a Pyk2-scaffold would potentially be used. In addition to the use of undifferentiated MSCs for proliferation studies, MSCs and calvarial OBs were cultured in osteogenic media for 7-21 days to induce OB differentiation, maturation and matrix deposition.

To examine the effect of PF-43 and PF-46 on OB precursor proliferation, mouse MSCs were plated overnight and then cultured in the presence or absence of 0.1 or 0.3 μM of each inhibitor for an additional 24 hours. A MTS assay was then performed to compare cell proliferation rates. As shown in Figure 30A, PF-43 (0.1 and 0.3 μM) and PF-46 (0.3 μM) significantly increased cell proliferation when compared to the untreated or control group ($p<0.05$). Moreover, 0.1 μM PF-46 exhibited the highest proliferation activity among the groups ($p<0.05$).

Bone marrow derived MSCs were then differentiated into mature OBs with 50 μM ascorbic acid and 5 mM β-GP in the presence or absence of PF-43 or PF-46. ALP activity assay and mineralizing activity were assayed at 7 and 21 days, respectively. Our results revealed that both PF-43 and PF-46 at 0.1 and 0.3 μM significantly increased the differentiation of OBs as assessed by increased ALP activity (Figure 30B). However, only PF-46 (0.1 and 0.3 μM) enhanced calcium deposition, a marker of mineralizing activity of OBs (Figure 30C).

We also examined the effect of PF-46 on the differentiation of calvarial OBs. Similar to MSCs, calvarial OBs treated with lower concentration of PF-46 for 21 days significantly promoted ALP activity (0.0125 and 0.05 μM) and mineral deposition levels (0.05 μM) in calvarial OBs when compared to control group ($p<0.05$) (Figure 31A and B).

These data suggest that PF-46, a Pyk2-targeted inhibitor, promotes ALP activity and mineralization to a greater extent than PF-43, the dual Pyk2/FAK inhibitor. Thus, we used PF-46 in all subsequent experiments. In addition, since a long-term goal of our studies is to identify a hydrogel suitable for *in vivo* bone regeneration applications, bone marrow derived MSCs were used to more closely approximate the bone microenvironment in which the scaffold will likely be used.

4.2.2 Characterization of PEGDA-gelatin hydrogels

4.2.2.1 P1000:G10 prepolymer solution reveals the highest viscosity and shear-thinning effect.

PEGDA and gelatin were chosen as the polymers for hydrogels since PEGDA properties can be tailored through the adjustment of molecular weight and PEGDA polymer concentration, which may influence the release behavior and degradation of hydrogels (Parlato et al. 2014). Gelatin incorporation has been shown to improve biodegradability and elasticity of the network (Burmania et al. 2003). We performed preliminary studies using PEGDA 400, 600, and 1000 Da with various w/v% of PEGDA and gelatin in prepolymer solutions and found that 25% PEGDA600 (P600), 25% PEGDA1000 (P1000), 25% PEGDA600 and 5% gelatin (P600:G5), and 25% PEGDA1000 and 10% gelatin (P1000:G10) showed the optimal consistency and did not form complete physical gels at room temperature for 5 minutes, which allowed us to have enough material working time. Thus, P600, P1000, P600:G5, and P1000:G10 prepolymer solutions were the candidate prepolymer solutions used in subsequent studies.

To measure the dynamic viscosity of the prepolymer solutions, all prepolymer solutions were prepared and examined for the controlled shear rate viscometry using a digital rheometer (viscometry mode) at room temperature. The viscometry was performed because we postulated that gelatin incorporated into PEGDA prepolymer solution could enhance the prepolymer solution viscosity, which would improve the handling of prepolymer solution. Our pilot results demonstrated that all groups exhibited a decrease in viscosity when shear rate was increased; this is the shear-thinning behavior. Furthermore, the addition of gelatin enhanced the shear-thinning effect in both P1000 and P600 prepolymer

solutions (Figure 32A). After prepolymer solutions reached Newtonian fluid behavior and exhibited a constant viscosity, P1000:G10 revealed the highest viscosity (44.8 mPa.s), followed by P600:G5 (39.1 mPa.s), P1000 (28.5 mPa.s) and lastly P600 (16.4 mPa.s).

Yield stress is the applied stress that needs to be exceeded in order to make materials flow. A material with this property is called a yield stress fluid, which is fully elastic when the stress value is below the yield stress, but it flows at stresses above yield stress (Moller et al. 2009). The presence of yield stress in the solution indicates that fluid will not be self-flowing. Regarding the plot of shear stress vs. shear rate or the flow curve (Figure 32B), incorporating gelatin in PEGDA prepolymer solutions allowed P1000:G10 solution to demonstrate a yield stress of about 16 Pa. This properly allows the gel to stay within the defect site when applied and not free-flowing before the prepolymer solution is polymerized by light curing.

4.2.2.2 Determination of hydrogel gelation times

The gelation times of P600, P1000, P600:G5, and P1000:G10 prepolymer solutions were determined using two methods; the probing technique and *in situ* photorheometry test. For the probing method, all prepolymer solutions were prepared and the disk-shaped gels (5x3 mm) were fabricated under visible light (LED dental curing light: 450-470 nm and 1000 J/cm^2) at room temperature (N=5/group). A periodontal probe was used to determine gelation time, which was the time when the surface of materials hardened and materials did not adhere to the tip of the periodontal probe. The gelation times of the four groups of hydrogels from the probing method are shown in Figure 33A. The statistical analysis indicated significant differences in the gelation times among the groups (p<0.05). The shortest mean gelation time (2.17±0.17 minutes) was recorded for P600. No significant difference in the gelation time was found between P600 and P600:G5. However, both P1000 and P1000:G10 showed a significantly higher gelation time than P600 and P600:G5. P1000:G10 exhibited the longest gelation time when compared to the other groups (5.4±0.15 minutes, p<0.05).

For the *in situ* photorheometry test, all prepolymer solutions were subjected to shear oscillation measurement using the digital rheometer with a light cure

attachment (Omnicure S1000: UV and visible light system: 320-500 nm and 1000J/cm^2). The photorheological analysis provides more accuracy in a gelation profile of hydrogels. Information about the gelation behavior of the gels is gained in terms of the measured storage or elasticity modulus (G') and loss or viscous modulus (G"). We observed that the moduli of P600, P600:G5, and P1000 that started from G" were greater than G' because the hydrogels exhibited a liquid behavior. Then, G' increased as the polymerization proceeded to a crossover point with G", which is recorded as the gelation time. Our results showed that P600 was cured fastest (2.4±0.04 minutes) followed by P1000 (5.71±0.01 minutes), and P600:G5 (6.8±0.13 minutes). Interestingly, we could not obtain the gel point for P1000:G10 by this method because G' of P1000:G10 exceeding G" at the starting point, so no crossover of G' and G" occurred. The plots of log G' and G" vs. time of a representative sample from each group are shown in Figure 33B-33E. The G' after curing of P600, P600:G5, P1000, and P1000:G10 were at 202.3×10^3, 327.8×10^3, 151.4×10^3, and 760 Pa, respectively.

Overall, different gelation times were found using the probing method and *in situ* photorheometry test, which will be discussed in greater detail in the discussion section of this chapter. Furthermore, both P600:G5 and P1000:G10 exhibited a gelation time between 2-6 minutes. Regarding the viscosity, the addition of gelatin enhanced the viscosity of P600 and P1000 prepolymer solutions. Thus, the gelation time and viscosity of our hydrogels would allow for sufficient handling time and fluid flow for future applications. Therefore, P600:G5 and P1000:G10 hydrogels were chosen for all subsequent experiments due to its viscosity and gelation which would make it useful as a carrier for drug delivery.

4.2.2.3 P600:G5 shows a greater swelling behavior and degradation than P1000:G10.

The swelling behavior of hydrogels can greatly affect the pore size of the network and the release behavior of gels. We evaluated the swelling ratio (Q) of PEGDA-gelatin hydrogels by fabricating P1000:G10 and P600:G5 gels (N=5/group), then soaking gels in PBS at 37°C and weight measuring up to 25 days. Both P1000:G10 and P600:G5 gels revealed rapid water absorption and

swelling and reached a maximum swelling ratio (Q_{max}) within 1 and 1.5 hours, respectively (Figure 34A). P1000:G10 showed significantly lower Q_{max} than P600:G500 (p<0.05).

Polymer degradation also affects drug release characteristics. Therefore, the extent of hydrogel degradation was examined by soaking P1000:G10 and P600:G5 hydrogels in PBS and measuring mass of samples up to 25 days (N=5/group). We found that P600:G5 gels exhibited greater degradation than P1000:G10 gels at days 3, 10, 20, and 25 (Figure 34B, p<0.05).

4.2.2.4 P1000:G10 hydrogels exhibit the highest loading efficiency and the slowest release behavior.

The loading efficiency mostly depends on the drug or substance solubility in the scaffold matrix material, the composition and molecular weight of the polymer, and the drug–polymer interaction (Asghar et al. 2012). To determine the loading efficacy, we used a fluorescent dye to mimic drug delivery of small molecule, PF-46. 7-amino-4-methylcoumarin was chosen because its excitation and emission spectrums (370 nm and 460 nm, respectively) are well defined and easily detectable. The 7-amino-4-methylcoumarin (2 mM) was loaded into P1000:G10 and P600:G5 prepolymer solutions before light curing and once set the hydrogels were immersed in PBS at 37 °C. In addition, we compared the loading efficacy of the hydrogels with 7-amino-4-methylcoumarin loaded collagen sponges, which are the control group. After 24 hours, all samples were completely disrupted using a sonicator (N=5/group). The total amount of fluorescent dye released into PBS was measured using fluorescence spectrophotometry. The 7-amino-4-methylcoumarin loaded collagen sponges had a loading efficiency of 100%. The loading efficiencies in P1000:G10 and P600:G5 were 99% and 83%, respectively (Figure 35).

To determine the release behavior of PEGDA-gelatin hydrogels, the *in vitro* release kinetics of 7-amino-4-methylcoumarin was measured in P1000:G10 and P600:G5 hydrogels, and collagen sponges (control). To replicate the physiological environment, the loaded hydrogels and collagen sponge with 7-amino-4-methylcoumarin were incubated in PBS at 37°C up to 25 days (N=5/group). The released fluorescent dye was measured using fluorescence

spectrophotometry over time. The total amount of 7-amino-4-methylcoumarin released from all candidate carriers is shown in Figure 36A. The percentage of cumulative *in vitro* release patterns of 7-amino-4-methylcoumarin loaded PEGDA-gelatin hydrogels and collagen sponges are shown in Figure 36B. On day 3, the cumulative initial burst of dye released from P1000:G10, P600:G5, and control were approximately 84%, 88%, and 93% of the loading amount, respectively. Approximately 100% of the loaded fluorescent dye was released from the control group by day 5, followed by P600:G5 at day 10 and P1000:G10 at day 15.

Generally, diffusion, erosion, and degradation are the mechanisms involved in molecule release from hydrogels (Fu and Kao 2009; Lin and Anseth 2009). A simple mathematical method to determine the release kinetics of molecules from a polymer matrix is derived by plotting the first 60% of cumulative drug release data vs. square root of time (Figure 36A, and insert figure), then fitting data in the Higuchi equation:

$$Q_t = Kt^{1/2}$$

where Q_t is the amount of drug released at time t, and K is the release constant rate. This equation is based on the Fickian diffusion and applicable to the diffusion of drugs that dispersed homogeneously in a polymer matrix (Dash et al. 2010; Grassi and Grassi 2005). By applying this model to our hydrogels, we found that data from all groups acceptably fit this equation ($R^2 > 0.96$). This finding indicated that the drug release mechanism of P1000:G10, P600:G5, and collagen sponge followed Fickian diffusion with the K values at 46.68±1.28, 48.68±1.27, and 49.59±1.73, respectively.

4.2.3 P1000:G10 and P600:G5 hydrogels are non-cytotoxic carriers.

According to the ISO 10993-5 guidelines (ISO-10993-5 1993), the materials that exhibit equal or more than 70% of the relative cell viability compared to the control group are considered as non-cytotoxic materials. We evaluated the cytotoxicity of P1000:G10 and P600:G5 hydrogels against MC3T3-E1 osteoblastic cells by following ISO 10993-5 guidelines (ISO-10993-5 1993). P1000:G10 and P600:G5 hydrogels, and collagen sponges were prepared, sterilized by sterilized

by UV light for 30 minutes per each side, and then soaked in α-MEM with 10% FBS and 1% P/S at 37ºC for 24 hours. Next, P1000:G10, P600:G5, and collagen sponge eluates were collected and used for the cytotoxicity tests. MC3T3-E1 osteoblastic cells were cultured with P1000:G10, P600:G5 or collagen sponge eluates (N=5/group) for 24 hours, and then cells were assayed for cell viability by performing an MTS assay. MC3T3-E1 cell viability was similar between P1000:G10 and P600:G5 eluates; cell viability after 24 hours was found to be 70% and 80%, respectively (Figure 37). MC3T3-E1 cell viability was found to be 100% in control media and collagen sponge eluates, which were used as positive controls. These data suggest that both P1000:G10 and P600:G5 hydrogels are non-cytotoxic hydrogels, with cell viability equal or greater than 70% after 24 hours.

4.2.4 The released PF-46 retains its efficacy to inhibit Pyk2 kinase activity.

P1000:G10 hydrogels were chosen to use as a carrier for PF-46 due to their viscosity, acceptable gelation time, release behavior, and cytocompatibility. PF-46 was reported to inhibit Pyk2 kinase activity with an IC_{50} value of 100 nM (Han et al. 2009). Since Pyk2 catalytic activity depends on its phosphorylation at key tyrosine residues (Bruzzaniti et al. 2009; Eleniste and Bruzzaniti 2012; Eleniste et al. 2012), we examined if the released PF-46 inhibited Pyk2 kinase activity by performing Pyk2 immunoprecipitation (IP) and tyrosine kinase activity assay.

PF-46 loaded P1000:G10 hydrogels were prepared, sterilized, and then soaked in α-MEM with 10% FBS and 1% P/S at 37ºC for 24 hours. Next, the released PF-46 was collected and the concentration estimated based on the release of 7-amino-4-methylcoumarin loaded P1000:G10 hydrogels after 24 hours. Three days prior to conducting the kinase assay, 293VnR cells were transfected with Pyk2 cDNA. 293VnR cells were used in this assay because they do not express Pyk2 and reveal high efficiency in transfection (Bruzzaniti et al. 2009). Pyk2-transfected 293VnR cells were then treated for 2 hours with released PF-46 at the estimated concentration of 0.1, 0.3, and 0.5 μM. Fresh PF-46 at 0.1 and 0.3 μM were used as positive controls and non-treated was used as a negative control group. In addition, Pyk2-expressing 293VnR cells were IP with a Pyk2 antibody to confirm that all groups had the same level of Pyk2. After this, the tyrosine kinase

activity assay was performed following the manufacturer's protocol (Takara Bio). (Figure 38A). As shown in Figure 38B, we found that all concentrations of the released PF-46 significantly inhibited Pyk2 kinase levels when compared to non-treated group (p<0.05). The ability of released PF-46 to inhibit Pyk2 kinase activity was comparable to fresh PF-46. This suggests that PF-46 released from P1000:G10 hydrogels retains its efficacy against the kinase activity of Pyk2.

4.2.5 The released PF-46 enhances ALP activity of stromal OBs.

To examine the bioactivity of PF-46 released from P1000:G10 hydrogels, bone marrow derived MSCs were differentiated into mature OBs under osteogenic conditions for 7 days in the presence or absence of the released PF-46 at the estimated concentrations of 0.1, 0.3, and 0.5 μM, and then ALP activity was examined. We used untreated stromal OBs as the negative control group. For the additional control, we used PF-46 incubated at 37°C for 24 hours as an additional control because we found that there was not statistical significant between fresh PF-46 and the one that incubated for 24 hours. The concentrations of PF-46 released from P1000:G10 were estimate values as described previously in section 4.2.4. As shown in Figure 39, released PF-46 at 0.1 and 0.5 μM markedly enhanced ALP activity as compared to the negative control group and the non-loaded P1000:G10 group (p<0.05). Furthermore, the ALP activity of OBs treated with released PF-46 at 0.1 and 0.5 μM was not statistically different from the 37°C-incubated PF-46 group. These findings indicate that the bioactivity of PF-46 released from P1000:G10 was retained and was effective in promoting OB differentiation.

4.3 Discussion

An ideal biomolecule carrier should not induce inflammatory or immune reactions. Furthermore, it should be absorbed concomitantly with bone healing without toxic residues, but still providing a slow delivery of biomolecules. Carriers should also be simply and cost-effectively fabricated, easily sterilized, and should

be stable for storage (Peppas et al. 2000; Seeherman and Wozney 2005). In addition, carriers should remain at their initial placement site.

We evaluated the viscosity, gelation time, swelling, degradation, and release behavior of several hydrogels and found a hydrogel composed of PEGDA1000 plus 10% gelatin exhibited viscosity and shear-thinning behavior suitable for use as an injectable-carrier. In addition, the P1000:G10 hydrogel was cytocompatible and PF-46 released from it retained its inhibitory activity against Pyk2, leading to an increase in OB activity. We found that P1000:G10 solution exhibited the most obvious shear-thinning behavior. Furthermore, the P1000:G10 solution exhibited the highest viscosity when it reached the Newtonion fluid behavior. These characteristics of P1000:G10 solution make it suitable as a drug delivery carrier because its viscosity is reduced when stress is applied and is rapidly recovered upon removal of the stress; then it can form the drug release gel depot (Choi et al. 2015) The viscosity of P1000:G10 solution can be affected by both increasing gelatin weight and PEGDA molecular weight (Hoch et al. 2012). As we can see that P1000 exhibited higher viscosity than P600, and the greater amount of gelatin also enhanced the viscosity of prepolymer solution. In addition, P1000:G10 solution is a yield stress fluid, which indicates that the solution will remain stationary after injection, allowing it to be cured without the concern of a free-flowing solution. This has the potential to prevent undesirable leakage of solution into neighboring tissues or blood circulation. This is important for one of our future applications, bone fracture healing application, that want to deliver the solution to the open surgical site, and the solution will stay in place next to the regeneration site.

As can be seen from our results, gelation times of our gels were increased when the molecular weight of PEGDA and the amount of gelatin were increased. This is true for both in situ photorheometry and probing techniques that we used to determine gelation time. However, the gelation times from *in situ* photorheometry were higher than the probing technique. The possible explanation may be from the probing technique examined only the surface of the gels, while

the oscillatory rheometry measured the entire gels. Another reason may be due to the difference in thickness of specimens in the two methods.

The thickness of specimens in the oscillatory measurement was 90 μm, while we used thicker specimens (3 mm) in the probing technique because it was the thickness of specimens that we used for all experiments in our project, and heat could be generated in the thick specimens during the curing process which may have accelerated the polymerization. These may have shortened the gelation times in the probing technique when compared to the *in situ* rheometry. Interestingly, the gelation time of P1000:G10 could not be detected by the rheometry. In contrast, we did not encounter difficulty in determining the gelation time in P600:G5. Our results are consistent with Fu et al. (Fu et al. 2012) that both covalently and physically crosslinked PEGDA-10%gelatin hydrogels exhibited a significantly higher value of G' than G" at both room temperature and 37 °C. The potential cause may be due to gelatin already in part forming a physical thermoreversible gel at room temperature, so that the rheometry could not detect the G" in P1000:G10. Using a temperature-adjusted rheometer may solve this problem. We also found that P1000:G10 showed a significantly lower swelling ratio than P600:G5. This suggests that higher PEGDA molecular weight exhibit lower water absorption and Q_{max}, and needs more time to reach $Q_{max,}$ which is consistent with the previous publication (Fu et al. 2012). Additionally, we found that the higher amount of gelatin decreased the swelling ratio, which corresponds with published studies showing that when the gelatin concentration is more than 6%, the swelling degree of gels tends to decrease because of a significant increase in the network chains density. This can lead to decreases in water absorption and polymer relaxation, resulting in a decrease in the degree of hydrogel swelling (Liu and Ballada 2014).

The degradation results reveal that P1000:G10 exhibited lower mass loss when compared to P600:G5. Our PEGDA-gelatin hydrogels consist of PEGDA chains with DTT to form $(-PEG-DTT-)_n$ PEG polymer chains, which are hydrolytically labile chains. Thus, the formed hydrogels can undergo hydrolytic degradation over time (Hudalla et al. 2008; Parlato et al. 2014). In addition, we

used gelatin, which is a natural polymer that is responsive to enzymatic degradation and can be degraded *in vivo* by several enzymes, such as collagenase and lysozyme (Bae et al. 2015; Hutson et al. 2011). This suggests that our PEGDA-gelatin hydrogels can be tailored to get desirable degradation time through the adjustment of the concentration of DTT and gelatin.

Although we used the same gelatin and PEGDA polymers for the synthesis of both PEGDA-gelatin hydrogels, we found that P600:G5 exhibited inferior loading efficiency than P1000:G10. This suggests that molecular weight of PEGDA and gelatin concentration may play a role in loading efficiency. As we know, the swelling and degradation of hydrogels in drug delivery applications facilitates local delivery of drugs through temporally modulated drug release. The release profile of 7-amino-4-methylcoumarin from PEGDA-gelatin hydrogels showed an initial burst release similar to what we found in collagen sponges, but the amount of dye release from PEGDA-gelatin hydrogels were slower than collagen sponges. P1000:G10 tended to exhibit the slowest release behavior even though we could not find the statistical significance, which resulted from P1000:G10 showing the lowest degree of swelling and degradation. Using released 7-amino-4-methylcoumarin we estimated the concentration of released PF-46. However, one limitation of this approach is that the detection of released 7-amino-4-methylcoumarin may differ from the released Pyk2 inhibitor due to differences in molecular weight, structure, and solubility between these two molecules, Nevertheless, the fluorescent dye was a cost-effective and amenable approach to examine molecule release kinetics of the PEGDA-gelatin hydrogels.As described above, several of our experiments suggested that P1000:G10 may make an appropriate carrier for delivery of small-molecule inhibitor of Pyk2. Overall, we selected P1000:G10 due to its viscosity and gelation because the long-term application of this technology will be as a drug-delivery system to promote OB bone formation, which does not require high mechanical properties. In load bearing area, we need to combine this gel with the other solid scaffolds to enhance mechanical properities. To identify an appropriate Pyk2 inhibitor, we examined the efficacy of two commercially available small molecule inhibitors of Pyk2, PF-43 and PF-46.

We found that both PF-43 and PF-46 enhanced the proliferation of mouse MSCs (OB precursors) and ALP activity in mature OBs. However, when OBs were differentiated for 21 days under osteogenic conditions, only PF-46 increased calcium deposition compared to the control group. These observations were consistent with our findings that Pyk2-KO OBs exhibit higher proliferation, ALP activity and mineralizing activity than WT OBs (Chapter 3). Furthermore, our results are consistent with published studies showing that both PF-43 and PF-46 can increase ALP activity of OBs, but only PF-46 enhances mineralization levels of OBs (Han et al. 2009). The possible reason for this is that PF-43 is a dual FAK/Pyk2 inhibitor, which is 20-fold more potent against FAK than Pyk2, whereas PF-46 is a Pyk2-targeted inhibitor with 100-fold more potent against Pyk2 than FAK. It has been reported that inhibition of FAK significantly reduces calcium deposition by human MSCs after 28 days of culture (Salasznyk et al. 2007). This suggests that FAK may play a role in the osteogenic mineralization process of OBs. Thus, the Pyk2-targeted inhibitor, PF-46, was used in subsequent *in vitro* experiments. Importantly, we found that the P1000:G10 hydrogel was cytocompatible. Importantly, the release PF-46 from P1000:G10 retained its efficacy against Pyk2 kinase activity and still effective in promoting ALP activity of OBs differentiated for 7 days. In addition, the ability to inhibit Pyk2 kinase activity and enhance OB activity was similar to the positive control, which was the PF-46 group. These signify that the bioactivity of PF-46 was not obliterated during PEGDA-gelatin hydrogel preparation.

4.4 Summary and conclusions

In summary, our results indicate that PF-46, a Pyk2-targeted inhibitor, enhances OB activity *in vitro*. Furthermore, P1000:G10 is appropriate to use as a carrier for PF-46 based on several physical characteristics as follows: 1) P1000:G10 prepolymer solutions exhibit a shear-thinning effect, 2) P1000:G10 prepolymer solutions exhibit high viscosity which can prevent undesirable leakage of the solution into neighboring tissues or blood circulation, 3) P1000:G10 can form

gel *in situ* by photopolymerization with a reasonable gelation time; allowing for sufficient handling time prior to light curing, 4) The P1000:G10 hydrogel is biodegradable and can be degraded by both hydrolytic and enzymatic degradation, 5) P1000:G10 is cytocompatible and exhibited the slowest drug-release behavior. Notably, the PF-46 released from P1000:G10 retained its inhibitory activity against Pyk2 kinase activity and enhanced ALP activity in OBs *in vitro*. The schema presentation of Pyk2-inhibitor loaded hydrogel preparation and utilization is shown in Figure 40. All of these findings strongly support the use of PEGDA-gelatin hydrogel incorporated with a Pyk2-targeted inhibitor for future bone regeneration studies.

CHAPTER 5

OVERALL DISCUSSION AND CONCLUSIONS

5.1 Discussion

The mechanisms that control bone mass and bone formation are not completely understood. Low bone mass diseases such as osteoporosis and periodontitis result from an imbalance in the bone resorption and bone formation processes. Therapeutic approaches have been developed to improve these low bone mass conditions in both systemic and local levels, but they still have some disadvantages. Therefore, a need for suitable approaches including biomolecules and biomaterials for both systemic and local levels still remains. The overall goals of this dissertation were to better understand the cellular mechanism of bone formation by OBs, and to develop novel therapies to increase bone mass.

Pyk2 is important for OB activity as well as OC activity (Buckbinder et al. 2007; Gil-Henn et al. 2007). While female Pyk2-KO mice exhibit increased BV/TV, unpublished studies from Dr. Bruzzaniti reveal that male Pyk2-KO mice exhibit a bone phenotype similar to WT mice. In addition, our unpublished studies indicate that E2 supplementation of OVX female Pyk2-KO mice resulted in a greater increase in BV/TV in Pyk2-KO OVX mice than in WT OVX mice. This suggests that Pyk2-KO mice may regulate OB activity and bone formation in part through estrogen signaling pathway.

In chapter 3 of this dissertation, we examined whether Pyk2 regulate bone mass in part by modulating the estrogen signaling in OBs. This is the first study to examine the role of Pyk2 and E2 in OB activity. A number of earlier studies examined only the role of Pyk2 in OB and OC activities (Buckbinder et al. 2007; Cheng et al. 2013; Eleniste et al. 2015; Gil-Henn et al. 2007; Kacena et al. 2012). Our results revealed that Pyk2-KO OBs showed significant increases in proliferation (cell number and metabolic activity), matrix formation and maturation, and mineralization. The addition of E2 or raloxifene led to a further increase in both matrix formation and maturation, and mineralization in Pyk2-KO OBs, but not in WT OBs. Consistent with a role of Pyk2 in OB activity, we found a decrease in ERα protein levels in Pyk2-KO OBs due to the degradation of cytosolic ERα via the ubiquitin proteasome pathway. These findings are consistent with published

reports that ERα can undergo proteasome mediated degradation (Chai et al. 2015; Lu et al. 2010; Petrel and Brueggemeier 2003; Zhou and Slingerland 2014). Although several reports indicate that ERβ can also be degraded by this mechanism (Sanchez et al. 2013; Tateishi et al. 2006), we found that ERβ protein levels in Pyk2-KO OBs were similar to WT OBs, suggesting the ERα and ERβ are differentially regulated in OBs. In addition to the proteasome-mediated degradation, ERα degradation can occur through a lysosome-dependent pathway. (Cooper 2000; Zhou and Slingerland 2014). A recent publication reported that chloroquine, a lysosomal inhibitor, abrogated the estrogen-dependent ERα breakdown in MCF-7 cells (Totta et al. 2014). Whether ERα is also degraded by lysosomes in Pyk2-KO OBs remains to be determined.

We also determined the role of Pyk2 and Pyk2-S isoforms and found they exhibit differential expression during OB differentiation. We also found Pyk2 and Pyk2-S are both negative regulators of OB activity, suggesting they may affect OBs at different stage of differentiation; Pyk2 may be active in early OBs, while Pyk2-S may inhibit OB activity in the mature OBs.

The results described in Chapter 3 strongly suggest that Pyk2 regulates OB activity and bone formation in part by modulating the estrogen signaling pathway. There are still many unanswered questions regarding the role of Pyk2 and estrogen in OB activity. For example, it will be interesting to determine if ERα degradation plays a role directly in OB differentiation and mineralization in the absence of Pyk2 or it is just a physiological coincidence. In addition, whether ERβ, plays a direct role in the regulation of OB activity in the absence of Pyk2 remains to be determined. Pyk2-KO OBs may also respond to E2 mechanisms other than ERα and/or ERβ, such as through the N-terminal truncated ERα isoform or ERRα. In addition, the role of Pyk2 in the regulation of the androgen receptor should not be overlooked especially in light of a recent publication which reported that Pyk2 promoted the expression and phosphorylation of the androgen receptor (Hsiao et al. 2016).

Pyk2-KO mice exhibit an osteopetrotic phenotype mostly from increasing cancellous bone volume. In this study, we found that Pyk2-KO OBs exhibited a

decrease in ERα protein levels compared to WT OBs. These in vitro findings correspond with what has been reported for the phenotype of global ERα-KO mice, which also exhibit high bone mass (Lindberg et al. 2001; Sims et al. 2002; Windahl et al. 1999). However, our findings are different from the phenotypes reported for bone-cell specific ERα-KO mice models. Controversy in the bone phenotypes of the bone-specific ERα-KO mice still exists due to the use of different Cre mice models, which affect different stages of OB differentiation. Almeida et al. (Almeida et al. 2013) found that cortical bone, not cancellous bone, was reduced in female mice when deleting ERα in MSCs ($ER\alpha^{f/f}$; *Prx-Cre*) or OB progenitors ($ER\alpha^{f/f}$; *Osx-Cre*). However, this bone loss disappeared in female mice in which ERα deletion was driven by the Cola1-promoter ($ER\alpha^{f/f}$; *Col1a1-Cre*). On the contrary, recent studies have reported that both cortical and cancellous bone volumes are decreased in the young female OB-specific deletion of ERα mice ($ER\alpha^{\Delta OB/\Delta OB}$; *OCN-Cre*) (Maatta et al. 2013; Melville et al. 2014). However, this phenotype disappeared when the age of mice was increased (Maatta et al. 2013). The bone phenotype of OB-specific ERα-KO mice suggests that deletion of ERα in OBs leads to a decrease in OB activity at least in young females. This conclusion contrasts with our results showing Pyk2-KO OBs which exhibit ERα protein degradation, exhibit a significant increase in OB activity, including proliferation, matrix maturation, and mineralization. Therefore, it is possible that decreased expression of ERα is unlikely to be the only mechanism involved in the regulation of OB activity in the absence of Pyk2.

In the current studies, we focused the role of Pyk2 and E2 in OB activity. However, Pyk2 is also expressed in OCs and Pyk2-deletion leads to OC impairment and reduced bone resorption (Bruzzaniti et al. 2009; Gil-Henn et al. 2007). In addition, it has been well established that estrogen promotes OC apoptosis (Hughes and Boyce 1997). Thus, it will be necessary to examine the combined effect of Pyk2 and estrogen on OC activity. To this end, we speculate that estrogen will enhance the effect of Pyk2-deletion on OCs as we found in OBs. Furthermore, the systemic effects such as the effect of hepatic IGF-1 which is known to stimulate OB formation (Imai et al. 2010; Sims et al. 2000) should be

evaluated in Pyk2-KO mice because it is known that estradiol can enhance the expression of IGF-1 and consequently promote bone formation (Bord et al. 2001). Thus, the high bone mass phenotype in Pyk2-KO mice with estradiol supplementation may also occur through this pathway.

In chapter 4 of this dissertation, we developed a Pyk2-inihbitor loaded hydrogel for future bone regeneration applications. We used bone marrow derived MSCs because they more closely approximate the bone microenvironment in which the hydrogel will be used in future studies. We found that PF-46, a Pyk2-selective inhibitor, enhanced OB proliferation, ALP activity, and mineral deposition *in vitro*. Importantly, our results support the hypothesis that our proposed drug carrier, P1000:G10, was cytocompatible and exhibited shear-thinning behavior, high viscosity and yield stress which would be favorable for a drug injectable carrier (Choi et al. 2015; Hoch et al. 2012). P1000:G10 also exhibited the slowest drug release behavior. Importantly, the released PF-46 retained its inhibitory activity against Pyk2 kinase activity and enhanced ALP activity in OBs *in vitro*.

To the best of our knowledge, this is the first study to develop a Pyk2-inihbitor loaded hydrogel for bone formation, and our *in vitro* results are promising and strongly support the therapeutic application of using a PEGDA-gelatin hydrogel incorporated with a Pyk2-selective inhibitor for bone regeneration *in vivo*. However, there are a number of limitations in our *in vitro* experiments that should not be overlooked. First, we used 7-amino-4-methylcoumarin, a fluorescent dye, as a representative of PF-46 because it is a small molecule that has the molecular weight quite close to PF-46 and the detection of this fluorescent dye can be performed by simple spectrophotometry. However, the release profile of the 7-amino-4-methylcoumarin may be different from the release profile of PF-46 due to the difference in molecular weight, structure, and solubility. Nevertheless, this still provides an approximation of the release behavior of PEGDA-gelatin hydrogels. Moreover, the released profile of 7-amino-4-methylcoumarin was a cost-effective method that can be useful for other carriers or scaffolds. However, it should be noted that there are the other methods that can be used to detect the release of PF-46 such as mass spectrometry or high performance liquid chromatography,

which require longer time to prepare and analyze. In future studies, we will examine the release profile of PF-46 using these techniques to obtain a more accurate release profile of PF-46 from PEGDA-gelatin hydrogels. Second, the gelation time of P1000:G10 could not be detected by the *in situ* photorheometry, which may be due to gelatin already forming physical gel at room temperature, so that the rheometry could not detect a crossover point of G" and G" in P1000:G10 at room temperature. This problem may be solved using the temperature-adjusted rheometer. However, the temperature should be above 37°C because a study found that both covalently and physically crosslinked PEGDA-10%gelatin hydrogels exhibit a significantly higher value of G' than G" at both room temperature and 37°C (Fu et al. 2012).

Furthermore, the release behavior of our PEGDA-gelatin hydrogels need to be improved, so that it will provide a more sustained released than collagen sponges, which will allow for the lower dosages of drugs or biomolecules (Fassbender et al. 2014). Therefore, Pyk2-inhibitor loaded hydrogel could be more efficient for promoting bone formation and regeneration. Theoretically, the initial release of biomolecules during first 3-7 days should be approximately 60% to initiate bone healing and then the remaining 30% bound biomolecules should show sustained release for 3-4 weeks to maintain an osteoinductive effect (Woo et al. 2001). The controlled and sustained release kinetics can be modified by various methods such as fabricating covalently PEGDA-gelatin hydrogels modification with cysteine (Fu et al. 2012) or incorporating methacrylate to retard drug release rate (Sutter et al. 2007).

In addition to bone marrow derived MSCs, future studies elucidate the efficacy of Pyk2-inhibitor loaded hydrogel in calvarial OBs will be useful in order to expand the therapeutic applications to the craniofacial skeleton, for example, for use in cranial defect regeneration or palatal suture expansion.

Given that deletion of Pyk2 increases OB activity and decreases OC resorption, Pyk2 inhibitors may have both anabolic and antiresorptive properties. However, to date, published studies have focused only on the anabolic effects of the Pyk2 inhibitors. Since OCs activity is decreased in the absence of Pyk2,

leading to a decrease in bone resorption, a possible concern regarding the use of a Pyk2-inihbitor based strategy for bone regeneration, especially in long bones, is whether the Pyk2 inhibitor will affect callus remodeling. Evidence shows that when antiresorptive agents such as bisphosphonates or Denosumab, which can impair OC activity, are used to enhance bone fracture healing, the quality and quantity of bone fracture repair is improved, although a delay in the time of bone healing may occur (Hegde et al. 2016). Another advantage of a hydrogel-based carrier is that the carrier and/or scaffold design can be tailored for timed release during the reparative phase of bone healing and be degraded prior to the remodeling phase, allowing for OC activity to proceed normally once the carrier and/or scaffold is degraded.

As we found an additive effect of estrogen on bone formation in the absence of Pyk2, we speculate that our Pyk2-inihbitor loaded carriers may provide more pronounced bone healing results in females than males. Furthermore, incorporating estrogen or raloxifene into a Pyk2-inihbitor based carriers may potentially promote bone healing in post-menopausal women. Based on our findings and other studies, Pyk2-inhibitor strategies may be useful for the treatment of post-menopausal osteoporosis. To date, estrogen replacement and raloxifene therapy still remain as effective treatments to protect and treat post-menopausal osteoporosis, but concerns exist regarding the non-skeletal risks related to long-term estrogen treatment, including the risk of uterine cancer, breast cancer and cardiovascular disease (Rosen 2005). One strategy to potentially reduce these risks is through the dual combination of estrogen or raloxifene with a Pyk2 inhibitor. This dual-combination drug approach could potentially reduce the dosage of estrogen or raloxifene and Pyk2 inhibitor being used, which may consequently decrease the adverse effects of the component drugs.

5.2 Conclusions

Taken together, our results indicate that Pyk2 is integrated into the estrogen and ERα/ERβ signaling cascade, and negatively regulates OB activity by

controlling the levels of ERα and phospho-ERK. Additionally, PF-46, a Pyk2-selective inhibitor, incorporated into P1000:G10 is cytocompatible and retains its ability to inhibit Pyk2, leading to an increase in OB differentiation *in vitro*. These findings strongly support that the inhibition of Pyk2 locally with PEGDA-gelatin hydrogel delivery may be a therapeutic tool for bone regeneration at sites of appendicular and/or craniofacial bone pathology. The schema presentation of the summary of key findings in this dissertation is shown in Figure 41. In the future, we will use the Pyk2 inhibitor incorporated into PEGDA-gelatin hydrogel for proof-of-concept bone healing application using a non-critical bone defect in a rat model system. Overall, our Pyk2-based strategy may be useful in the bone regeneration field, and may be valuable as a therapeutic treatment for those suffering from systemic bone loss, such as osteoporosis. Thus, targeting Pyk2 may be a novel strategy for bone regeneration at the local and systemic levels.

TABLES

Table 1. Experimental design for cell studies described in Chapter 3

Figure	Cell type	Number of cells	Treatment	Time	Analysis method
13 and 14B	WT OB Pyk2-KO OB	5×10^4 cells/well in 12-well plate	100 nM E2	1-4 days	Cell counting
14A	WT OB Pyk2-KO OB	2×10^3 cells/well in 96-well plate	100 nM E2	12 hours	MTS
15, 19 16 17	WT OB Pyk2-KO OB	5×10^4 cells/well in 12-well plate	100 nM E2	4, 7, 14, 21, and 28 days	QPCR ALP activity Mineralization
18	WT OB Pyk2-KO OB	5×10^4 cells/well in 12-well plate	0.1-10 nM Raloxifene	28 days	ALP activity Mineralization
20, 23, 24, 28	WT OB Pyk2-KO OB	2×10^5 cells/well in 6-well plate	100 nM E2	4, 21 and 28 days	Western blotting
21	WT OB Pyk2-KO OB	2×10^5 cells/well in 6-well plate	100 nM E2 ± 20 μM MG-132	E2 for 4 days and MG-132 for final 3 hours	Western blotting
22	WT OB Pyk2-KO OB	5×10^4 cells/well in 12-well plate	100 nM E2 ± 0.04, 0.1, and 0.4 μM PPT or DPN	21 days	ALP activity Mineralization
26	MC3T3-E1 cells	6.7×10^4 cell/well in 24-well plate	Pyk2/Pyk2-S transfection	2-3 days after transfection	MTS ALP activity Mineralization
27	WT OB Pyk2-KO OB	2×10^5 cells/well in 6-well plate	100 nM E2	6 hours on day 0 and day 14	Western blotting

Table 2. Oligonucleotide primers used for QPCR and RT-PCR

Primers	Primer sequences	Expression
18S	Forward: AGTCCCTGCCCTTTGTACACA Reverse: CGATCCGAGGGCCTCACTA	Housekeeping gene
β-Actin	Forward: TCACCCACACTGTGCCCATCTACGA Reverse: CAGCGGAACCGCTCATTGCCAATGG	Housekeeping gene
GAPDH	Forward: GGTCGGTGTGAACGGATTTGGC Reverse: GCAGTGATGGCATGGACTGTGG	Housekeeping gene
c-fos	Forward: ACTTCTTGTTTCCGGC Reverse: AGCTTCAGGGTAGGTG	OB proliferation
ALP	Forward: ACTGATGTGGAATACGAACTGGATGAGAAGG Reverse: CAGTCAGGTTGTTCCGATTCAATTCATACTGC	OB differentiation (early mature OB)
Collagen type I	Forward: AACCTGGTGCGAAAGGTGAA Reverse: AGGAGCACCAACGTTACCAA	OB differentiation (matrix synthesis)
OCN	Forward: TCTCTCTGACCTCACAGATGCCAAGC Reverse: GGACTGAGGCTCCAAGGTAGCG	OB differentiation (matrix synthesis and mineralization)
ERα	Forward: CTCAACCGCCCGCAGCTCAA Reverse: GTAGGCGATGCCCGACTGGC	Highly expressed during early OB differentiation
ERβ	Forward: ACCCTCACTGGCACGTTGCG Reverse: GGCTTGCGGTAGCCAAGGGG	remain constant throughout OB differentiation
Pyk2/ Pyk2-S	Forward: AGCAAGAAAGGAATGCTCGCTACC Reverse: TTCCACCATCTGCTTCTGCTGTCT	Pyk2 isoforms; differentially expressed during OB differentiation

Table 3. Experimental design for cell studies described in Chapter 4

Figure	Cell type	Number of cells	Treatment	Time	Analysis method
30A	Bone marrow derived MSCs	2×10^3 cells/well in 96-well plate	0.0125, 0,025, 0.05, 0.1 and 0.3 μM of PF-43 or PF-46	24 hours	MTS
30B and 30C	Bone marrow derived MSCs differentiated to mature OBs	4×10^4 cells/well in 12-well plate	Osteogenic media comtaining 0.0125, 0,025, 0.05, 0.1 and 0.3 μM of PF-43 or PF-46	7 -21 days	ALP activity Mineralization
31	Calvarial OBs	4×10^4 cells/well in 12-well plate	Osteogenic media comtaining 0.0125, and 0.05 μM of PF-46	7 -21 days	ALP activity Mineralization
37	MC3T3-E1	2×10^3 cells/well in 96-well plate	Hydrogels and collagen sponges' eluates	24 hours	Cytotoxicity
38	293 VnR cells	1×10^6 cells/dish in 10 cm^2-dish	0.1 and 0.3 μM of released PF-46	2 hours	In vitro kinase activity
39	Bone marrow derived MSCs differentiated to mature OBs	4×10^4 cells/well in 12-well plate	0.1 and 0.3 μM of released PF-46	7 days	ALP activity

FIGURES

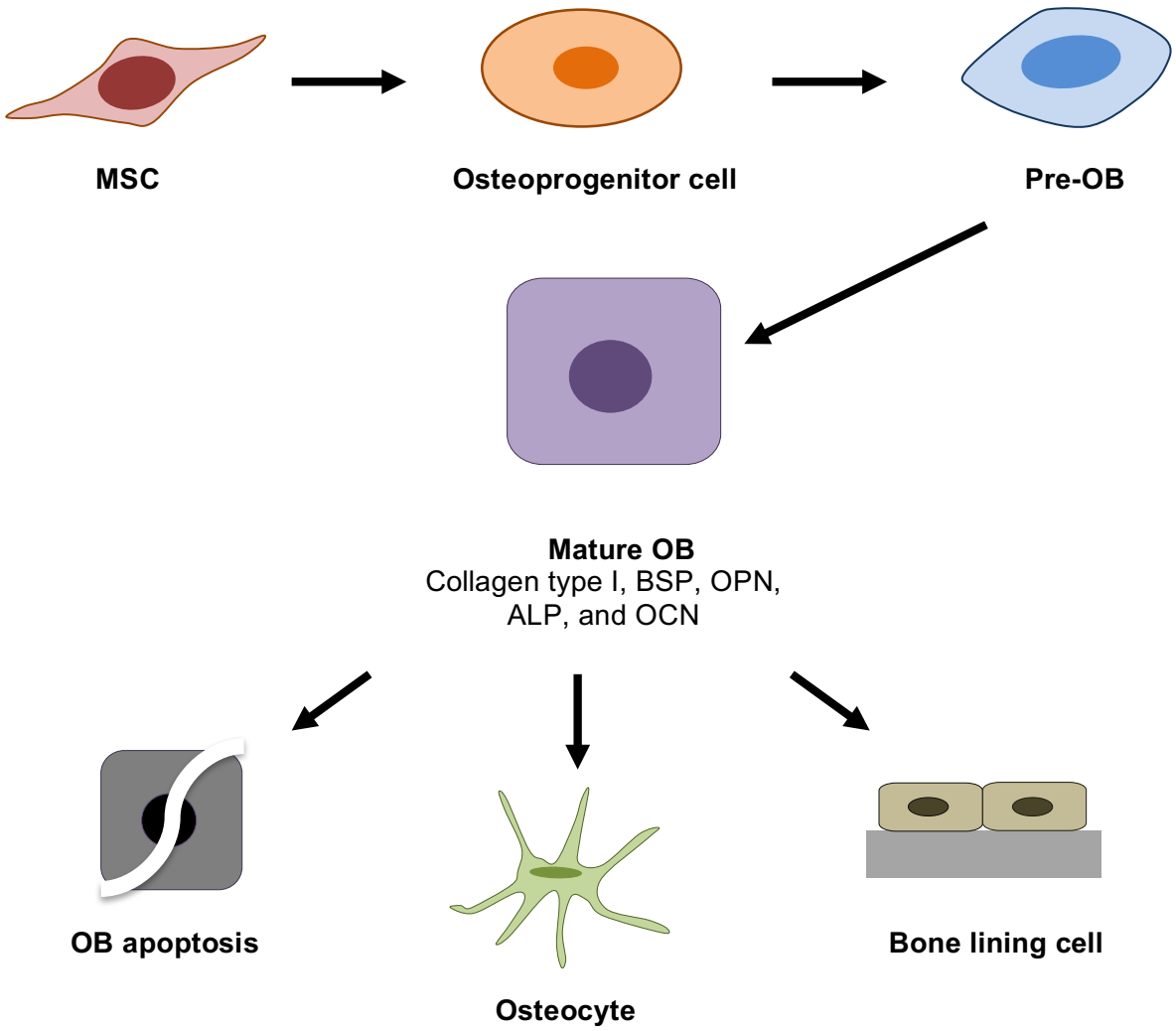

Figure 1. Schema for osteoblastogenesis.

Osteoprogenitor cells differentiate from MSCs, and then differentiate into pre-OBs and then into mature OBs. OB maturation is associated with an increase in collagen type I, ALP, BSP, OPN, and OCN expression. At the end of differentiation, mature OBs enter apoptosis or further differentiate into either osteocytes or bone lining cells.

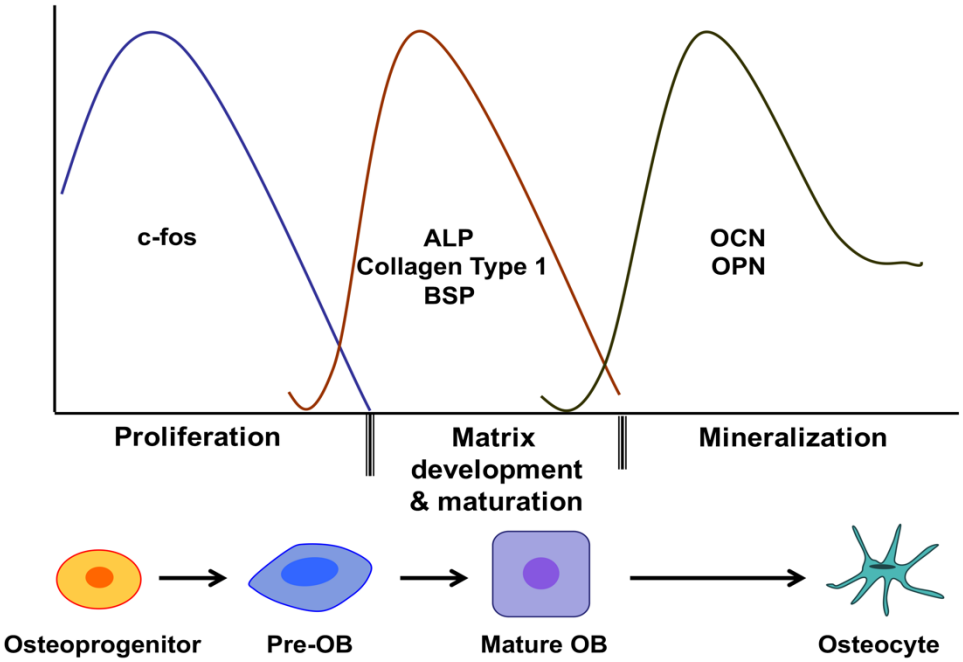

Figure 2. Gene expression during OB proliferation and differentiation.
OB proliferation is associated with cell-cycle progression and the induction of key transcription factors such as c-fos. The maturation of OBs requires the ECM-related proteins including ALP and collagen type 1. The induction of OCN, OPN and other genes is required for the mineralization of the ECM. (Adapted from Stein et al. 2004)

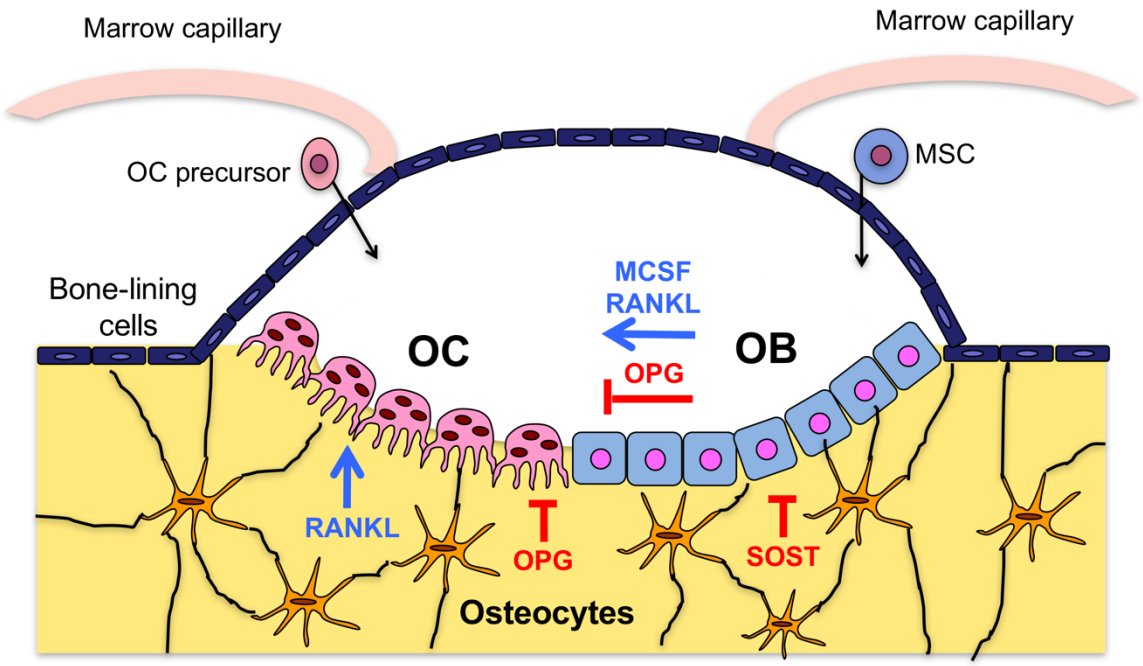

Figure 3. Interplay of bone cells in the basic multicellular unit.

Bone remodeling process is carried out by the coupling between bone resorption and bone formation within BMUs. The BMU is located on bone surface and covered by a bone remodeling compartment (BRC). In the BRC, intercellular communication occurs among bone cells, endothelial and vascular cells. OCs are derived from the hematopoietic lineage, while OBs are originated from MSCs in the marrow cavity. The cytokines MCSF, RANKL, and OPG necessary for OC formation and are produced by OBs and osteocytes. Osteocytes also secrete sclerostin which inhibits the actions of OBs.

17β-estradiol

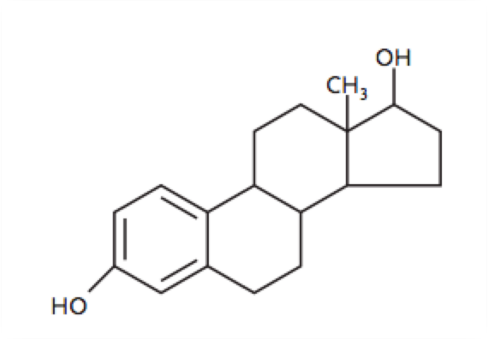

Raloxifene

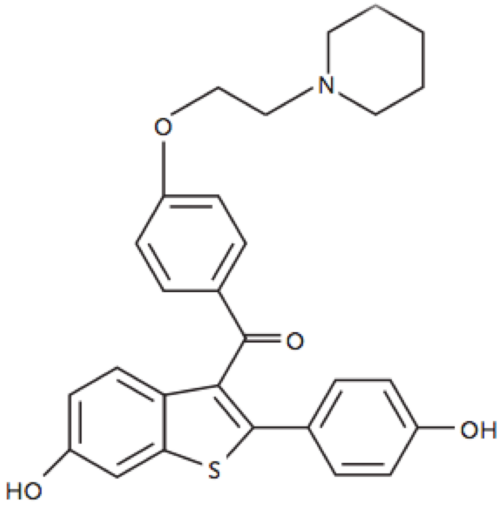

Figure 4. Chemical structures of 17β-estradiol and raloxifene.

17β-estradiol has a cyclophenanthrene structure, whereas raloxifene has a benzothiophene structure. Even though the raloxifene structure differs from estrogen, both have a conformation that allows them to bind to the ligand-binding domain of the ER (Riggs and Hartmann 2003). Unlike 17β-Estradiol that has similar binding affinity to both ERs, raloxifene has a preferential binding affinity to ERα than ERβ (Zhu et al. 2006).

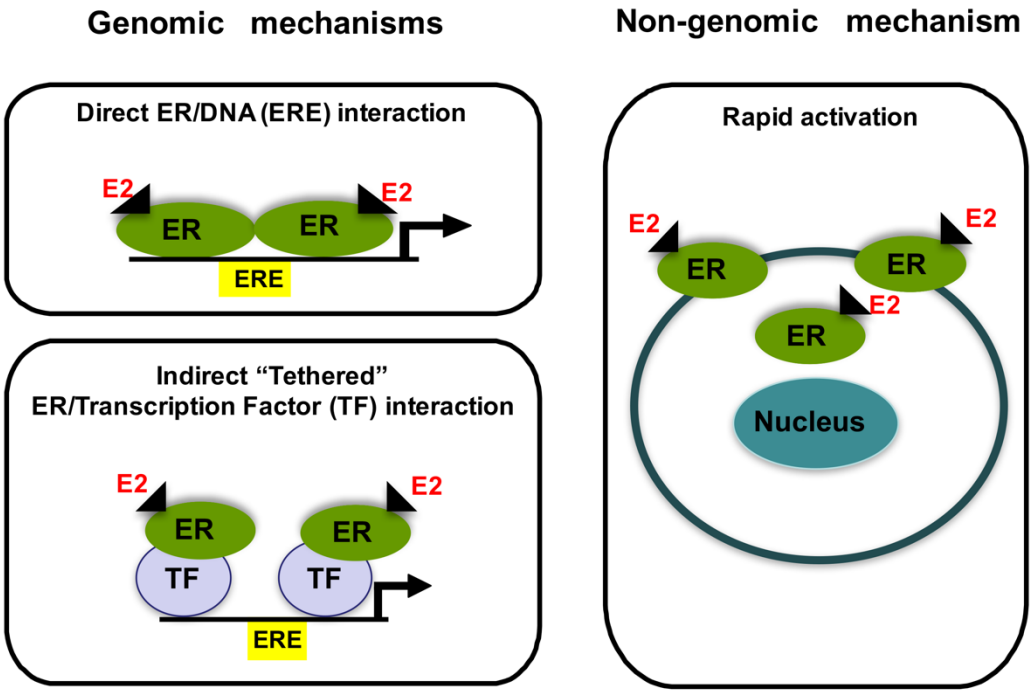

Figure 5. Schema of the mechanisms of estrogen response.

Estrogen actions are mediated by genomic and non-genomic pathways. The genomic pathway of estrogen (E2) occurs through its binding to nuclear estrogen receptors (ERs) either by direct interaction between E2-ER with the estrogen response element (ERE) in transcription promoter regions or by indirect binding of E2- ER to ERE via other transcription factors. In contrast, the non-genomic actions of E2 occur via the interaction of E2 with ERs present at the cell membrane or in the cytoplasm (Adapted from Burr and Allen, 2013)

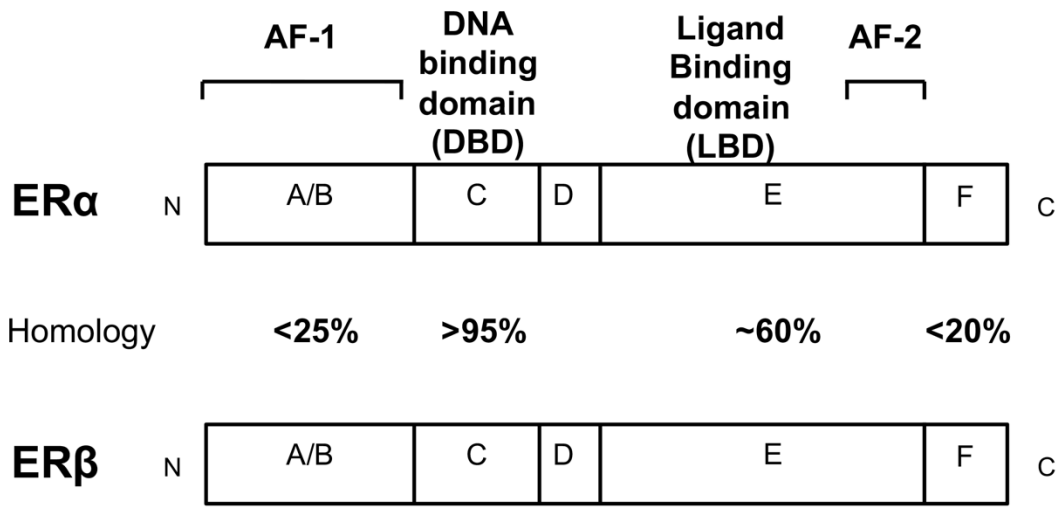

Figure 6. ERα and ERβ protein structure and functional domains.

ERα and ERβ shared a conserved domain structure. The N terminal A/B domain contains activation function sites 1 (AF-1). The C region consists of the DNA-binding domain (DBD). The D domain, hinge region, contributes to the specificity of DNA binding and nuclear localization of ERs. The E domain is the ligand binding domain (LBD), and AF-2 is also in this domain. The F domain is at the C terminal. The percentage in the figure demonstrates the structural homology of each domain between ERα and ERβ; these are similar in mouse, rat, and human (Adapted from Compston et al. 2001 and Hewitt et al. 2016).

A

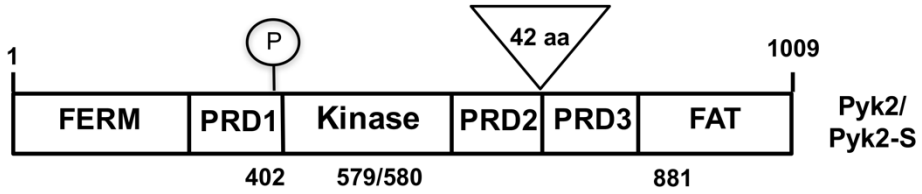

B

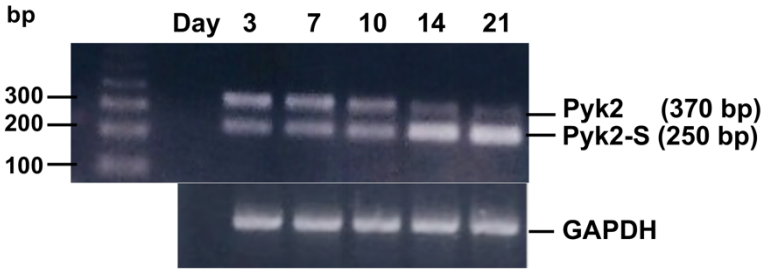

Figure 7. The structures of Pyk2 isoforms and their expression during OB differentiation.

(A) Pyk2 has two isoforms, the full-length Pyk2 (118 KDa) and Pyk2-S (106 KDa), which lacks 42 amino acids compared to the full-length Pyk2. Pyk2 and Pyk2-S can be autophosphorylated at tyrosine residue Y402, which is important for kinase activity and downstream signaling. (B) RT-PCR of OB differentiated for 3-21 days, OBs express full-length Pyk2 (370-bp PCR product) and Pyk2-S (250-bp PCR product). The ratio of Pyk2 to Pyk2-S decreases during OB differentiation with Pyk2-S expression exceeding Pyk2 by day 14 and day 21.

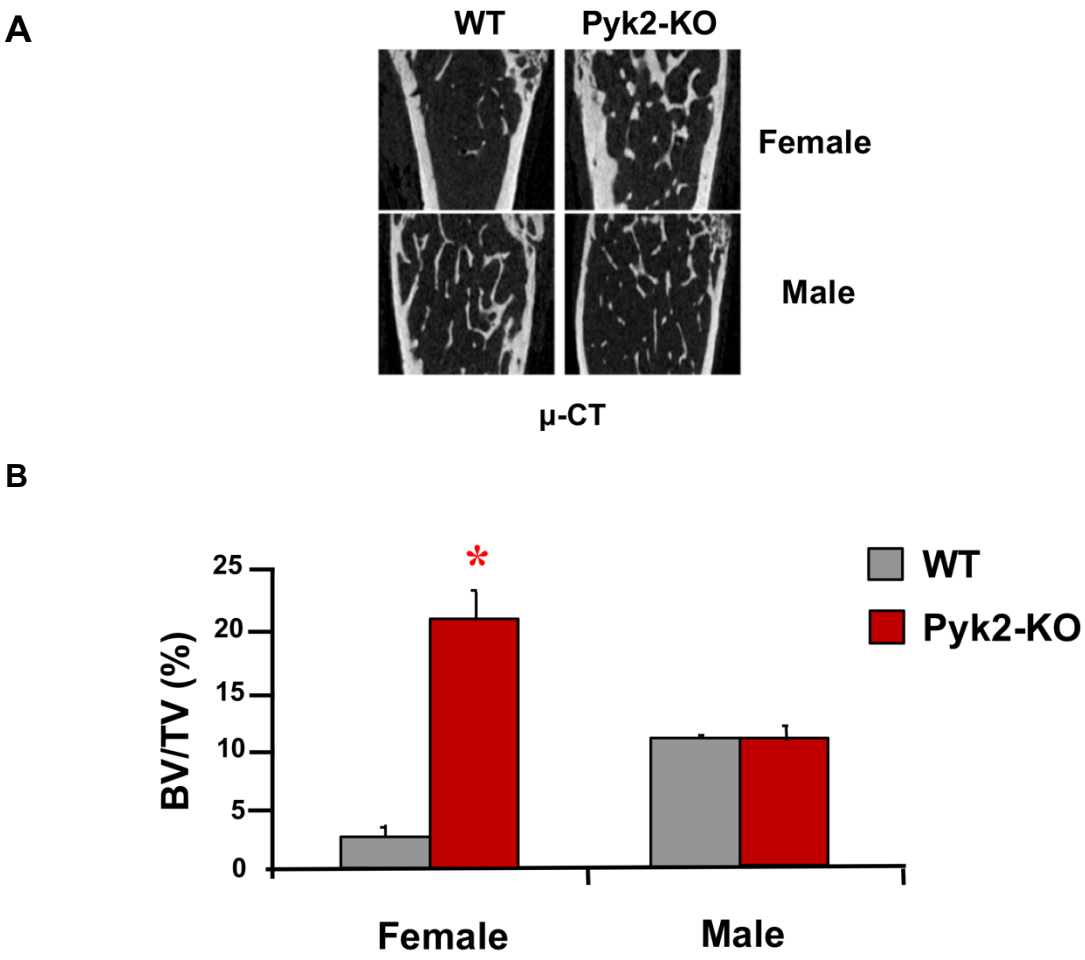

Figure 8. μ-CT analyses of long bones in female and male mice.

(A) Representative images of μ-CT at the distal femur of 32-week-old male and female WT and Pyk2-KO mice showing an increase in trabecular BMD in Pyk2-KO female mice compared to WT female mice, but not in male mice. (B) BV/TV% of female Pyk2-KO mice (20.98 ± 2.68) was significantly higher than female WT mice (3.28 ± 0.46%), whereas no difference between the male WT and Pyk2-KO mice ($p<0.05$) (Nguyen et al., unpublished data).

A

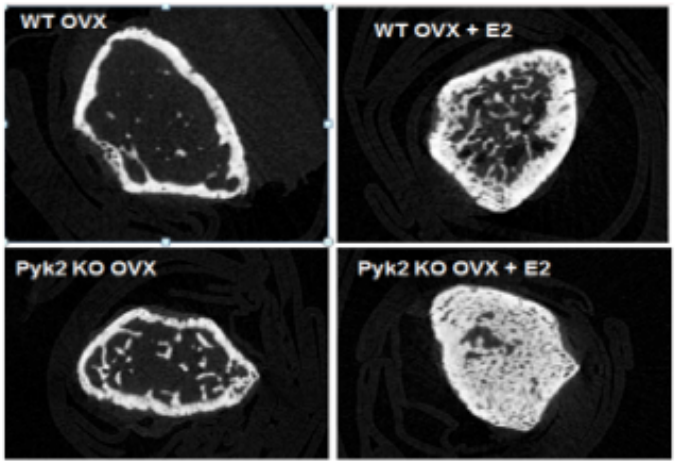

B

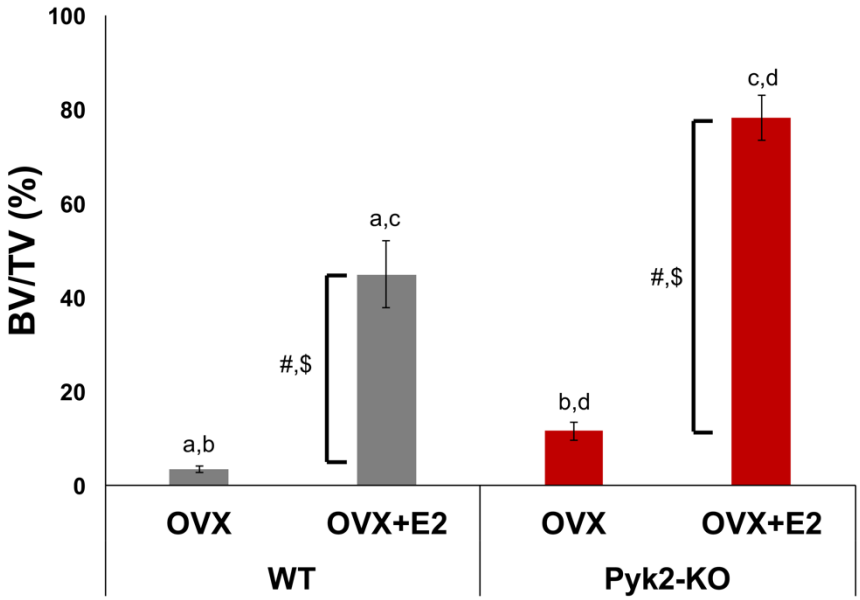

Figure 9. Effect of 17β-estradiol supplementation on bone volume in Pyk2-KO mice.

(A) Representative images of μ-CT analysis of femoral trabecular bone of OVX mice with or without OVX and 17β-estradiol (E2) supplementation (167 ng/day) at 4 weeks post-operatively. OVX Pyk2-KO + E2 exhibited the highest increased BV/TV% among groups. (B) The relative change in BV/TV% of OVX Pyk2-KO + E2 (#) relative to OVX ($) was significantly higher than the change in BV/TV% of WT mice ($p<0.05$) (Bruzzaniti, unpublished data).

A. PF-431396

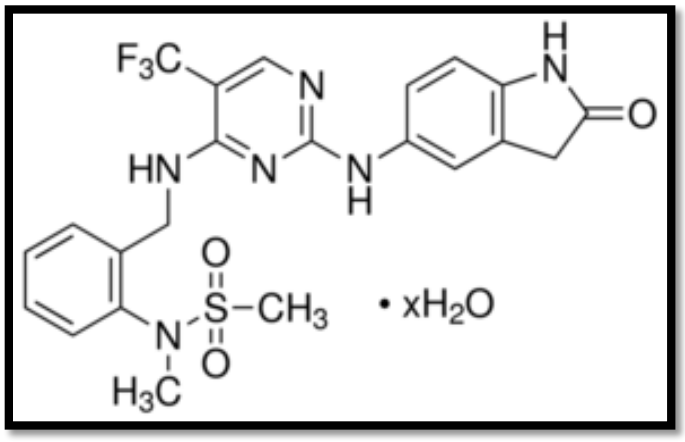

B. PF-4618433

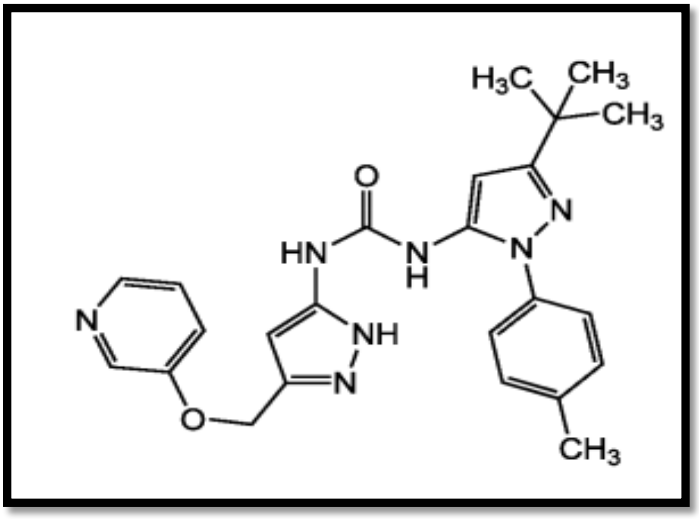

Figure 10. Chemical structures of the Pyk2 inhibitors.

(A) PF-431396 ($C_{22}H_{21}F_3N_6O_3S \cdot xH_2O$) is a dual FAK/Pyk2 inhibitor with IC_{50} values of 1.5 nM of FAK and 11-32 nM of Pyk2. (B) PF-4618433 ($C_{24}H_{27}N_7O_2$) is a Pyk2-targeted inhibitor that has IC_{50} values of 100 nM for Pyk2 and 10,000 nM for FAK.

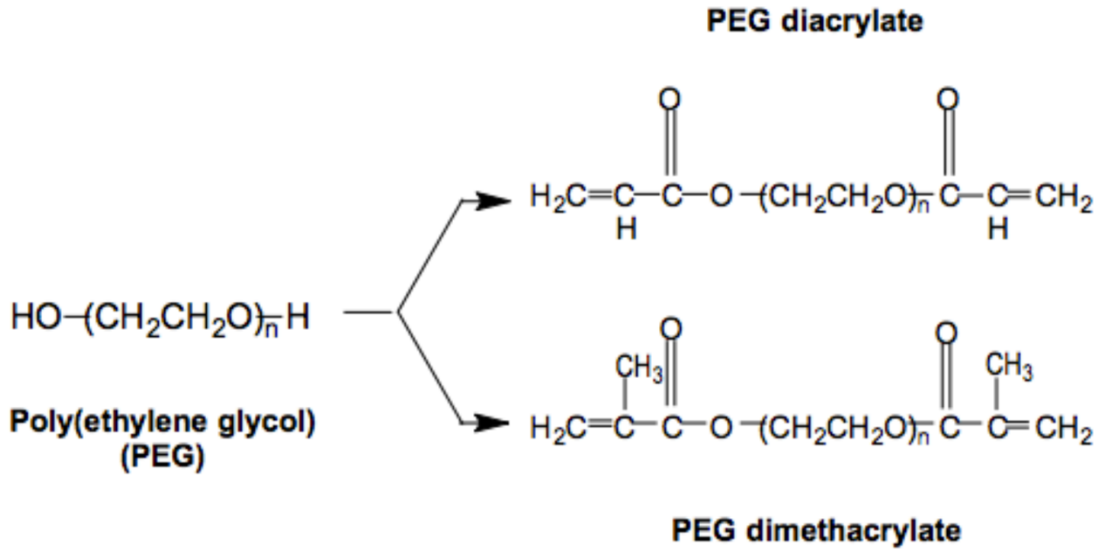

Figure 11. Chemical structures of PEG, PEGDA, and PEGDM.

PEG diacrylate (PEGDA) or PEG dimethacrylate (PEGDM) are PEG-based macromers with reactive termini that highly used in hydrogel fabrication due to the controllable material properties and the simplicity of synthesis. (Adapted from Lin and Anseth 2009).

A

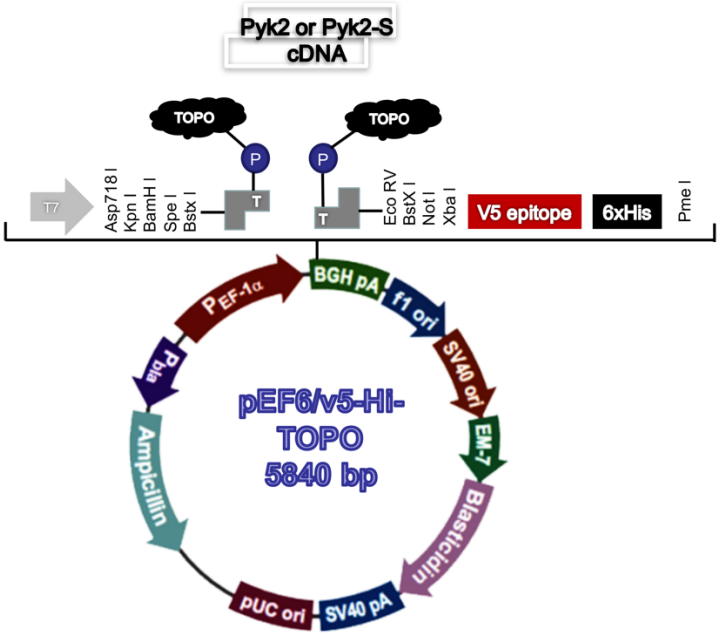

B

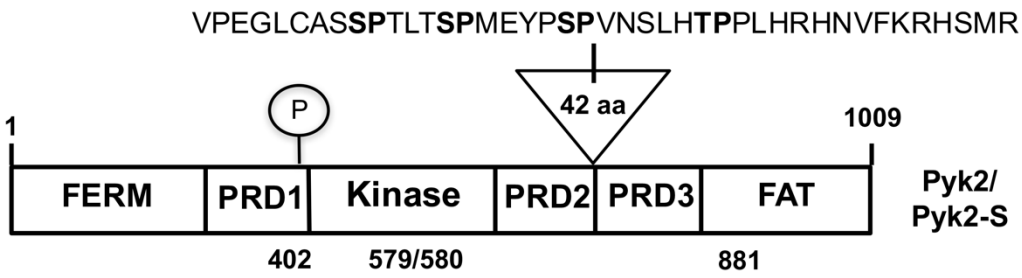

Figure 12. Pyk2 and Pyk2-S expression constructs.

(A) Schematic representation of the plasmid vector for Pyk2/Pyk2-S expression constructs is shown. The vector was tagged with histidine (His) and V5. (B) The domain structures of Pyk2/Pyk2-S are shown. Pyk2-S lacks 42 amino acids compared to the full-length Pyk2 as indicated.

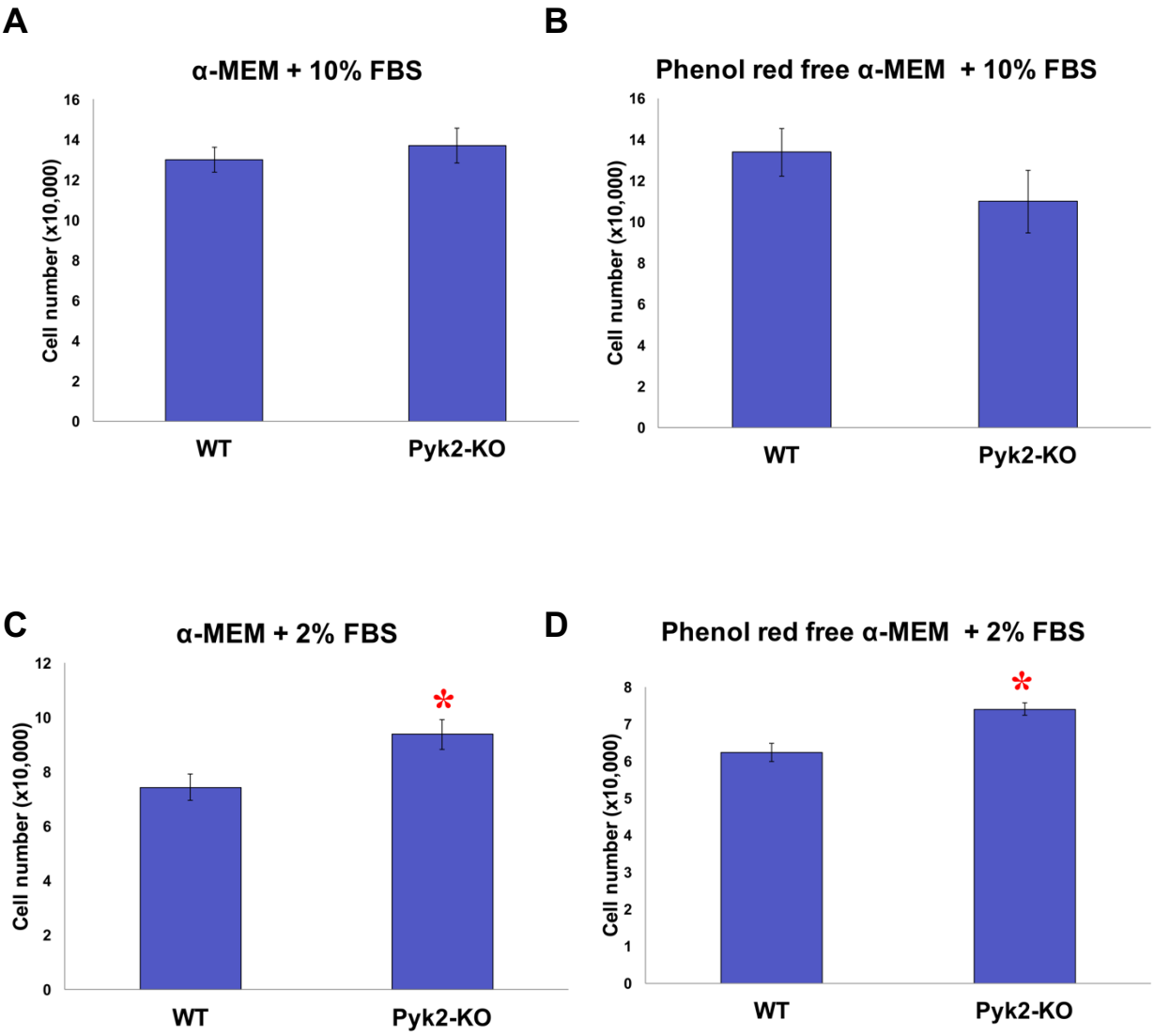

Figure 13. Effect of media and FBS concentration on OB number.

(A and B) An equal number of WT and Pyk2-KO OBs were cultured in α-MEM or phenol red free α-MEM plus 10% FBS, or (C and D) in α-MEM or phenol red free α-MEM plus 2% FBS. Cells were cultured for 4 days and then cell numbers excluding Trypan blue were counted (N=6/group). The data are shown as mean and SEM of six samples. Asterisks (*) indicate statistical significance between WT and Pyk2-KO OBs.

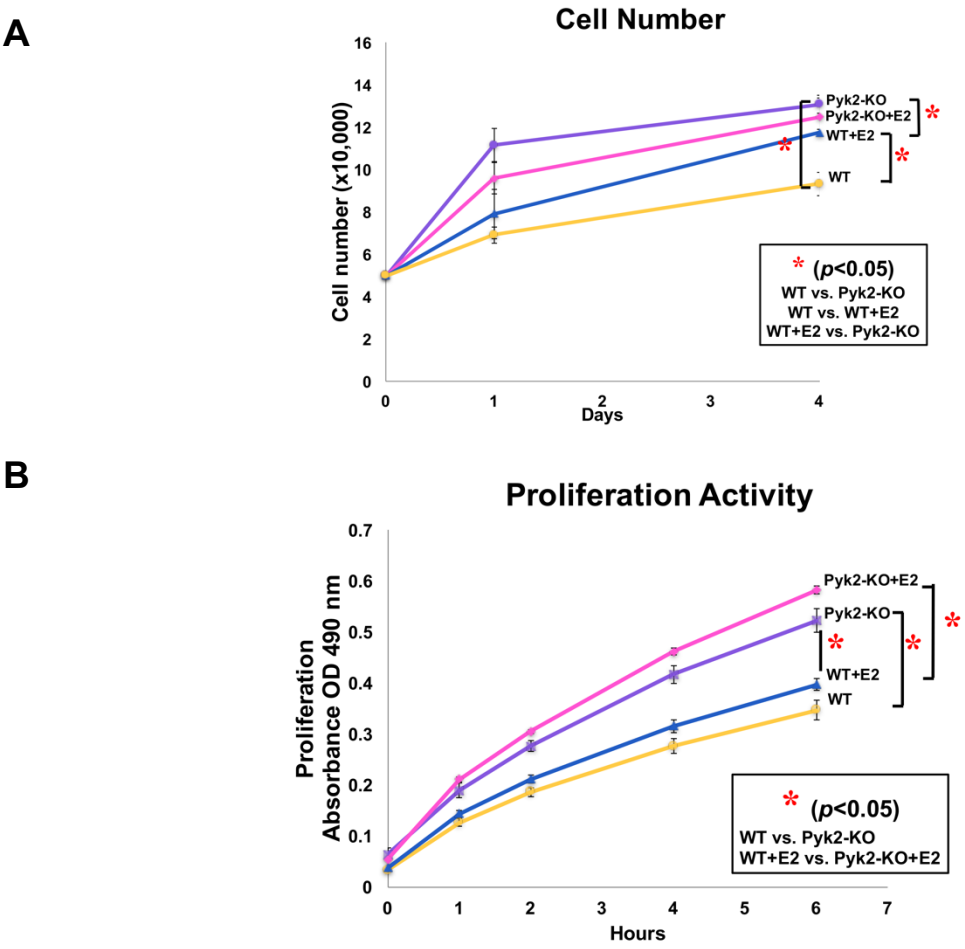

Figure 14. Effect of Pyk2-deletion and estrogen on OB proliferation and number.

(A). Calvarial WT and Pyk2-KO OBs were cultured for 1 or 4 days in the presence or absence of 100 nM E2. At days 1 and 4, cells from each group were trypsinized and counted under a microscope using a hemacytometer. (B) Calvarial WT and Pyk2-KO OBs were cultured for 24 hours then treated with or without 100 nM E2 for 12 hours, and an MTS assay was performed for 0 to 6 hours. The data shown as mean and SEM of triplicate samples. Experiments were performed a minimum of three times and representative data are shown. Asterisks (*) indicate statistical significance between WT and Pyk2-KO, WT and Pyk2-KO with E2, and WT with E2 and Pyk2-KO for the proliferation activity ($p<0.05$). For cell number, statistical significant differences were found between WT and Pyk2-KO, WT and WT with E2, and WT with E2 and Pyk2-KO ($p<0.05$).

Day 4

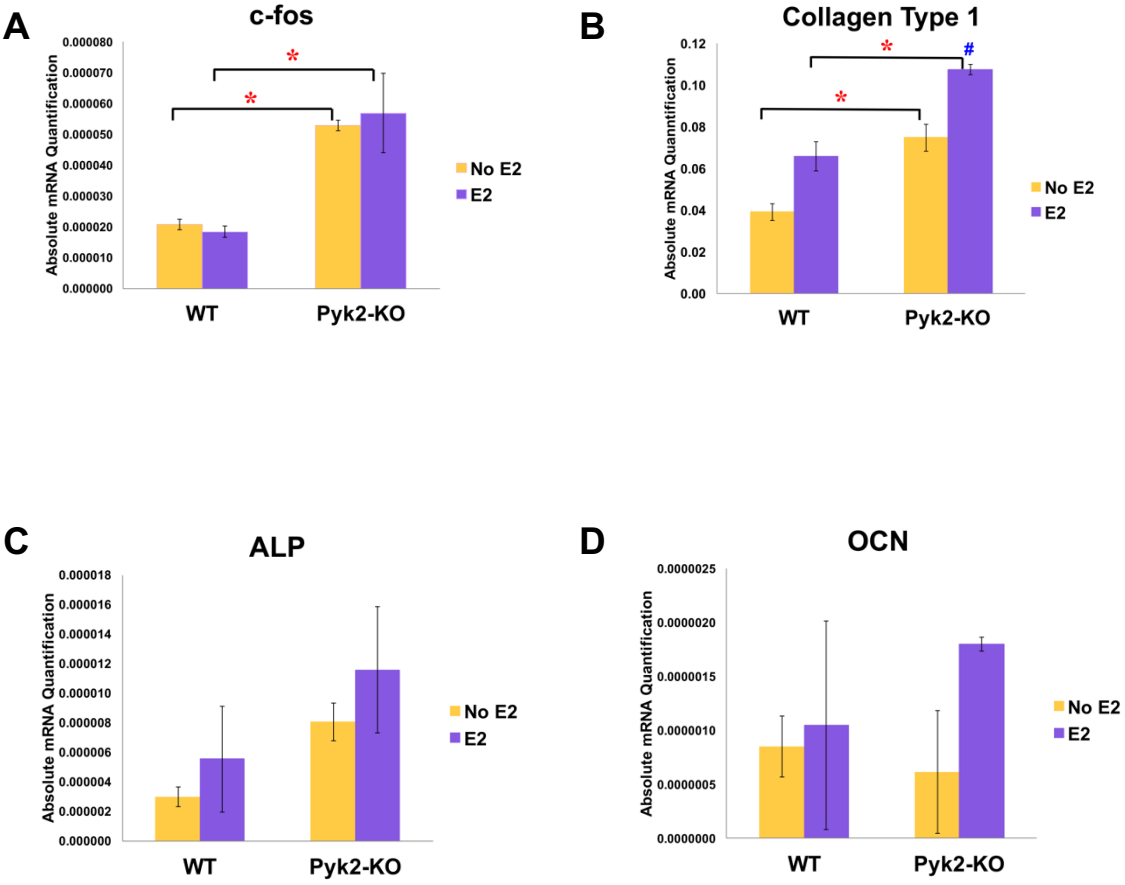
A
c-fos
Absolute mRNA Quantification
0.000080
0.000070
0.000060
0.000050
0.000040
0.000030
0.000020
0.000010
0.000000
*
*
WT
Pyk2-KO
No E2
E2
B
Collagen Type 1
Absolute mRNA Quanntification
0.12
0.10
0.08
0.06
0.04
0.02
0.00
*
#
*
WT
Pyk2-KO
No E2
E2
C
ALP
Absolute mRNA Quantification
0.000018
0.000016
0.000014
0.000012
0.000010
0.000008
0.000006
0.000004
0.000002
0.000000
WT
Pyk2-KO
No E2
E2
D
OCN
Absolute mRNA Quantification
0.0000025
0.0000020
0.0000015
0.0000010
0.0000005
0.0000000
WT
Pyk2-KO
No E2
E2

Day 28

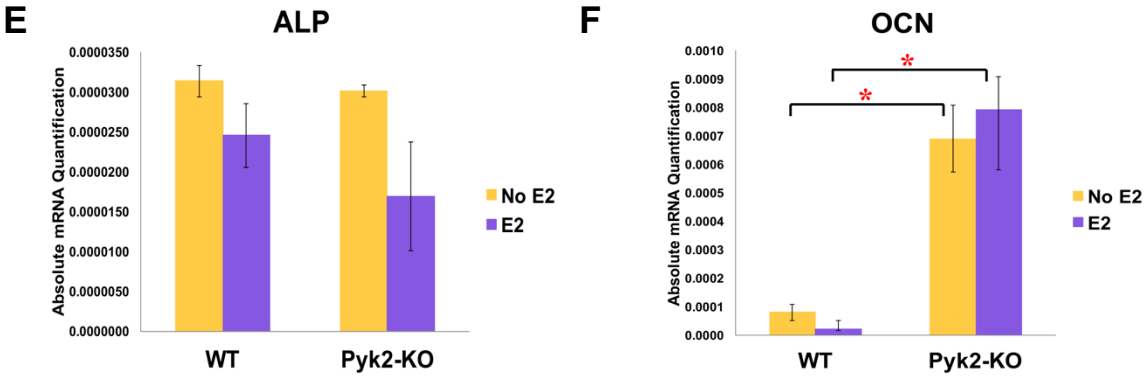
E
ALP
Absolute mRNA Quantification
0.0000350
0.0000300
0.0000250
0.0000200
0.0000150
0.0000100
0.0000050
0.0000000
WT
Pyk2-KO
No E2
E2
F
OCN
Absolute mRNA Quantification
0.0010
0.0009
0.0008
0.0007
0.0006
0.0005
0.0004
0.0003
0.0002
0.0001
0.0000
*
*
WT
Pyk2-KO
No E2
E2

Figure 15. Effect of Pyk2-deletion and estrogen on markers of OB activity. WT and Pyk2-KO calvarial OBs were cultured for 4-28 days with or without 100 nM E2 supplementation, and QPCR analysis was used to determine mRNA expression of osteoblastic genes. On day 4, (A) c-fos, (B) collagen type I, (C) ALP, and (D) OCN mRNA expression levels were evaluated. In addition, (E) ALP, and (F) OCN mRNA levels on day 28 were examined. 18S was used as the housekeeping control to normalize the amount of the mRNA transcript under investigation. The data are shown as mean and SEM of triplicate samples. Experiments were performed a minimum of three times and representative data are shown. Asterisks (*) indicate statistically significant difference ($p<0.05$) between WT and Pyk2-KO OBs, whereas pound signs (#) indicate statistical significance of estrogen supplementation (($p<0.05$).

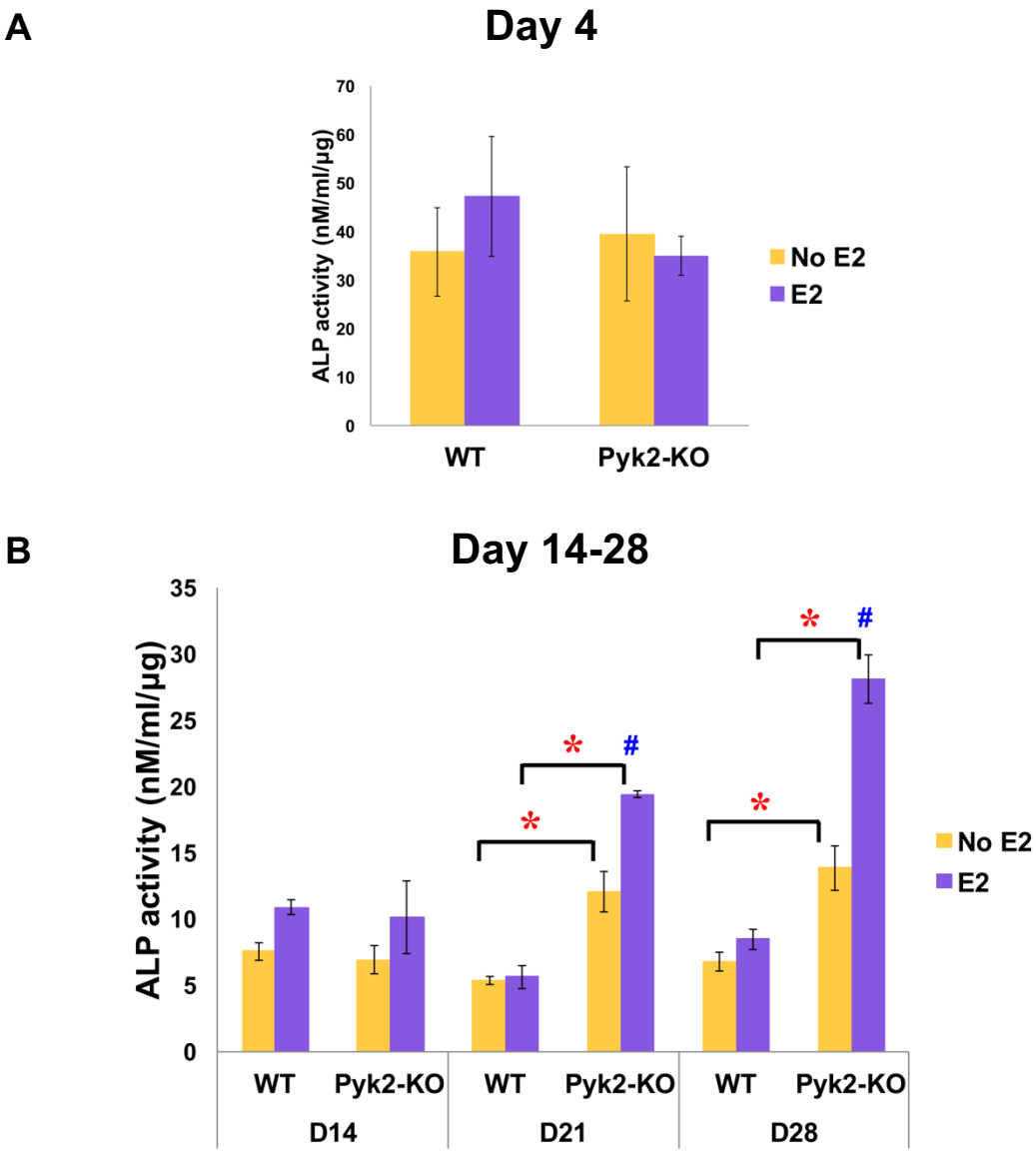

Figure 16. Effect of Pyk2-deletion and estrogen supplementation on ALP activity during OB differentiation.

WT and Pyk2-KO calvarial OBs were cultured for 4-28 days under osteogenic conditions containing ascorbic acid and β-GP with or without 100 nM E2 supplementation. (A) Results of quantitative ALP activity assay on day 4, (B) and days 14 to 28 are shown. Asterisks (*) indicate statistically significant difference (p<0.05) between WT and Pyk2-KO OBs, whereas pound signs (#) indicate statistical significance of estrogen supplementation ((p<0.05)

.

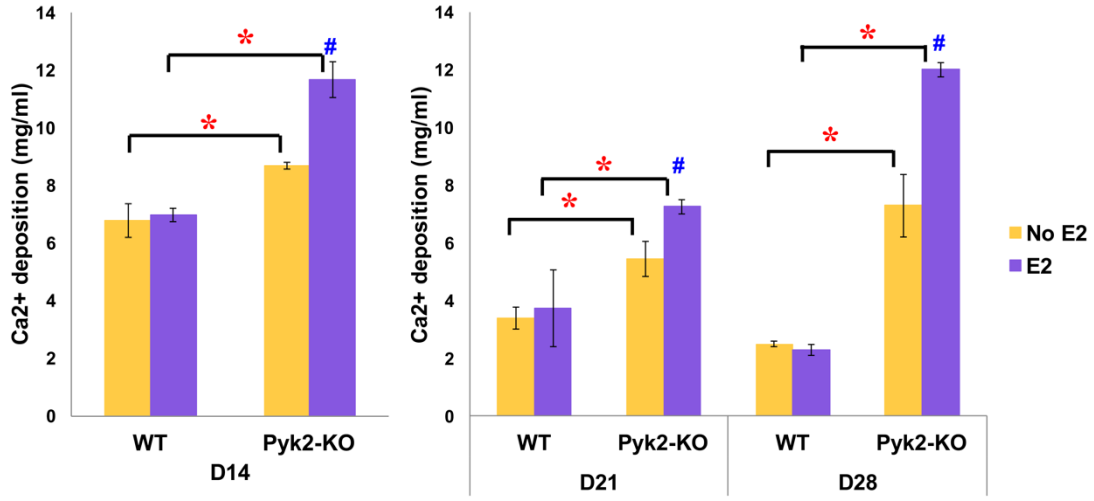

Figure 17. Mineralization of WT and Pyk2-KO OBs in the presence or absence of E2.

WT and Pyk2-KO calvarial OBs were cultured for 14-28 days under osteogenic conditions containing ascorbic acid and β-GP with or without 100 nM E2 supplementation. Results of quantitative Alizarin Red S staining are shown. Asterisks (*) indicate a statistically significant difference ($p<0.05$) between WT and Pyk2-KO OBs, whereas pound signs (#) indicate statistical significance of estrogen supplementation (($p<0.05$).

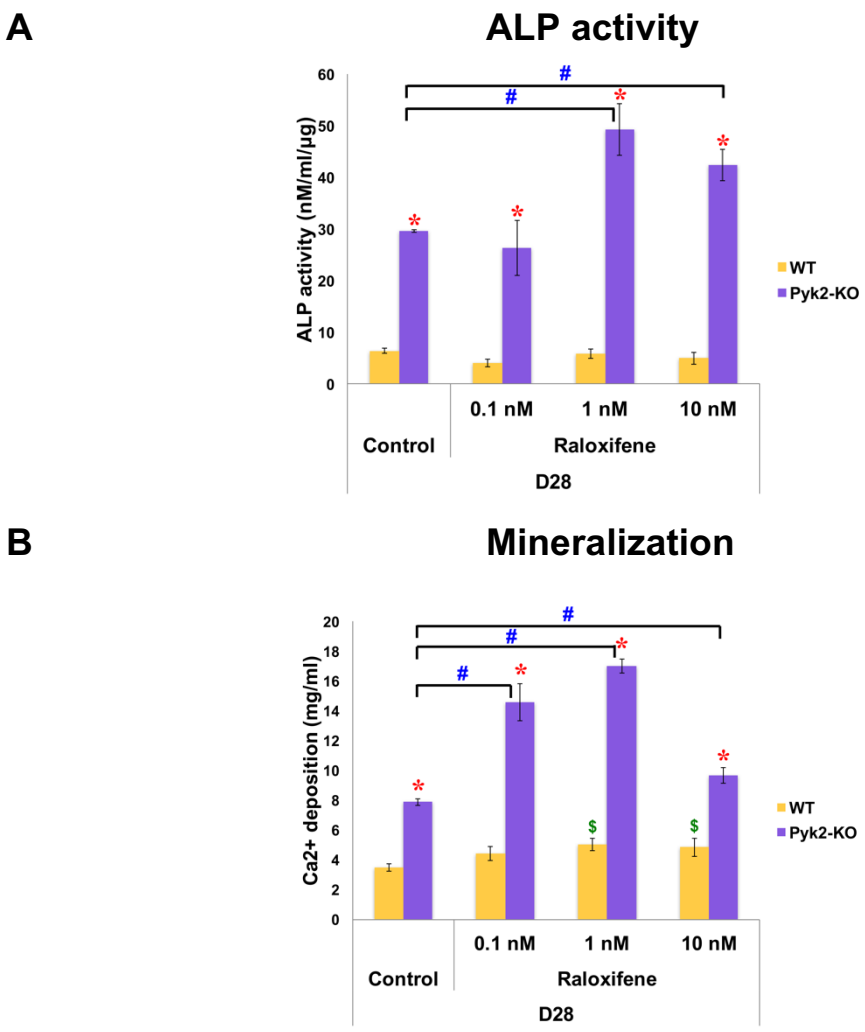

Figure 18. The effect of raloxifene on ALP activity and mineralization in WT and Pyk2-KO OBs.

WT and Pyk2-KO calvarial OBs were cultured for 28 days under osteogenic conditions containing ascorbic acid and β-GP with or without 0.1 nM, 1 nM and 10 nM raloxifene. (A) Results of quantitative ALP activity assay, (B) and quantitative Alizarin Red S staining are shown. The data are shown as mean and SEM of triplicate samples. Experiments were performed three times and representative data are shown. Asterisks (*) indicate statistical significance ($p<0.05$) between WT and Pyk2-KO OBs, whereas pound signs (#) and dollar signs ($) indicate statistical significance of raloxifene supplementation (($p<0.05$) in Pyk2-KO and WT OBs, respectively.

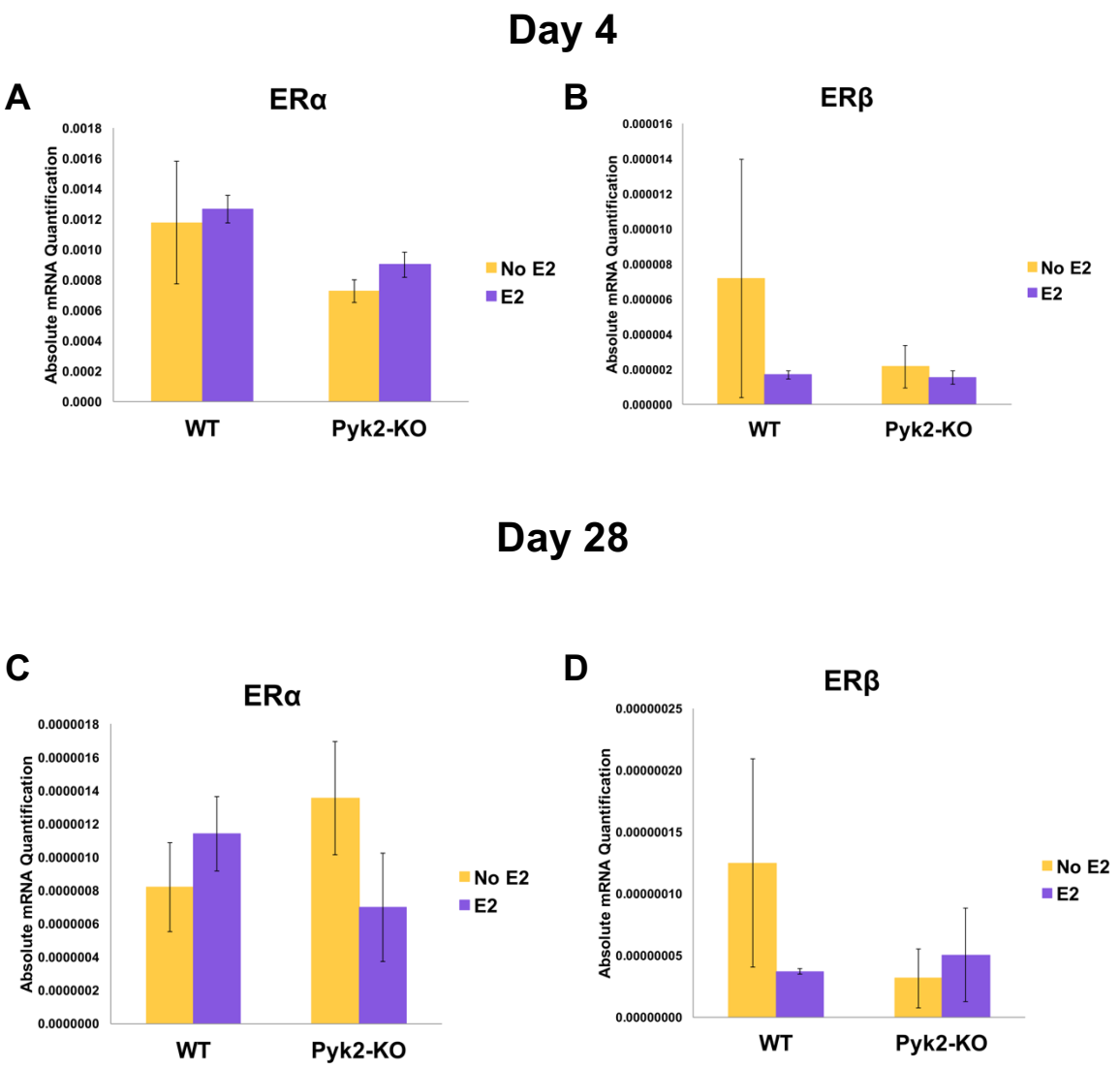

Figure 19. ERα and ERβ mRNA levels in WT and Pyk2-KO OBs in the presence or absence of E2.

WT and Pyk2-KO calvarial OBs were cultured for 4 (A and B) and 28 (C and D) days with or without 100 nM E2 supplementation. ERα and ERβ mRNA expressions were determined using QPCR analysis. 18S was used as the control to normalize the amount of the mRNA transcript under investigation. The data are shown as mean and SEM of triplicate samples.

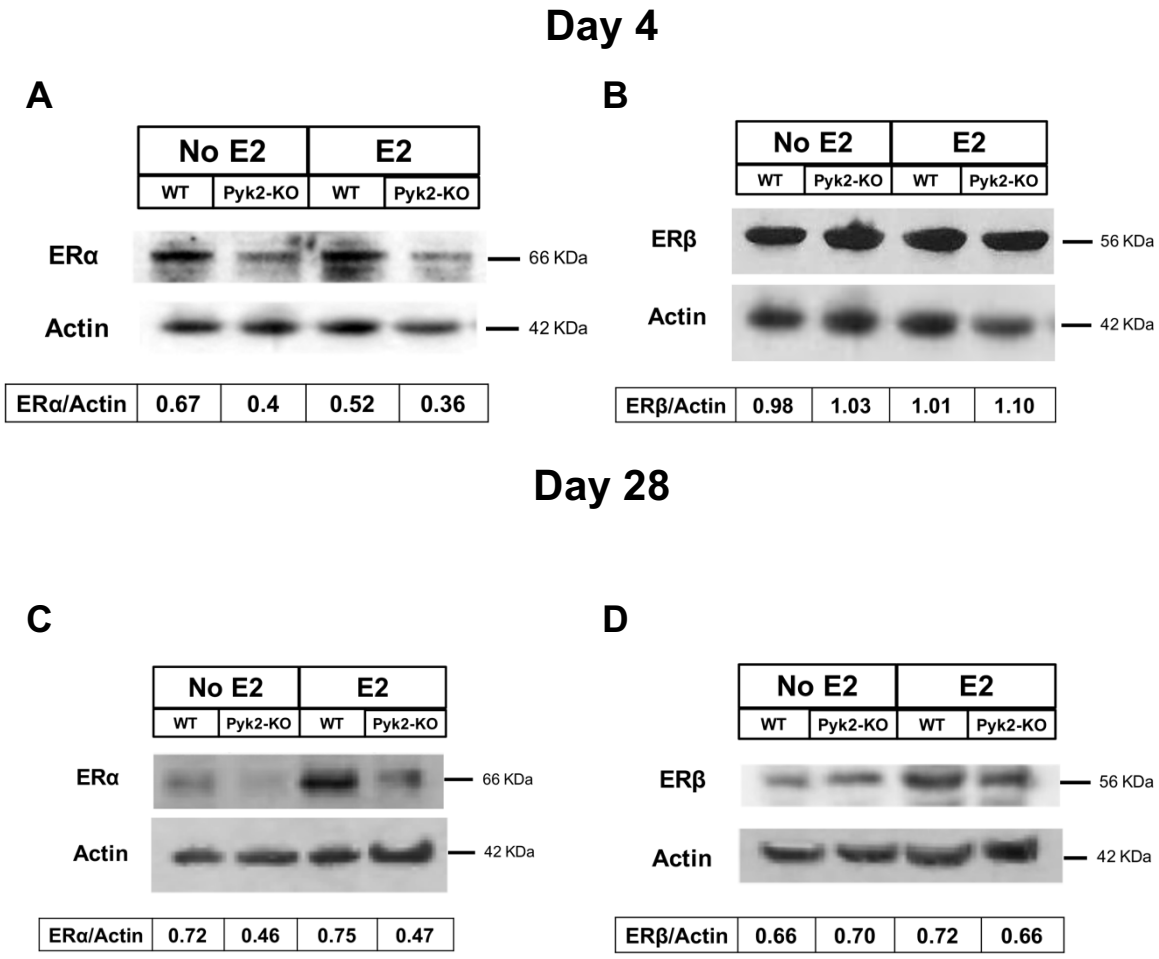

Figure 20. ERα and ERβ protein levels in WT and Pyk2-KO OBs in the presence or absence of E2.

WT and Pyk2-KO calvarial OBs were cultured for 4 (A and B) and 28 (C and D) days with or without 100 nM E2 supplementation. Western blotting was performed to determine ERα and ERβ protein expressions. Cells were lysed with mRIPA buffer, and then sonicated. The ratio of ERα or ERβ to β-actin was determined by densitometry using ImageJ software. Experiments were performed 4 times in a 4-day experiment and twice in a 28-day experiment and representative data are shown.

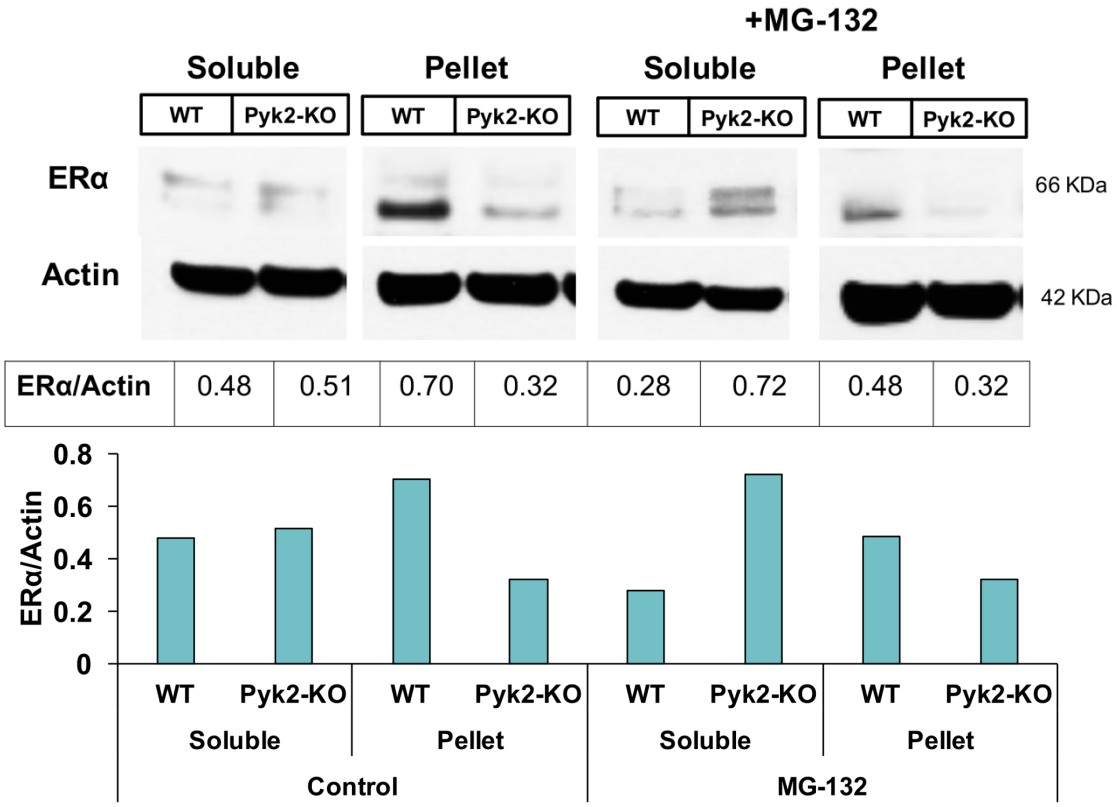

Figure 21. Effect of MG-132 on the subcellular distribution of ERα.

WT and Pyk2-KO calvarial OBs were cultured for 4 days, then a proteasome inhibitor, MG-132 (20 μM), was added for the final 3 hours of culture. Cells were lysed with mRIPA buffer and the soluble fraction was separated from the insoluble pellet fraction. Forty μg of soluble proteins and 20 μg of proteins from the pellet fraction were resolved by SDS-PAGE. Western blotting and densitometry was performed to determine the ratio of ERα/β-actin in WT and Pyk2-KO OBs in the presence or absence of MG-132. Experiments were performed twice and representative data are shown.

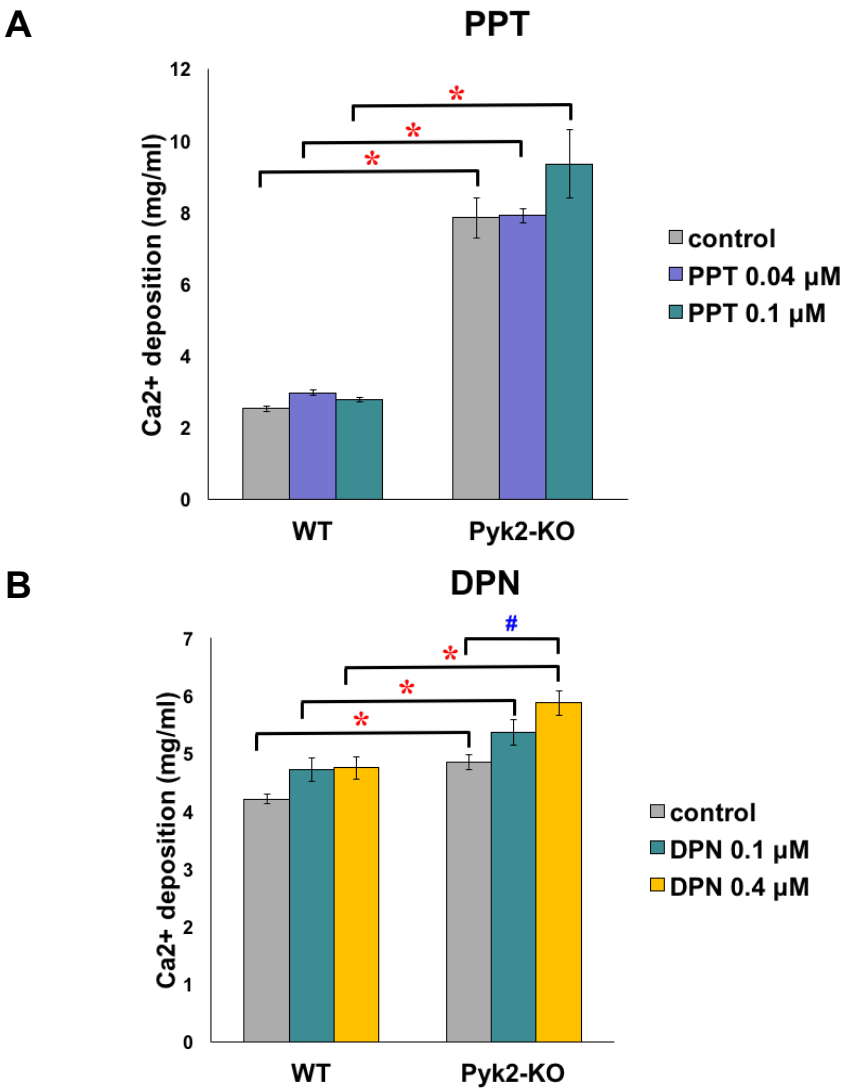

Figure 22. The effect of the activation of ERα and ERβ on OB mineralization. WT and Pyk2-KO calvarial OBs were cultured under osteogenic conditions for 21 days. An ERα-specific agonist (PPT; 0.04, 0.1, and 0.4 μM) or an ERβ-specific agonist (DPN; 0.1, and 0.4 μM) was added for the whole culture time. The effects of (A) PPT and (B) DPN on mineralization levels are shown. Experiments were performed twice, in triplicate, and representative data are shown. Asterisks (*) indicate statistical significance (p<0.05) between WT and Pyk2-KO OBs, whereas pound signs (#) indicate statistical significance of PPT or DPN supplementation ((p<0.05).

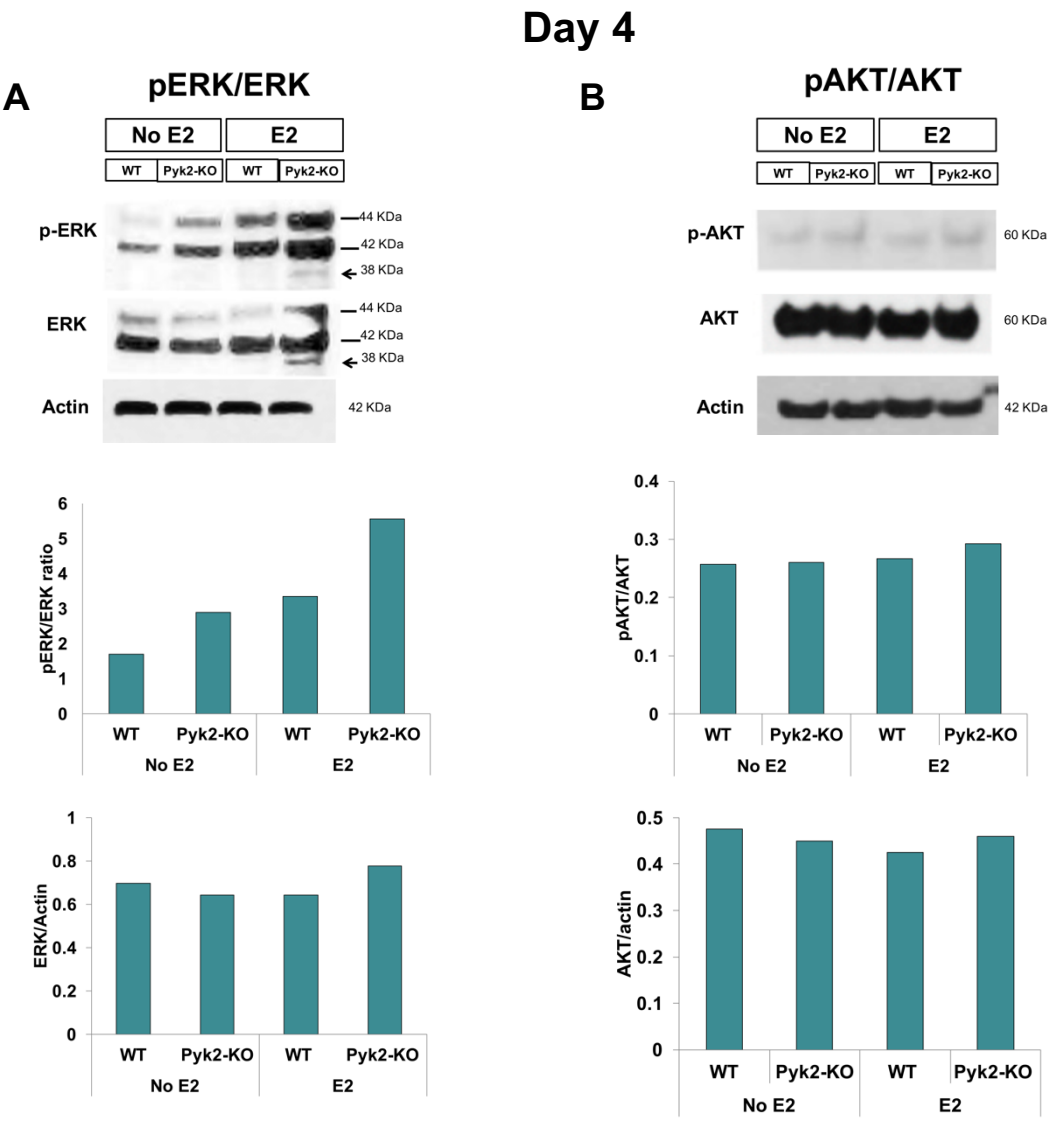

Figure 23. The effect of Pyk2-deletion and E2 on ERK and AKT phosphorylation in undifferentiated OBs.

WT and Pyk2-KO calvarial OBs were cultured for 4 days with or without 100 nM E2 supplementation, and then cell pellets were lysed with mRIPA buffer. Western blotting was performed to determine pERK, ERK, pAKT, AKT, and actin protein levels. The ratio of p-ERK/ERK, ERK/actin, pAKT/AKT, and AKT/actin are shown. Experiments were performed twice and representative data are shown. An additional band approximating the molecular weight of p-p38 and p38 was also detected with the p-ERK antibody, although the identify of this protein remains to be confirmed.

Day 21

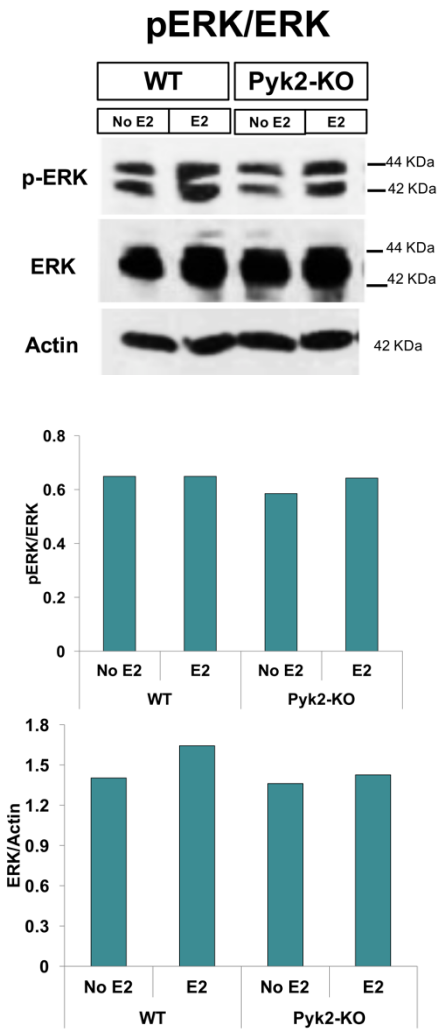

Figure 24. The effect of Pyk2-deletion and E2 on ERK phosphorylation in differentiated OBs for 21 days.

WT and Pyk2-KO calvarial OBs were cultured under osteogenic conditions for 21 days with or without 100 nM E2 supplementation, and then cell pellets were lysed with mRIPA buffer. Western blotting was performed to determine pERK, ERK, and actin protein levels. The ratio of p-ERK/ERK and ERK/actin are shown. Experiments were performed twice and representative data are shown.

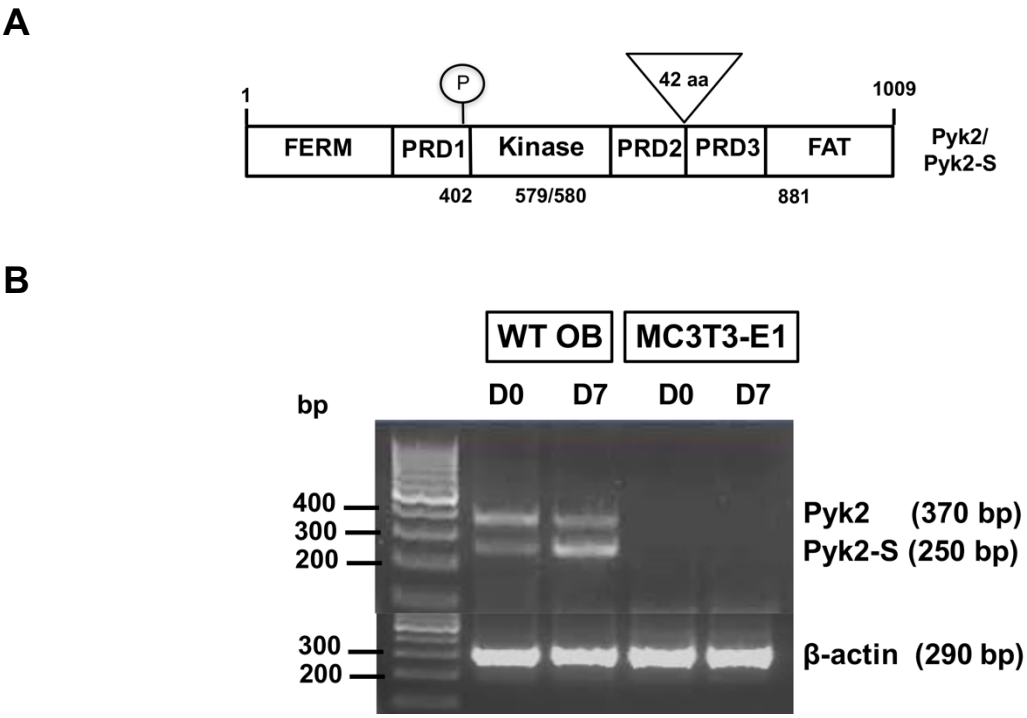

Figure 25. Pyk2 and Pyk2-S expression in primary OBs and MC3T3-E1 cells. (A) Schema of Pyk2 and Pyk2-S isoforms. (B) Calvarial OBs and MC3T3-E1 cells were cultured for 0-7 days. Ethidium bromide-stained gel shows the expression of Pyk2 and Pyk2-S mRNA expressions in calvarial OBs and MC3T3-E1 by RT-PCR. β-actin was used as the housekeeping control. Molecular weight standards are shown.

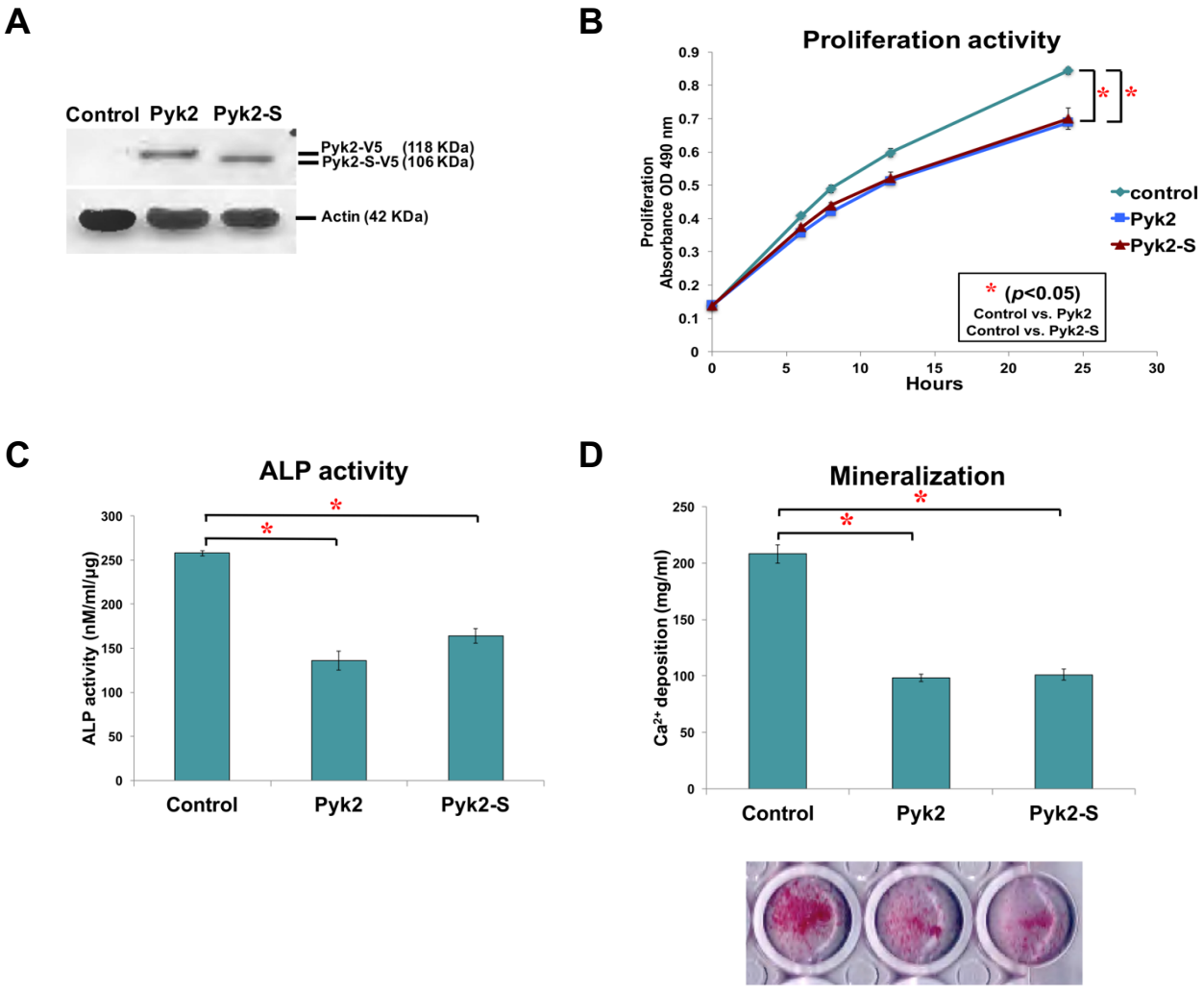

Figure 26. The effect of Pyk2 and Pyk2-S on OB proliferation, differentiation, and mineralization.

MC3T3-E1 cells were transiently transfected with expression constructs for Pyk2 or Pyk2-S. (A) Equivalent expression of Pyk2 and Pyk2-S proteins in MCT3-E1 cells was confirmed by Western blotting. (B) Results of MTS assay after 2 days of transfection, (C) Quantitative ALP activity assay of MCT3-E1 cells expressing Pyk2 or Pyk2-S cultured for 3 days in osteogenic media. (D) Alizarin Red S staining to determine quantitative mineralization after 3 days are shown. Experiments were performed three times and representative data are shown. Asterisks (*) indicate statistically significant differences ($p<0.05$).

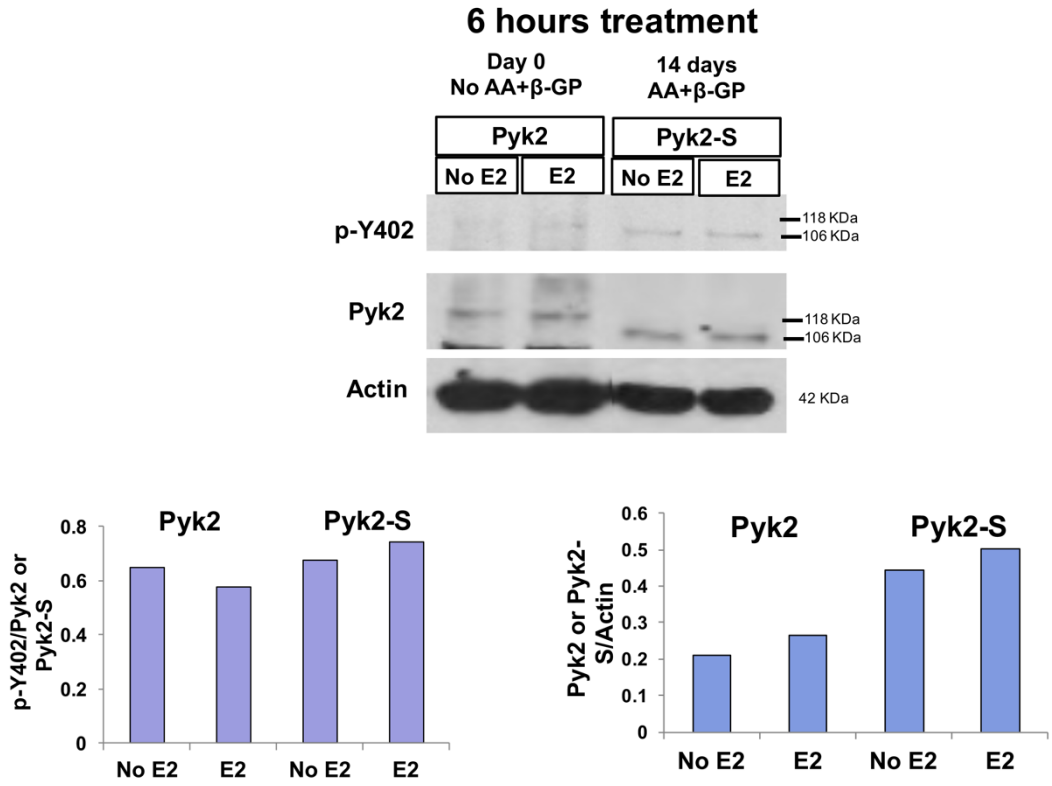

Figure 27. Expression of phospho-Y402 and Pyk2 isoforms in undifferentiated and differentiated OBs treated with E2 for 6 hours.

WT calvarial OBs were cultured under osteogenic conditions for 0 or 14 days and 100 nM E2 was added for the final 6 hours of culture. Western blotting was performed for Pyk2-Y402 phosphorylation (p-Y402) and total Pyk2. β–actin was used to normalize for protein loading. Densitometry was performed using ImageJ software and used to calculate the ratio of p-Y402/Pyk2, p-Y402/Pyk2-S, Pyk2/Actin, and Pyk2-S/Actin. Studies were replicated twice and representative data are shown. The two molecular weight isoforms of Pyk2 are indicated.

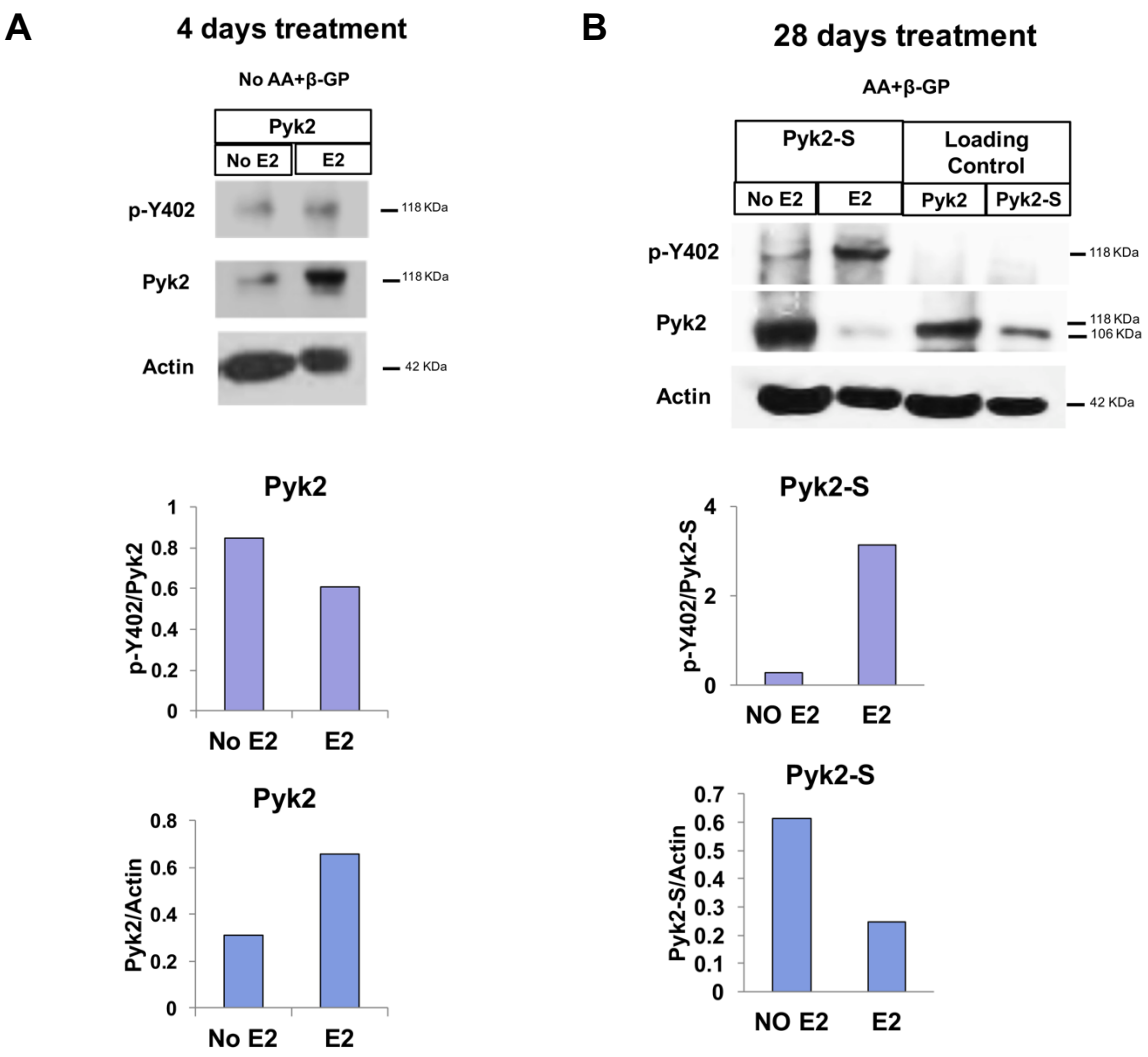

Figure 28. Expression of phospho-Y402 and Pyk2 isoforms in undifferentiated and differentiated OBs treated with E2 for 4 and 28 days.

(A) WT calvarial OBs were cultured in the presence or absence 100 nM E2 for 4 days. (B) WT calvarial OBs were differentiated in osteogenic media with or without 100 nM E2 for 28 days. Western blotting was performed for Pyk2-Y402 phosphorylation (p-Y402), total Pyk2 and β-actin. Densitometry was performed using ImageJ software and used to calculate the ratio of p-Y402/Pyk2, p-Y402/Pyk2-S, Pyk2/Actin, and Pyk2-S/Actin. Studies were replicated twice and representative data are shown. MC3T3-E1 cells expressing Pyk2 or Pyk2-S were used as a positive control for Western blotting.

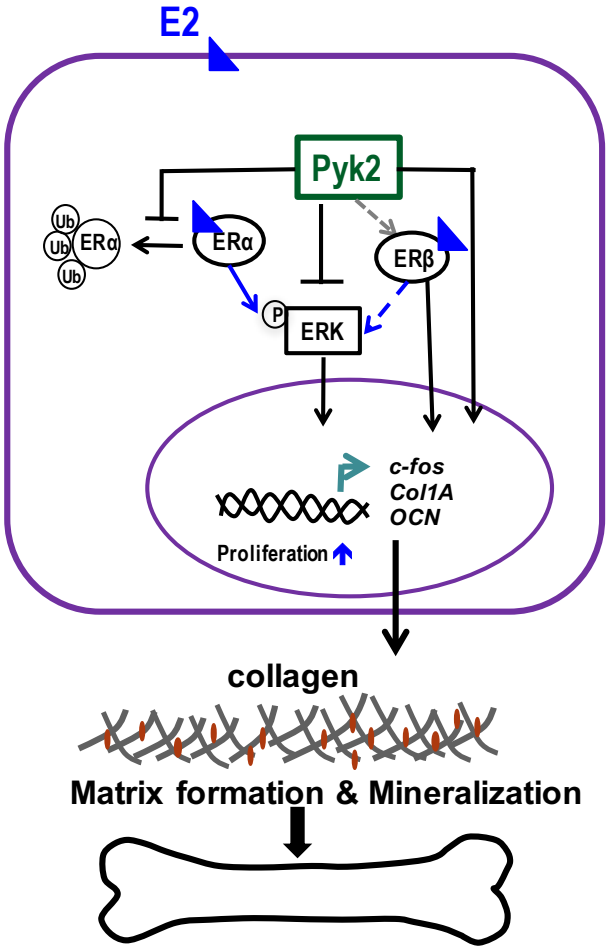

Figure 29. Working model for the mechanism of action of Pyk2 and E2 in OBs.

Pyk2 protects ERα protein degradation by the ubiquitin-proteasome pathway. In addition, Pyk2 inhibits ERK phosphorylation which consequently suppresses OB proliferation and differentiation. Pyk2 integrates to E2-ERα/ERβ signaling cascade via ERK pathway. Overall, our findings suggest Pyk2 negatively affects E2, ERα and ERK signaling in OBs. Thus, Pyk2 deletion combined with E2 stimulation has a positive effect on matrix formation and mineralization of OBs, resulting in a further increase in bone mass. Pyk2 and Pyk2-S (not shown) may exert unique effects on early and late stages of the OB differentiation process, respectively.

A

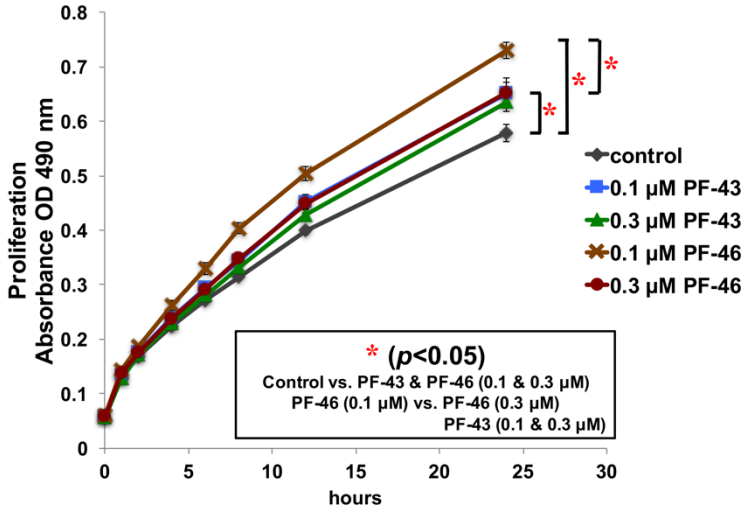
Proliferation Absorbance OD 490 nm
hours
control
0.1 μM PF-43
0.3 μM PF-43
0.1 μM PF-46
0.3 μM PF-46
* (p<0.05)
Control vs. PF-43 & PF-46 (0.1 & 0.3 μM)
PF-46 (0.1 μM) vs. PF-46 (0.3 μM)
PF-43 (0.1 & 0.3 μM)

B

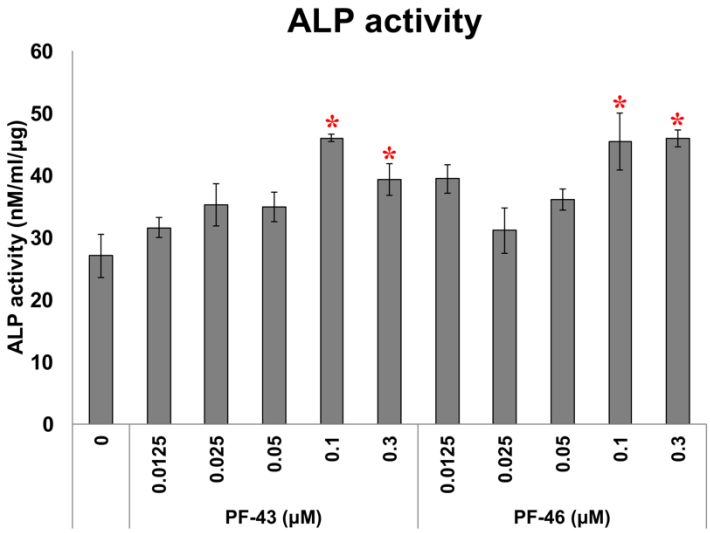
ALP activity
ALP activity (nM/ml/μg)
PF-43 (μM)
PF-46 (μM)

C

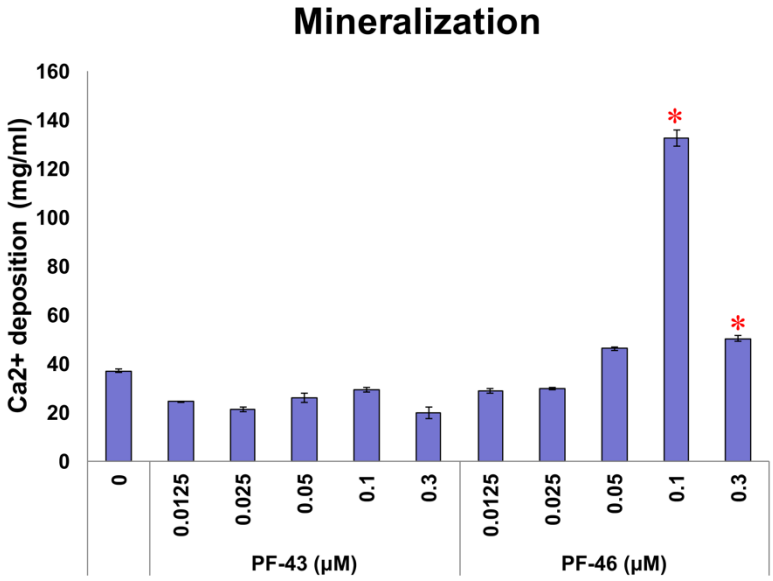
Mineralization
Ca2+ deposition (mg/ml)
PF-43 (μM)
PF-46 (μM)

Figure 30. The efficacy of Pyk2 inhibitors, PF-43 and PF-46, on the activity of bone marrow derived MSCs.

(A) MSCs were treated with a dual FAK/Pyk2 inhibitor (PF-43) or a Pyk2-targeted inhibitor (PF-46) at 0.1 and 0.3 μM for 24 hours, and then proliferation activity was determined using the MTS assay. (B; C) MSCs were differentiated into mature OBs under osteogenic conditions for 7 or 21 days in the presence or absence of PF-43 or PF-46, and the ALP activity and mineralization assays were performed, respectively. The data are shown as mean and SEM of triplicate samples. Experiments were performed a minimum of three times and representative data are shown. Asterisks (*) indicate statistical significance ($p<0.05$).

A

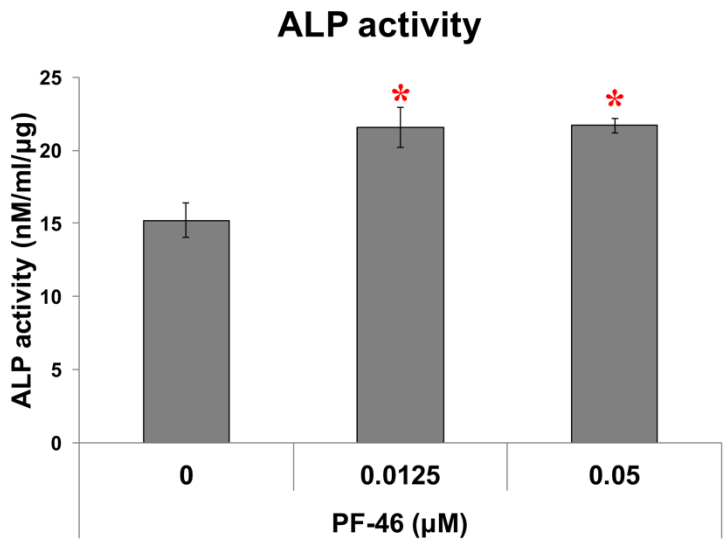

B

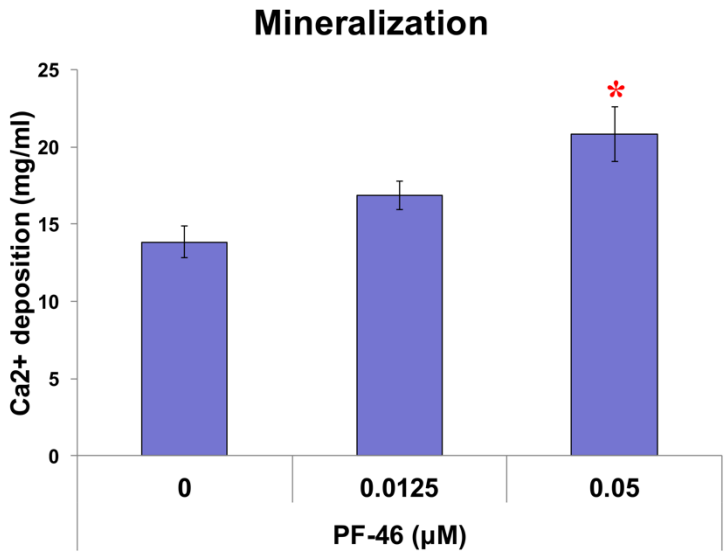

Figure 31. The efficacy of Pyk2 inhibitor, PF-46, on calvarial OB activity. Calvarial OBs were differentiated under osteogenic conditions for 7 or 21 days in the presence or absence of a Pyk2-targeted inhibitor, PF-46, at 0.0125 and 0.05 µM. (A) The quantitative ALP activity assay and (B) the mineralization assay were performed. The data are shown as mean and SEM of triplicate samples. Experiments were performed three times and representative data are shown. Asterisks (*) indicate statistical significance ($p<0.05$).

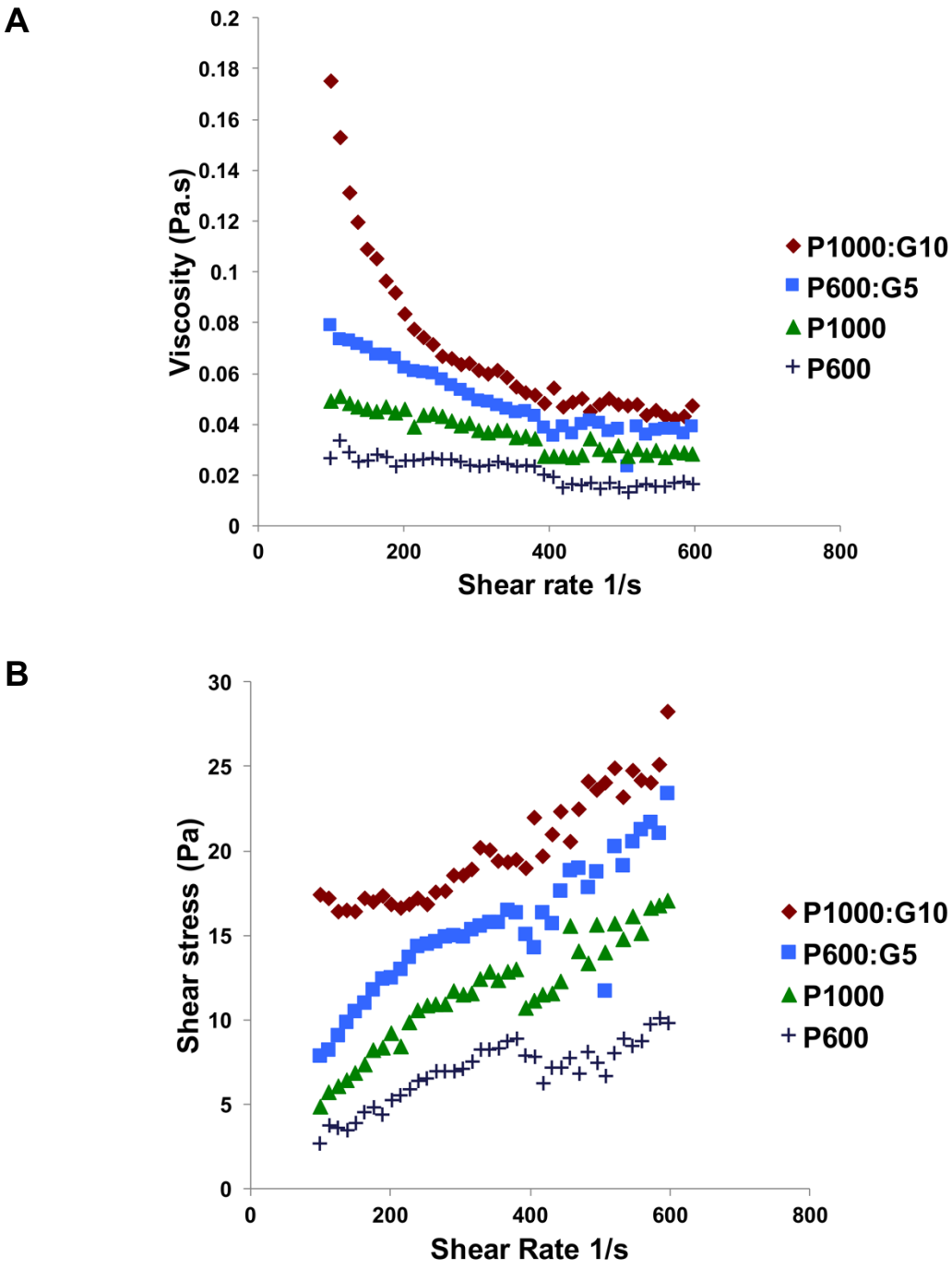

Figure 32. The dynamic viscosity of PEGDA and PEGDA-gelatin hydrogels. The dynamic viscosity of P600, P600:G5, P1000, and P1000:G10 prepolymer solutions was measured using a digital rheometer (viscometry mode) at room temperature. The plots of (A) viscosity vs. shear rate, and (B) shear stress vs. shear rate of a representative sample from each group are shown.

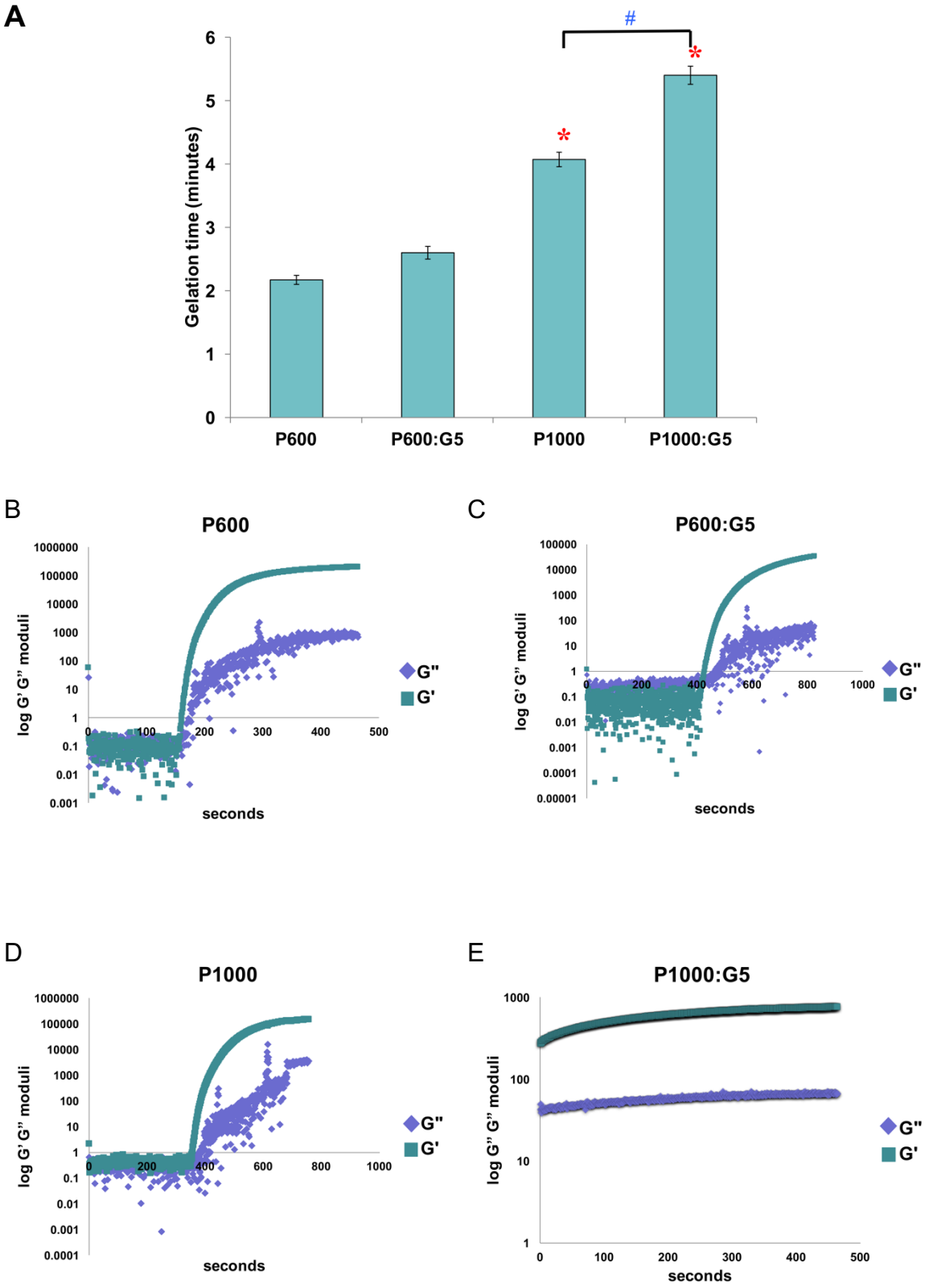
A
Gelation time (minutes)
P600
P600:G5
P1000
P1000:G5
#
*
B
P600
log G' G" moduli
seconds
G"
G'
C
P600:G5
D
P1000
E
P1000:G5

Figure 33. The gelation times of PEGDA and PEGDA-gelatin hydrogels.
(A) P600, P600:G5, P1000, and P1000:G10 prepolymer solutions were prepared and pipetted into a disk-shaped mold of 5 mm in diameter and 3 mm in thickness and exposed under visible light at room temperature. Gelation times were determined using a periodontal probe to verify the hardened material surfaces. The data are shown as mean and SEM of five samples (N=5). Asterisks (*) indicate statistical significant differences between different molecular weights of PEGDA, while the pound sign (#) shows significance for the effect of gelatin (p<0.05). (B to E) The *in situ* photorheometry was performed in four groups of prepolymer solutions using a digital rheometer with a light cure attachment at room temperature. Gelation times were defined as the time when storage modulus (G′) crossover loss modulus (G″), and the plots of log G' and G" moduli vs. time of a representative sample from each group are shown.

A

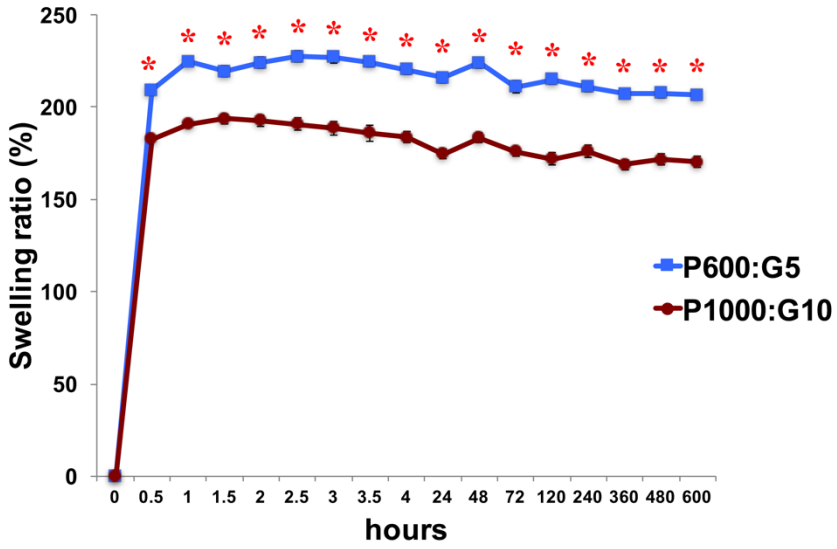

B

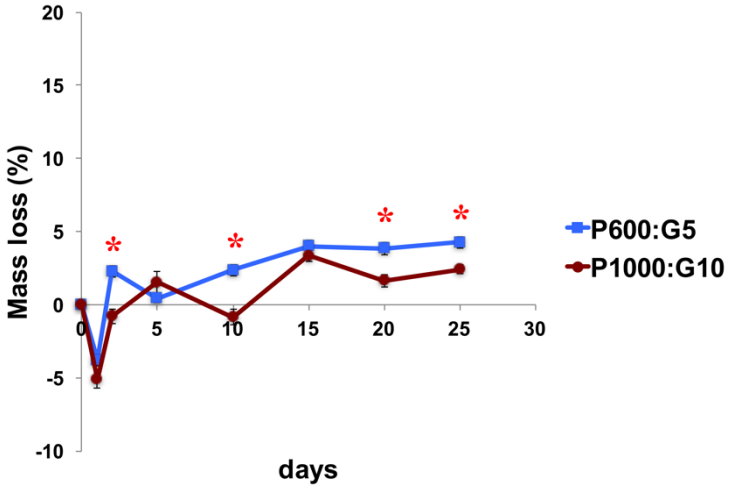

Figure 34. The swelling ratio and degradation of PEGDA-gelatin hydrogels. (A) P600:G5 and P1000:G10 gels were prepared and dried under the vacuum for 48 hours before soaking gels in PBS at 37°C and weight measuring up to 25 days. (B) The degradation of P600:G5 and P1000:G10 gels were also evaluated using the same method as the swelling experiment. The data are shown as mean and SEM of five samples (N=5). Experiments were performed twice and representative data are shown. Asterisks (*) indicate statistical significance (p<0.05).

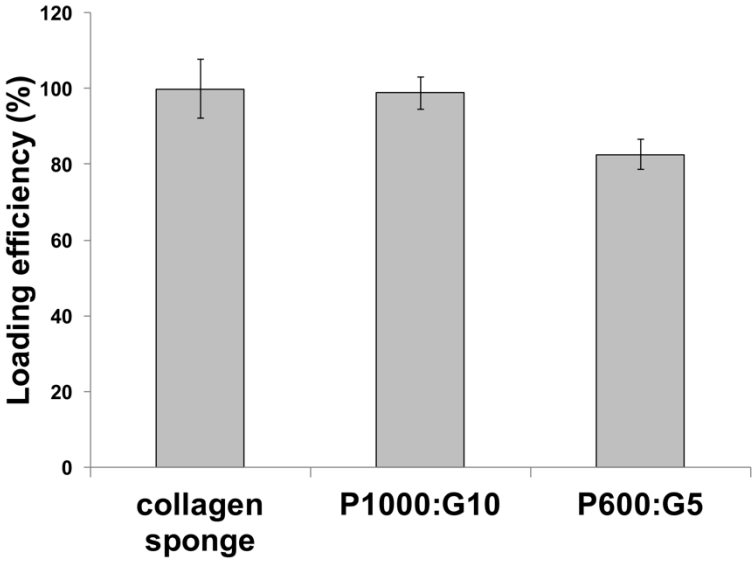

Figure 35. The loading efficiency of 7-amino-4-methylcoumarin in hydrogels. 7-amino-4-methylcoumarin was used as a representative of PF-46 and loaded into P600:G5 or P1000:G10 prepolymer solution before photopolymerization, or were dripped on collagen sponge (control) (N=5). Samples were then incubated in PBS at 37°C for 24 hours, and then were completely disrupted using a sonicator. The total amount of eluted dye was measured using a fluorescence spectrophotometer.

A

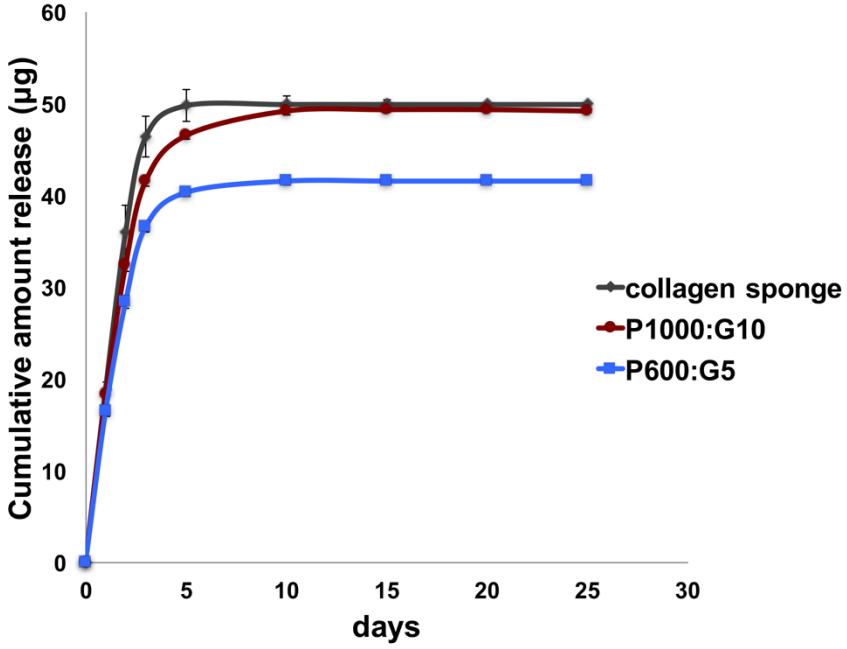
Cumulative amount release (µg)
60
50
40
30
20
10
0
0
5
10
15
20
25
30
days
collagen sponge
P1000:G10
P600:G5

B

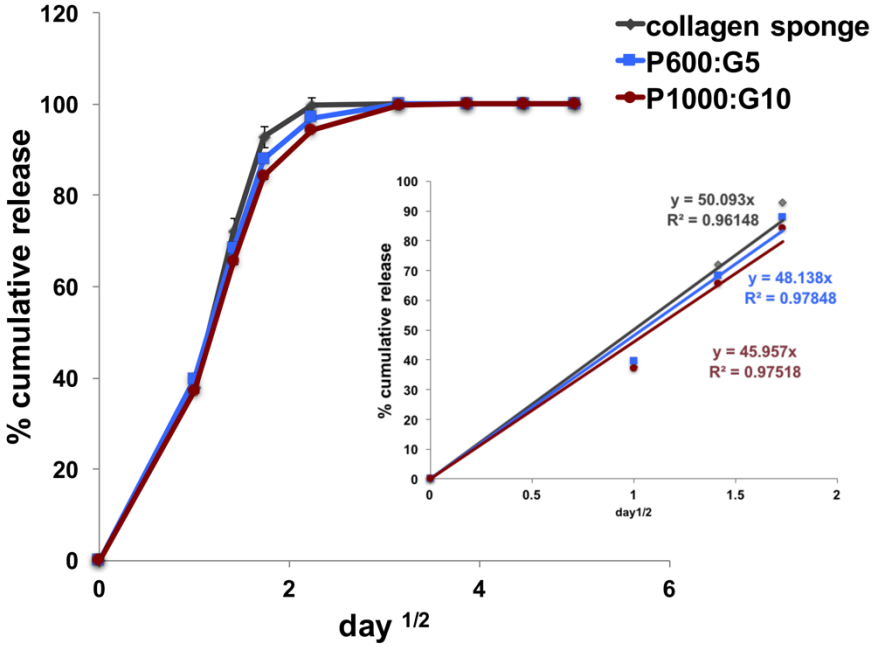
% cumulative release
120
100
80
60
40
20
0
0
2
4
6
day 1/2
collagen sponge
P600:G5
P1000:G10
y = 50.093x
R² = 0.96148
y = 48.138x
R² = 0.97848
y = 45.957x
R² = 0.97518
% cumulative release
day1/2
0
0.5
1
1.5
2

Figure 36. The release profiles of 7-amino-4-methylcoumarin loaded PEGDA-gelatin hydrogels.

7-amino-4-methylcoumarin was used as a representative of PF-46 and loaded into P600:G5, P1000:G10, or collagen sponge (control) (N=5). Carriers were then incubated in PBS at 37°C, and eluted dye was collected every 30 minutes up to 4 hours and at days 1, 2, 3, 5, 10, 15, 20, and 25. (A) The cumulative amount of dye released from carriers is shown. (B) The plots of % cumulative release vs. time square root of the three candidate carriers are shown for the whole period of release. The insert shows the plot of the first 60% cumulative release vs. time square root of all carriers. The correlation efficient (R^2) and slope (y) for each candidate are also indicated.

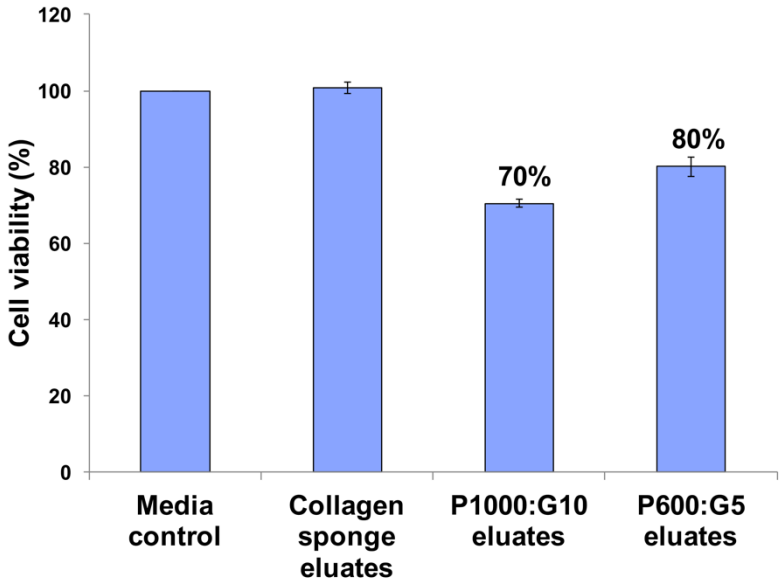

Figure 37. *In vitro* cytotoxicity of PEGDA-gelatin containing eluates.
P600:G5, P1000:G10 and collagen sponge disks were prepared and immersed in α-MEM supplemented with 10% FBS and 1%P/S at 37ºC for 24 hours, and eluates were collected. MC3T3-E1 cells were then cultured in the presence or absence of eluates for 24 hours and MTS assay was performed to determine the cytotoxicity of eluates. Non-treated MC3T3-E1 cells were used as a positive control. The data are shown as mean and SEM of five samples (N=5). Experiments were performed twice and representative data are shown.

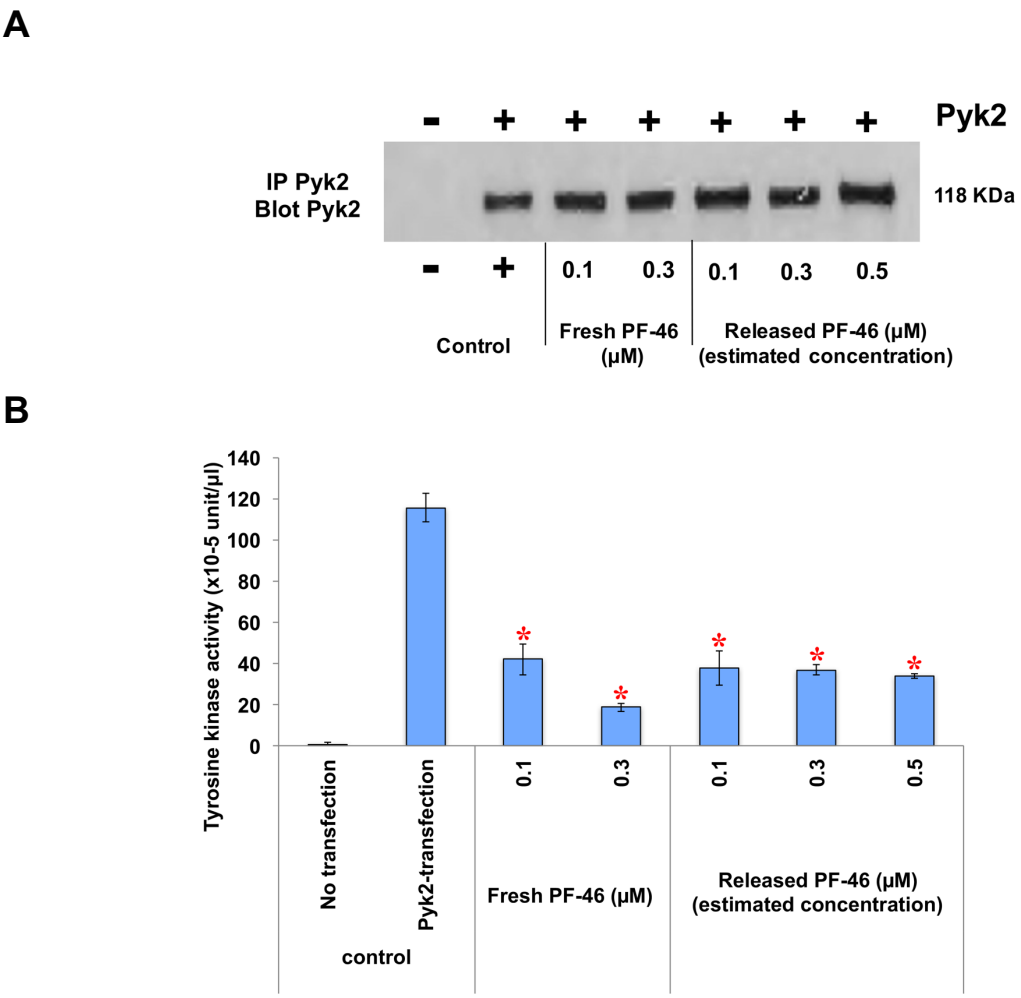

Figure 38. Inhibition of Pyk2 tyrosine kinase activity by the released PF-46. PF-46 loaded P1000:G10 gels were immersed in α-MEM supplemented with 10% FBS and 1%P/S at 37ºC for 24 hours, and released PF-46 were collected. 293 VnR cells were transfected with Pyk2 cDNA for 3 days and then treated with released PF-46 at different concentrations for 2 hours. (A) Pyk2 immunoprecipitates (IP) from cells were immunoblotted for Pyk2 as controls. (B) The effect of released PF-46 on the intracellular Pyk2 tyrosine kinase activity was examined using Universal Tyrosine Kinase Assay Kit. The data are shown as mean and SEM of five samples (N=5). Experiments were performed twice and representative data are shown. Asterisks (*) indicate statistically significant differences from the Pyk2 transfection control group (p<0.05).

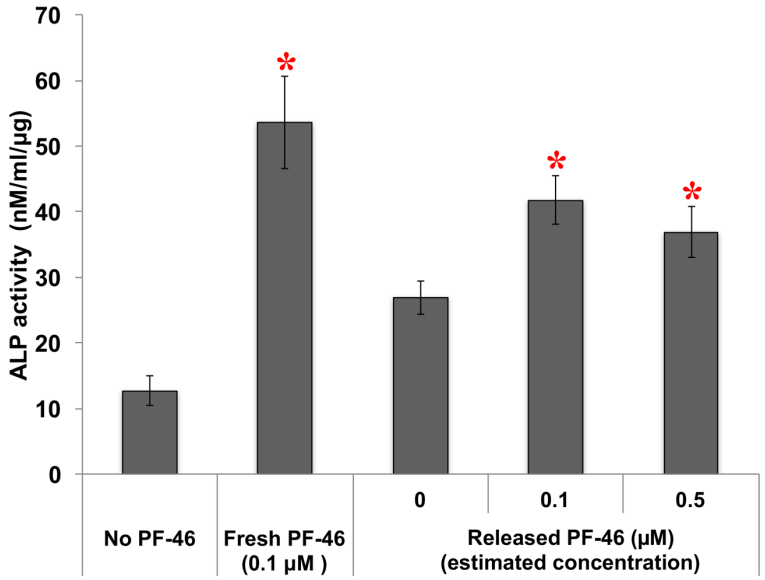

Figure 39. Effect of released PF-46 on ALP activity in OBs.

PF-46 loaded P1000:G10 gels were immersed in α-MEM supplemented with 10% FBS and 1%P/S at 37ºC for 24 hours, and released PF-46 were collected. Bone marrow derived MSCs were differentiated into mature OBs under osteogenic conditions for 7 days in the presence or absence of released PF-46 at various concentrations, and ALP activity assay was performed. Fresh PF-46 was used as positive controls, and untreated cells were used as the negative control. The data are shown as mean and SEM of five samples (N=5). Experiments were performed twice and representative data are shown. Asterisks (*) indicate statistically significant differences from the negative control (p<0.05).

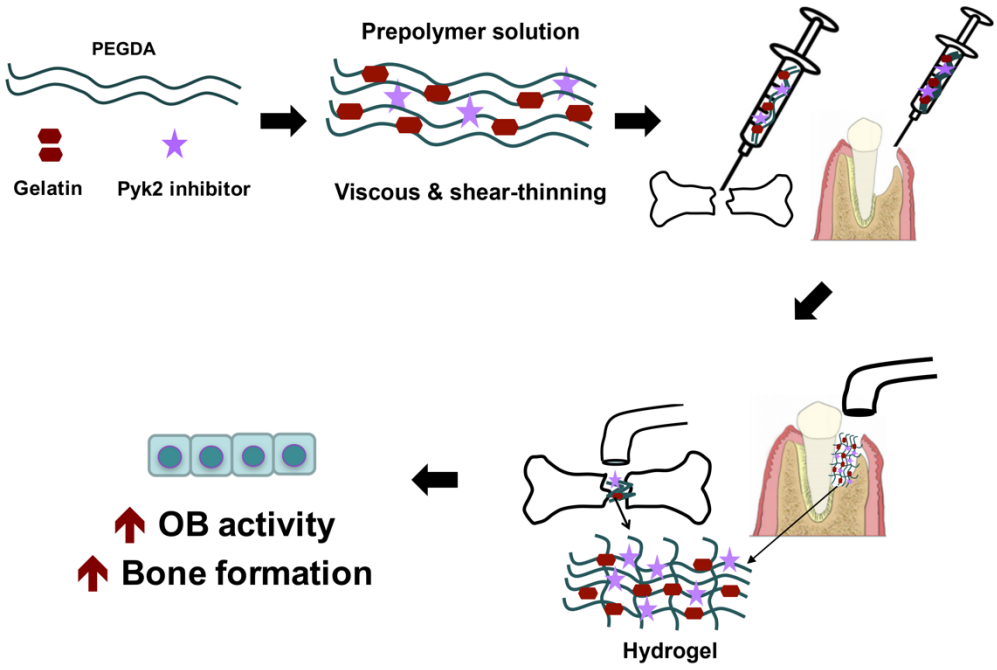

Figure 40. Schema of Pyk2-inhibitor loaded hydrogel preparation and utilization.

The PEGDA-gelatin prepolymer solution exhibits high viscosity, yield stress, and shear-thinning behavior, which is suitable for injectable delivery, keeping the solution within the defect site prior to photopolymerization. Importantly, a Pyk2-targeted inhibitor incorporated into PEGDA-hydrogel enhances OB activity, which strongly supports the use of a Pyk2 inhibitor-loaded hydrogel for future bone regeneration studies.

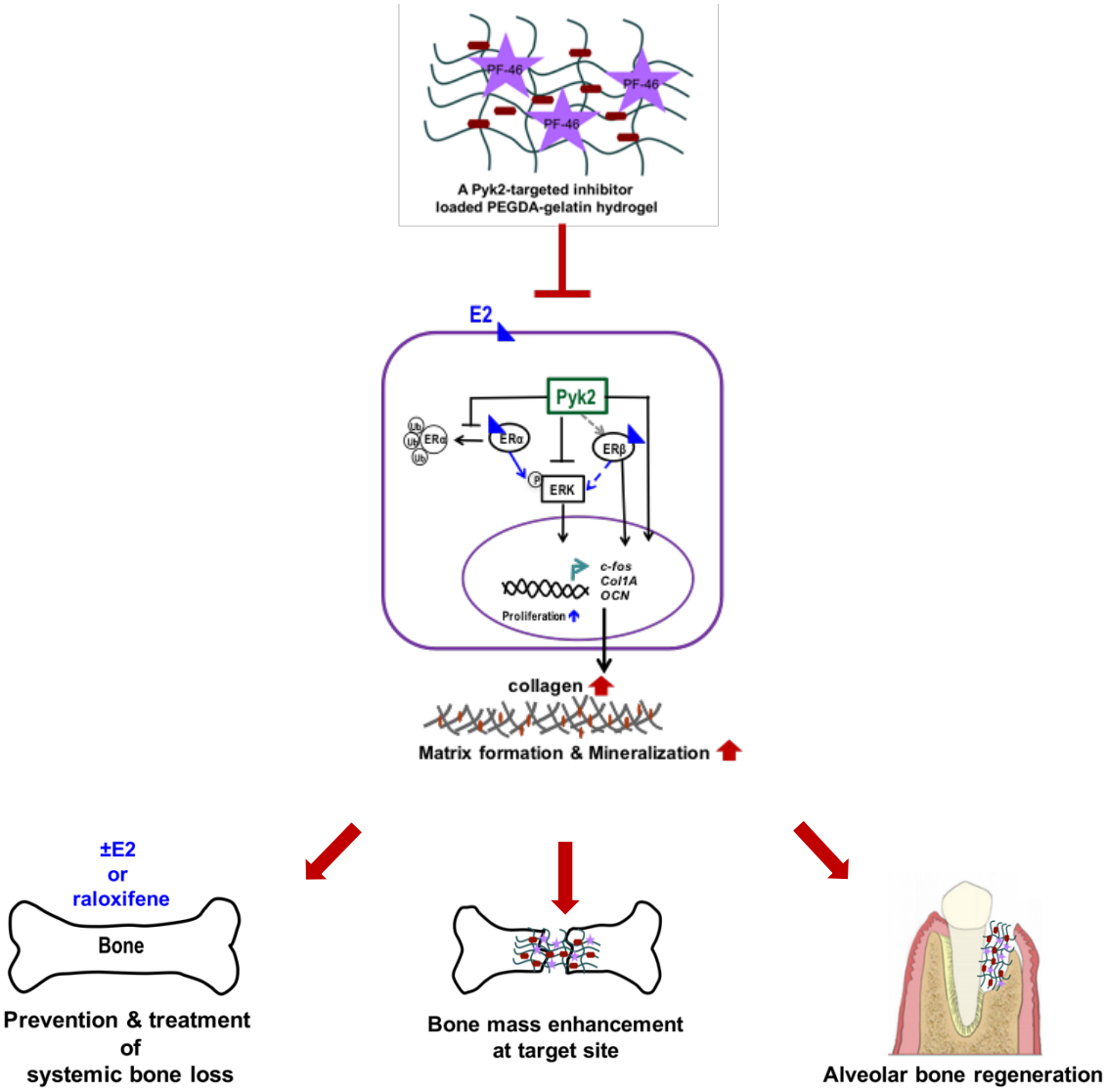

Figure 41. Schematic illustrating the key findings from Chapter 3 and Chapter 4 and the potential clinical applications.

A Pyk2-targeted inhibitor loaded PEGDA-gelatin hydrogel inhibits Pyk2 activity and enhances OB activity. We propose the Pyk2 inhibitor will act in a similar manner as genetic deletion of Pyk2 to augments bone formation. Thus, the inhibition of Pyk2 locally with hydrogel delivery may be a therapeutic tool for bone regeneration at sites of craniofacial bone and the other skeletal defects. Furthermore, therapeutic strategies that target Pyk2 at the systemic level, with or without with estrogen or raloxifene supplementation may improve bone mass in low bone mass diseases such as osteoporosis.

REFERENCES

Alford AI, Kozloff KM, Hankenson KD. 2015. Extracellular matrix networks in bone remodeling. The international journal of biochemistry & cell biology. 65:20-31.

Allen JG, Fotsch C, Babij P. 2010. Emerging targets in osteoporosis disease modification. Journal of medicinal chemistry. 53(11):4332-4353.

Allen JG, Lee MR, Han CY, Scherrer J, Flynn S, Boucher C, Zhao H, O'Connor AB, Roveto P, Bauer D et al. 2009. Identification of small molecule inhibitors of proline-rich tyrosine kinase 2 (pyk2) with osteogenic activity in osteoblast cells. Bioorganic & medicinal chemistry letters. 19(17):4924-4928.

Almeida M, Han L, Martin-Millan M, Plotkin LI, Stewart SA, Roberson PK, Kousteni S, O'Brien CA, Bellido T, Parfitt AM et al. 2007. Skeletal involution by age-associated oxidative stress and its acceleration by loss of sex steroids. The Journal of biological chemistry. 282(37):27285-27297.

Almeida M, Iyer S, Martin-Millan M, Bartell SM, Han L, Ambrogini E, Onal M, Xiong J, Weinstein RS, Jilka RL et al. 2013. Estrogen receptor-alpha signaling in osteoblast progenitors stimulates cortical bone accrual. The Journal of clinical investigation. 123(1):394-404.

Amini AR, Laurencin CT, Nukavarapu SP. 2012. Bone tissue engineering: Recent advances and challenges. Critical reviews in biomedical engineering. 40(5):363-408.

Anderson HC, Garimella R, Tague SE. 2005. The role of matrix vesicles in growth plate development and biomineralization. Frontiers in bioscience : a journal and virtual library. 10:822-837.

Armstrong VJ, Muzylak M, Sunters A, Zaman G, Saxon LK, Price JS, Lanyon LE. 2007. Wnt/beta-catenin signaling is a component of osteoblastic bone cell early responses to load-bearing and requires estrogen receptor alpha. The Journal of biological chemistry. 282(28):20715-20727.

Arts J, Kuiper GG, Janssen JM, Gustafsson JA, Lowik CW, Pols HA, van Leeuwen JP. 1997. Differential expression of estrogen receptors alpha and beta mrna during differentiation of human osteoblast sv-hfo cells. Endocrinology. 138(11):5067-5070.

Asghar W, Islam M, Wadajkar AS, Wan Y, Ilyas A, Nguyen KT, Iqbal SM. 2012. Plga micro-and nanoparticles loaded into gelatin scaffold for controlled drug release. IEEE Transactions on Nanotectology. 11(3):546-553.

Aubin JE. 1998. Advances in the osteoblast lineage. Biochemistry and cell biology = Biochimie et biologie cellulaire. 76(6):899-910.

Aubin JE, Liu F, Malaval L, Gupta AK. 1995. Osteoblast and chondroblast differentiation. Bone. 17(2 Suppl):77S-83S.

Ayala-Pena VB, Scolaro LA, Santillan GE. 2013. Atp and utp stimulate bone morphogenetic protein-2,-4 and -5 gene expression and mineralization by rat primary osteoblasts involving pi3k/akt pathway. Experimental cell research. 319(13):2028-2036.

Bae JW, Choi JH, Lee Y, Park KD. 2015. Horseradish peroxidase-catalysed in situ-forming hydrogels for tissue-engineering applications. Journal of tissue engineering and regenerative medicine. 9(11):1225-1232.

Bagi CM, Roberts GW, Andresen CJ. 2008. Dual focal adhesion kinase/pyk2 inhibitor has positive effects on bone tumors: Implications for bone metastases. Cancer. 112(10):2313-2321.

Barrett-Connor E, Mosca L, Collins P, Geiger MJ, Grady D, Kornitzer M, McNabb MA, Wenger NK. 2006. Effects of raloxifene on cardiovascular events and breast cancer in postmenopausal women. The New England journal of medicine. 355(2):125-137.

Bellido T, Plotkin LI. 2011. Novel actions of bisphosphonates in bone: Preservation of osteoblast and osteocyte viability. Bone. 49(1):50-55.

Berthois Y, Katzenellenbogen JA, Katzenellenbogen BS. 1986. Phenol red in tissue culture media is a weak estrogen: Implications concerning the study of estrogen-responsive cells in culture. Proceedings of the National Academy of Sciences of the United States of America. 83(8):2496-2500.

Bigi A, Cojazzi G, Panzavolta S, Rubini K, Roveri N. 2001. Mechanical and thermal properties of gelatin films at different degrees of glutaraldehyde crosslinking. Biomaterials. 22(8):763-768.

Bigi A, Panzavolta S, Rubini K. 2004. Relationship between triple-helix content and mechanical properties of gelatin films. Biomaterials. 25(25):5675-5680.

Bonnelye E, Aubin JE. 2002. Differential expression of estrogen receptor-related receptor alpha and estrogen receptors alpha and beta in osteoblasts in vivo and in vitro. Journal of bone and mineral research : the official journal of the American Society for Bone and Mineral Research. 17(8):1392-1400.

Bonnelye E, Merdad L, Kung V, Aubin JE. 2001. The orphan nuclear estrogen receptor-related receptor alpha (erralpha) is expressed throughout osteoblast differentiation and regulates bone formation in vitro. The Journal of cell biology. 153(5):971-984.

Bord S, Horner A, Beavan S, Compston J. 2001. Estrogen receptors alpha and beta are differentially expressed in developing human bone. The Journal of clinical endocrinology and metabolism. 86(5):2309-2314.

Bord S, Ireland DC, Beavan SR, Compston JE. 2003. The effects of estrogen on osteoprotegerin, rankl, and estrogen receptor expression in human osteoblasts. Bone. 32(2):136-141.

Bose S, Tarafder S. 2012. Calcium phosphate ceramic systems in growth factor and drug delivery for bone tissue engineering: A review. Acta biomaterialia. 8(4):1401-1421.

Boutahar N, Guignandon A, Vico L, Lafage-Proust MH. 2004. Mechanical strain on osteoblasts activates autophosphorylation of focal adhesion kinase and proline-rich tyrosine kinase 2 tyrosine sites involved in erk activation. The Journal of biological chemistry. 279(29):30588-30599.

Boyce BF, Xing L. 2008. Functions of rankl/rank/opg in bone modeling and remodeling. Archives of biochemistry and biophysics. 473(2):139-146.

Boyle WJ, Simonet WS, Lacey DL. 2003. Osteoclast differentiation and activation. Nature. 423(6937):337-342.

Braidman IP, Hainey L, Batra G, Selby PL, Saunders PT, Hoyland JA. 2001. Localization of estrogen receptor beta protein expression in adult human bone. Journal of bone and mineral research : the official journal of the American Society for Bone and Mineral Research. 16(2):214-220.

Bruzzaniti A, Neff L, Sandoval A, Du L, Horne WC, Baron R. 2009. Dynamin reduces pyk2 y402 phosphorylation and src binding in osteoclasts. Molecular and cellular biology. 29(13):3644-3656.

Bruzzaniti A, Neff L, Sanjay A, Horne WC, De Camilli P, Baron R. 2005. Dynamin forms a src kinase-sensitive complex with cbl and regulates podosomes and osteoclast activity. Molecular biology of the cell. 16(7):3301-3313.

Buckbinder L, Crawford DT, Qi H, Ke HZ, Olson LM, Long KR, Bonnette PC, Baumann AP, Hambor JE, Grasser WA, 3rd et al. 2007. Proline-rich tyrosine kinase 2 regulates osteoprogenitor cells and bone formation, and offers an anabolic treatment approach for osteoporosis. Proceedings of the National Academy of Sciences of the United States of America. 104(25):10619-10624.

Burmania JA, Martinez-Diaz GJ, Kao WJ. 2003. Synthesis and physicochemical analysis of interpenetrating networks containing modified gelatin and poly(ethylene glycol) diacrylate. Journal of biomedical materials research Part A. 67(1):224-234.

Burr D, Allen M. 2013. Basic and applied bone biology. Burr D, M. A, editors. China: Elsevier.

Cai Y, Yu X, Hu S, Yu J. 2009. A brief review on the mechanisms of mirna regulation. Genomics, proteomics & bioinformatics. 7(4):147-154.

Callige M, Richard-Foy H. 2006. Ligand-induced estrogen receptor alpha degradation by the proteasome: New actors? Nuclear receptor signaling. 4:e004.

Cao L, Bu R, Oakley JI, Kalla SE, Blair HC. 2003. Estrogen receptor-beta modulates synthesis of bone matrix proteins in human osteoblast-like mg63 cells. Journal of cellular biochemistry. 89(1):152-164.

Carroll JS, Meyer CA, Song J, Li W, Geistlinger TR, Eeckhoute J, Brodsky AS, Keeton EK, Fertuck KC, Hall GF et al. 2006. Genome-wide analysis of estrogen receptor binding sites. Nature genetics. 38(11):1289-1297.

Chai F, Liang Y, Bi J, Chen L, Zhang F, Cui Y, Jiang J. 2015. Reggamma regulates eralpha degradation via ubiquitin-proteasome pathway in breast cancer. Biochemical and biophysical research communications. 456(1):534-540.

Chang WH, Chang Y, Lai PH, Sung HW. 2003. A genipin-crosslinked gelatin membrane as wound-dressing material: In vitro and in vivo studies. Journal of biomaterials science Polymer edition. 14(5):481-495.

Chen CH, Chang CH, Wang KC, Su CI, Liu HT, Yu CM, Wong CB, Wang IC, Whu SW, Liu HW. 2011. Enhancement of rotator cuff tendon-bone healing with injectable periosteum progenitor cells-bmp-2 hydrogel in vivo. Knee surgery, sports traumatology, arthroscopy : official journal of the ESSKA. 19(9):1597-1607.

Chen FP, Hsu T, Hu CH, Wang WD, Wang KC, Teng LF. 2004. Expression of estrogen receptors alpha and beta in human osteoblasts: Identification of exon-2 deletion variant of estrogen receptor beta in postmenopausal women. Chang Gung medical journal. 27(2):107-115.

Cheng MZ, Rawlinson SC, Pitsillides AA, Zaman G, Mohan S, Baylink DJ, Lanyon LE. 2002. Human osteoblasts' proliferative responses to strain and 17beta-estradiol are mediated by the estrogen receptor and the receptor for insulin-like growth factor i. Journal of bone and mineral research : the official journal of the American Society for Bone and Mineral Research. 17(4):593-602.

Cheng YH, Hooker RA, Nguyen K, Gerard-O'Riley R, Waning DL, Chitteti BR, Meijome TE, Chua HL, Plett AP, Orschell CM et al. 2013. Pyk2 regulates megakaryocyte-induced increases in osteoblast number and bone formation. Journal of bone and mineral research : the official journal of the American Society for Bone and Mineral Research. 28(6):1434-1445.

Chesnut CH, 3rd, Silverman S, Andriano K, Genant H, Gimona A, Harris S, Kiel D, LeBoff M, Maricic M, Miller P et al. 2000. A randomized trial of nasal spray salmon calcitonin in postmenopausal women with established osteoporosis: The prevent recurrence of osteoporotic fractures study. Proof study group. The American journal of medicine. 109(4):267-276.

Choi B, Loh XJ, Tan A, Loh CK, Ye E, Joo MK, Jeong B. 2015. Introduction to in situ forming hydrogels for biomedical applications. In: Loh JX, editor. In-situ gelling polymers: For biomedical applications. Singapore: Springer Singapore. p. 5-35.

Chu TM, Warden SJ, Turner CH, Stewart RL. 2007. Segmental bone regeneration using a load-bearing biodegradable carrier of bone morphogenetic protein-2. Biomaterials. 28(3):459-467.

Cohen FJ, Watts S, Shah A, Akers R, Plouffe L, Jr. 2000. Uterine effects of 3-year raloxifene therapy in postmenopausal women younger than age 60. Obstetrics and gynecology. 95(1):104-110.

Compston JE. 2001. Sex steroids and bone. Physiological reviews. 81(1):419-447.

Cooper G. 2000. The cell: A molecular approach. Sinauer Associates.

Cummings SR, San Martin J, McClung MR, Siris ES, Eastell R, Reid IR, Delmas P, Zoog HB, Austin M, Wang A et al. 2009. Denosumab for prevention of fractures in postmenopausal women with osteoporosis. The New England journal of medicine. 361(8):756-765.

Das S, Crockett JC. 2013. Osteoporosis - a current view of pharmacological prevention and treatment. Drug design, development and therapy. 7:435-448.

Dash S, Murthy PN, Nath L, Chowdhury P. 2010. Kinetic modeling on drug release from controlled drug delivery systems. Acta poloniae pharmaceutica. 67(3):217-223.

Datta HK, Ng WF, Walker JA, Tuck SP, Varanasi SS. 2008. The cell biology of bone metabolism. Journal of clinical pathology. 61(5):577-587.

de Oliveira GS, Miziara MN, Silva ER, Ferreira EL, Biulchi AP, Alves JB. 2013. Enhanced bone formation during healing process of tooth sockets filled with demineralized human dentine matrix. Australian dental journal. 58(3):326-332.

Dimitriou R, Jones E, McGonagle D, Giannoudis PV. 2011. Bone regeneration: Current concepts and future directions. BMC medicine.9-66.

Dobnig H, Turner RT. 1995. Evidence that intermittent treatment with parathyroid hormone increases bone formation in adult rats by activation of bone lining cells. Endocrinology. 136(8):3632-3638.

Downey PA, Siegel MI. 2006. Bone biology and the clinical implications for osteoporosis. Physical therapy. 86(1):77-91.

Drake MT, Clarke BL, Khosla S. 2008. Bisphosphonates: Mechanism of action and role in clinical practice. Mayo Clinic proceedings. 83(9):1032-1045.

Eghbali-Fatourechi G, Khosla S, Sanyal A, Boyle WJ, Lacey DL, Riggs BL. 2003. Role of rank ligand in mediating increased bone resorption in early postmenopausal women. The Journal of clinical investigation. 111(8):1221-1230.

Eleniste PP, Bruzzaniti A. 2012. Focal adhesion kinases in adhesion structures and disease. Journal of signal transduction. 2012:296450.

Eleniste PP, Du L, Shivanna M, Bruzzaniti A. 2012. Dynamin and ptp-pest cooperatively regulate pyk2 dephosphorylation in osteoclasts. The international journal of biochemistry & cell biology. 44(5):790-800.

Eleniste PP, Patel V, Posritong S, Zero O, Largura H, Cheng YH, Himes ER, Hamilton M, Baughman J, Kacena MA et al. 2015. Pyk2 and megakaryocytes regulate osteoblast differentiation and migration via distinct and overlapping mechanisms. Journal of cellular biochemistry.

Eriksen EF, Keaveny TM, Gallagher ER, Krege JH. 2014. Literature review: The effects of teriparatide therapy at the hip in patients with osteoporosis. Bone. 67:246-256.

Ernst M, Rodan GA. 1991. Estradiol regulation of insulin-like growth factor-i expression in osteoblastic cells: Evidence for transcriptional control. Molecular endocrinology (Baltimore, Md). 5(8):1081-1089.

Fallon MD, Whyte MP, Teitelbaum SL. 1980. Stereospecific inhibition of alkaline phosphatase by l-tetramisole prevents in vitro cartilage calcification. Laboratory investigation; a journal of technical methods and pathology. 43(6):489-494.

Fassbender M, Minkwitz S, Strobel C, Schmidmaier G, Wildemann B. 2014. Stimulation of bone healing by sustained bone morphogenetic protein 2 (bmp-2) delivery. International journal of molecular sciences. 15(5):8539-8552.

Fazeli PK, Wang IS, Miller KK, Herzog DB, Misra M, Lee H, Finkelstein JS, Bouxsein ML, Klibanski A. 2014. Teriparatide increases bone formation and bone mineral density in adult women with anorexia nervosa. The Journal of clinical endocrinology and metabolism. 99(4):1322-1329.

Fu R, Selph S, McDonagh M, Peterson K, Tiwari A, Chou R, Helfand M. 2013. Effectiveness and harms of recombinant human bone morphogenetic protein-2 in spine fusion: A systematic review and meta-analysis. Annals of internal medicine. 158(12):890-902.

Fu Y, Kao WJ. 2009. Drug release kinetics and transport mechanisms from semi-interpenetrating networks of gelatin and poly(ethylene glycol) diacrylate. Pharmaceutical research. 26(9):2115-2124.

Fu Y, Xu K, Zheng X, Giacomin AJ, Mix AW, Kao WJ. 2012. 3d cell entrapment in crosslinked thiolated gelatin-poly(ethylene glycol) diacrylate hydrogels. Biomaterials. 33(1):48-58.

Galea GL, Meakin LB, Sugiyama T, Zebda N, Sunters A, Taipaleenmaki H, Stein GS, van Wijnen AJ, Lanyon LE, Price JS. 2013. Estrogen receptor alpha mediates proliferation of osteoblastic cells stimulated by estrogen and mechanical strain, but their acute down-regulation of the wnt antagonist sost is mediated by estrogen receptor beta. The Journal of biological chemistry. 288(13):9035-9048.

Ganguly S, Ashley LA, Pendleton CM, Grey RD, Howard GC, Castle LD, Peyton DK, Fultz ME, DeMoss DL. 2008. Characterization of osteoblastic properties of 7f2 and umr-106 cultures after acclimation to reduced levels of fetal bovine serum. Canadian journal of physiology and pharmacology. 86(7):403-415.

Ganss B, Kim RH, Sodek J. 1999. Bone sialoprotein. Critical reviews in oral biology and medicine : an official publication of the American Association of Oral Biologists. 10(1):79-98.

Ge C, Xiao G, Jiang D, Franceschi RT. 2007. Critical role of the extracellular signal-regulated kinase-mapk pathway in osteoblast differentiation and skeletal development. The Journal of cell biology. 176(5):709-718.

Ge C, Yang Q, Zhao G, Yu H, Kirkwood KL, Franceschi RT. 2012. Interactions between extracellular signal-regulated kinase 1/2 and p38 map kinase pathways in the control of runx2 phosphorylation and transcriptional activity. Journal of bone and mineral research : the official journal of the American Society for Bone and Mineral Research. 27(3):538-551.

Ghosh-Choudhury N, Abboud SL, Nishimura R, Celeste A, Mahimainathan L, Choudhury GG. 2002. Requirement of bmp-2-induced phosphatidylinositol 3-kinase and akt serine/threonine kinase in osteoblast differentiation and smad-dependent bmp-2 gene transcription. The Journal of biological chemistry. 277(36):33361-33368.

Gifre L, Vidal J, Carrasco JL, Muxi A, Portell E, Monegal A, Guanabens N, Peris P. 2016. Denosumab increases sublesional bone mass in osteoporotic individuals with recent spinal cord injury. Osteoporosis international : a journal established as result of cooperation between the European Foundation for Osteoporosis and the National Osteoporosis Foundation of the USA. 27(1):405-410.

Gil-Henn H, Destaing O, Sims NA, Aoki K, Alles N, Neff L, Sanjay A, Bruzzaniti A, De Camilli P, Baron R et al. 2007. Defective microtubule-dependent podosome organization in osteoclasts leads to increased bone density in pyk2(-/-) mice. The Journal of cell biology. 178(6):1053-1064.

Goldstein SR, Scheele WH, Rajagopalan SK, Wilkie JL, Walsh BW, Parsons AK. 2000. A 12-month comparative study of raloxifene, estrogen, and placebo on the postmenopausal endometrium. Obstetrics and gynecology. 95(1):95-103.

Gomes-Filho IS, Passos Jde S, Cruz SS, Vianna MI, Cerqueira Ede M, Oliveira DC, dos Santos CA, Coelho JM, Sampaio FP, Freitas CO et al. 2007. The association between postmenopausal osteoporosis and periodontal disease. Journal of periodontology. 78(9):1731-1740.

Grassi M, Grassi G. 2005. Mathematical modelling and controlled drug delivery: Matrix systems. Current drug delivery. 2(1):97-116.

Greene T, Lin C. 2015. Modular crosslinking of gelatin-based thiol-ene hydrogels for in vitro culture of hepatocellular carcinoma cells. . ACS Biomaterials Science & Engineering. 1:1314-1323.

Han S, Mistry A, Chang JS, Cunningham D, Griffor M, Bonnette PC, Wang H, Chrunyk BA, Aspnes GE, Walker DP et al. 2009. Structural characterization of proline-rich tyrosine kinase 2 (pyk2) reveals a unique (dfg-out) conformation and enables inhibitor design. The Journal of biological chemistry. 284(19):13193-13201.

Hao Y, Lin CC. 2014. Degradable thiol-acrylate hydrogels as tunable matrices for three-dimensional hepatic culture. Journal of biomedical materials research Part A. 102(11):3813-3827.

Harada S, Rodan GA. 2003. Control of osteoblast function and regulation of bone mass. Nature. 423(6937):349-355.

Hauschka PV, Lian JB, Cole DE, Gundberg CM. 1989. Osteocalcin and matrix gla protein: Vitamin k-dependent proteins in bone. Physiological reviews. 69(3):990-1047.

Hegde V, Jo JE, Andreopoulou P, Lane JM. 2015. Effect of osteoporosis medications on fracture healing. Osteoporosis international : a journal established as result of cooperation between the European Foundation for Osteoporosis and the National Osteoporosis Foundation of the USA.

Hegde V, Jo JE, Andreopoulou P, Lane JM. 2016. Effect of osteoporosis medications on fracture healing. Osteoporosis international : a journal established as result of cooperation between the European Foundation for Osteoporosis and the National Osteoporosis Foundation of the USA. 27(3):861-871.

Heldring N, Pike A, Andersson S, Matthews J, Cheng G, Hartman J, Tujague M, Strom A, Treuter E, Warner M et al. 2007. Estrogen receptors: How do they signal and what are their targets. Physiological reviews. 87(3):905-931.

Henriksen K, Neutzsky-Wulff AV, Bonewald LF, Karsdal MA. 2009. Local communication on and within bone controls bone remodeling. Bone. 44(6):1026-1033.

Hessle L, Johnson KA, Anderson HC, Narisawa S, Sali A, Goding JW, Terkeltaub R, Millan JL. 2002. Tissue-nonspecific alkaline phosphatase and plasma cell membrane glycoprotein-1 are central antagonistic regulators of bone mineralization. Proceedings of the National Academy of Sciences of the United States of America. 99(14):9445-9449.

Hewitt SC, Winuthayanon W, Korach KS. 2016. What's new in estrogen receptor action in the female reproductive tract. Journal of molecular endocrinology. 56(2):R55-71.

Hoch E, Schuh C, Hirth T, Tovar GE, Borchers K. 2012. Stiff gelatin hydrogels can be photo-chemically synthesized from low viscous gelatin solutions using molecularly functionalized gelatin with a high degree of methacrylation. Journal of materials science Materials in medicine. 23(11):2607-2617.

Hsiao YH, Huang YT, Hung CY, Kuo TC, Luo FJ, Yuan TC. 2016. Pyk2 via s6k1 regulates the function of androgen receptors and the growth of prostate cancer cells. Endocrine-related cancer. 23(8):651-663.

Hu Y, Chan E, Wang SX, Li B. 2003. Activation of p38 mitogen-activated protein kinase is required for osteoblast differentiation. Endocrinology. 144(5):2068-2074.

Hudalla GA, Eng TS, Murphy WL. 2008. An approach to modulate degradation and mesenchymal stem cell behavior in poly(ethylene glycol) networks. Biomacromolecules. 9(3):842-849.

Hughes DE, Boyce BF. 1997. Apoptosis in bone physiology and disease. Molecular pathology : MP. 50(3):132-137.

Hunter GK, Goldberg HA. 1993. Nucleation of hydroxyapatite by bone sialoprotein. Proceedings of the National Academy of Sciences of the United States of America. 90(18):8562-8565.

Hutson CB, Nichol JW, Aubin H, Bae H, Yamanlar S, Al-Haque S, Koshy ST, Khademhosseini A. 2011. Synthesis and characterization of tunable poly(ethylene glycol): Gelatin methacrylate composite hydrogels. Tissue engineering Part A. 17(13-14):1713-1723.

Igwe JC, Gao Q, Kizivat T, Kao WW, Kalajzic I. 2011. Keratocan is expressed by osteoblasts and can modulate osteogenic differentiation. Connective tissue research. 52(5):401-407.

Imai Y, Kondoh S, Kouzmenko A, Kato S. 2010. Minireview: Osteoprotective action of estrogens is mediated by osteoclastic estrogen receptor-alpha. Molecular endocrinology (Baltimore, Md). 24(5):877-885.

Ishibe M, Nojima T, Ishibashi T, Koda T, Kaneda K, Rosier RN, Puzas JE. 1995. 17 beta-estradiol increases the receptor number and modulates the action of 1,25-dihydroxyvitamin d3 in human osteosarcoma-derived osteoblast-like cells. Calcified tissue international. 57(6):430-435.

Ismail A, Nawaz Z. 2005. Nuclear hormone receptor degradation and gene transcription: An update. IUBMB life. 57(7):483-490.

ISO-10993-5. 1993. Biological evaluation of medical devices. Part 5: Tests for cytotoxicity: In vitro methods. In: ISO, editor.

Iwasaki M, Taylor GW, Nakamura K, Yoshihara A, Miyazaki H. 2013. Association between low bone mineral density and clinical attachment loss in japanese postmenopausal females. Journal of periodontology. 84(12):1708-1716.

Jaiswal RK, Jaiswal N, Bruder SP, Mbalaviele G, Marshak DR, Pittenger MF. 2000. Adult human mesenchymal stem cell differentiation to the osteogenic or adipogenic lineage is regulated by mitogen-activated protein kinase. The Journal of biological chemistry. 275(13):9645-9652.

Janicki P, Schmidmaier G. 2011. What should be the characteristics of the ideal bone graft substitute? Combining scaffolds with growth factors and/or stem cells. Injury. 42 Suppl 2:S77-81.

Jeffcoat MK. 1993. Bone loss in the oral cavity. Journal of bone and mineral research : the official journal of the American Society for Bone and Mineral Research. 8 Suppl 2:S467-473.

Jikko A, Harris SE, Chen D, Mendrick DL, Damsky CH. 1999. Collagen integrin receptors regulate early osteoblast differentiation induced by bmp-2. Journal of bone and mineral research : the official journal of the American Society for Bone and Mineral Research. 14(7):1075-1083.

Jilka RL, Weinstein RS, Bellido T, Roberson P, Parfitt AM, Manolagas SC. 1999. Increased bone formation by prevention of osteoblast apoptosis with parathyroid hormone. The Journal of clinical investigation. 104(4):439-446.

Johnson PD, Besselsen DG. 2002. Practical aspects of experimental design in animal research. ILAR journal. 43(4):202-206.

Jordan VC, Gapstur S, Morrow M. 2001. Selective estrogen receptor modulation and reduction in risk of breast cancer, osteoporosis, and coronary heart disease. Journal of the National Cancer Institute. 93(19):1449-1457.

Kacena MA, Eleniste PP, Cheng YH, Huang S, Shivanna M, Meijome TE, Mayo LD, Bruzzaniti A. 2012. Megakaryocytes regulate expression of pyk2 isoforms and caspase-mediated cleavage of actin in osteoblasts. The Journal of biological chemistry. 287(21):17257-17268.

Kalamajski S, Aspberg A, Lindblom K, Heinegard D, Oldberg A. 2009. Asporin competes with decorin for collagen binding, binds calcium and promotes osteoblast collagen mineralization. The Biochemical journal. 423(1):53-59.

Kawamura N, Kugimiya F, Oshima Y, Ohba S, Ikeda T, Saito T, Shinoda Y, Kawasaki Y, Ogata N, Hoshi K et al. 2007. Akt1 in osteoblasts and osteoclasts controls bone remodeling. PloS one. 2(10):e1058.

Keeting PE, Scott RE, Colvard DS, Han IK, Spelsberg TC, Riggs BL. 1991. Lack of a direct effect of estrogen on proliferation and differentiation of normal human osteoblast-like cells. Journal of bone and mineral research : the official journal of the American Society for Bone and Mineral Research. 6(3):297-304.

Khosla S, Oursler MJ, Monroe DG. 2012. Estrogen and the skeleton. Trends in endocrinology and metabolism: TEM. 23(11):576-581.

Kimble RB, Srivastava S, Ross FP, Matayoshi A, Pacifici R. 1996. Estrogen deficiency increases the ability of stromal cells to support murine osteoclastogenesis via an interleukin-1and tumor necrosis factor-mediated stimulation of macrophage colony-stimulating factor production. The Journal of biological chemistry. 271(46):28890-28897.

Kinane DF, Marshall GJ. 2001. Periodontal manifestations of systemic disease. Australian dental journal. 46(1):2-12.

Kokabu S, Lowery JW, Jimi E. 2016. Cell fate and differentiation of bone marrow mesenchymal stem cells. Stem cells international. 2016:3753581.

Kondoh S, Inoue K, Igarashi K, Sugizaki H, Shirode-Fukuda Y, Inoue E, Yu T, Takeuchi JK, Kanno J, Bonewald LF et al. 2014. Estrogen receptor alpha in osteocytes regulates trabecular bone formation in female mice. Bone. 60:68-77.

Krall EA, Garcia RI, Dawson-Hughes B. 1996. Increased risk of tooth loss is related to bone loss at the whole body, hip, and spine. Calcified tissue international. 59(6):433-437.

Krause C, Korchynskyi O, de Rooij K, Weidauer SE, de Gorter DJ, van Bezooijen RL, Hatsell S, Economides AN, Mueller TD, Lowik CW et al. 2010. Distinct modes of inhibition by sclerostin on bone morphogenetic protein and wnt signaling pathways. The Journal of biological chemistry. 285(53):41614-41626.

Krum SA. 2011. Direct transcriptional targets of sex steroid hormones in bone. Journal of cellular biochemistry. 112(2):401-408.

Krum SA, Brown M. 2008. Unraveling estrogen action in osteoporosis. Cell cycle (Georgetown, Tex). 7(10):1348-1352.

Krum SA, Miranda-Carboni GA, Hauschka PV, Carroll JS, Lane TF, Freedman LP, Brown M. 2008a. Estrogen protects bone by inducing fas ligand in osteoblasts to regulate osteoclast survival. The EMBO journal. 27(3):535-545.

Krum SA, Miranda-Carboni GA, Lupien M, Eeckhoute J, Carroll JS, Brown M. 2008b. Unique eralpha cistromes control cell type-specific gene regulation. Molecular endocrinology (Baltimore, Md). 22(11):2393-2406.

Kuiper GG, Carlsson B, Grandien K, Enmark E, Haggblad J, Nilsson S, Gustafsson JA. 1997. Comparison of the ligand binding specificity and transcript tissue distribution of estrogen receptors alpha and beta. Endocrinology. 138(3):863-870.

Lai CF, Chaudhary L, Fausto A, Halstead LR, Ory DS, Avioli LV, Cheng SL. 2001. Erk is essential for growth, differentiation, integrin expression, and cell function in human osteoblastic cells. The Journal of biological chemistry. 276(17):14443-14450.

Lemon JC, Okay DJ, Powers JM, Martin JW, Chambers MS. 2003. Facial moulage: The effect of a retarder on compressive strength and working and setting times of irreversible hydrocolloid impression material. The Journal of prosthetic dentistry. 90(3):276-281.

Levi-Montalcini R, Skaper SD, Dal Toso R, Petrelli L, Leon A. 1996. Nerve growth factor: From neurotrophin to neurokine. Trends in neurosciences. 19(11):514-520.

Lewandrowski KU, Nanson C, Calderon R. 2007. Vertebral osteolysis after posterior interbody lumbar fusion with recombinant human bone morphogenetic protein 2: A report of five cases. The spine journal : official journal of the North American Spine Society. 7(5):609-614.

Li J, Baker BA, Mou X, Ren N, Qiu J, Boughton RI, Liu H. 2014. Biopolymer/calcium phosphate scaffolds for bone tissue engineering. Advanced healthcare materials. 3(4):469-484.

Li X, Xie J, Yuan X, Xia Y. 2008. Coating electrospun poly(epsilon-caprolactone) fibers with gelatin and calcium phosphate and their use as biomimetic scaffolds for bone tissue engineering. Langmuir : the ACS journal of surfaces and colloids. 24(24):14145-14150.

Li X, Zhang Y, Kang H, Liu W, Liu P, Zhang J, Harris SE, Wu D. 2005. Sclerostin binds to lrp5/6 and antagonizes canonical wnt signaling. The Journal of biological chemistry. 280(20):19883-19887.

Lim ST, Chen XL, Lim Y, Hanson DA, Vo TT, Howerton K, Larocque N, Fisher SJ, Schlaepfer DD, Ilic D. 2008. Nuclear fak promotes cell proliferation and survival through ferm-enhanced p53 degradation. Molecular cell. 29(1):9-22.

Lim ST, Miller NL, Nam JO, Chen XL, Lim Y, Schlaepfer DD. 2010. Pyk2 inhibition of p53 as an adaptive and intrinsic mechanism facilitating cell proliferation and survival. The Journal of biological chemistry. 285(3):1743-1753.

Lin CC, Anseth KS. 2009. Peg hydrogels for the controlled release of biomolecules in regenerative medicine. Pharmaceutical research. 26(3):631-643.

Lin CC, Ki CS, Shih H. 2015. Thiol-norbornene photo-click hydrogels for tissue engineering applications. Journal of applied polymer science. 132(8).

Lin CC, Metters AT. 2006. Hydrogels in controlled release formulations: Network design and mathematical modeling. Advanced drug delivery reviews. 58(12-13):1379-1408.

Lin CC, Raza A, Shih H. 2011. Peg hydrogels formed by thiol-ene photo-click chemistry and their effect on the formation and recovery of insulin-secreting cell spheroids. Biomaterials. 32(36):9685-9695.

Lin Y, Liu LJ, Murray T, Sodek J, Rao L. 2004. Effect of raloxifene and its interaction with human pth on bone formation. Journal of endocrinological investigation. 27(5):416-423.

Lindberg MK, Alatalo SL, Halleen JM, Mohan S, Gustafsson JA, Ohlsson C. 2001. Estrogen receptor specificity in the regulation of the skeleton in female mice. The Journal of endocrinology. 171(2):229-236.

Lipinski CA, Loftus JC. 2010. Targeting pyk2 for therapeutic intervention. Expert opinion on therapeutic targets. 14(1):95-108.

Liu, Ballada A. 2014. Engineering of polymers and chemical complexity, volume i: Current state of the art and perspectives. New Jersy, USA: Apple Academic Press

Liu F, Malaval L, Gupta AK, Aubin JE. 1994. Simultaneous detection of multiple bone-related mrnas and protein expression during osteoblast differentiation: Polymerase chain reaction and immunocytochemical studies at the single cell level. Developmental biology. 166(1):220-234.

Liu XH, Kirschenbaum A, Weinstein BM, Zaidi M, Yao S, Levine AC. 2010. Prostaglandin e2 modulates components of the wnt signaling system in bone and prostate cancer cells. Biochemical and biophysical research communications. 394(3):715-720.

Loe H. 1993. Periodontal disease. The sixth complication of diabetes mellitus. Diabetes care. 16(1):329-334.

Loftus JC, Ross JT, Paquette KM, Paulino VM, Nasser S, Yang Z, Kloss J, Kim S, Berens ME, Tran NL. 2012. Mirna expression profiling in migrating glioblastoma cells: Regulation of cell migration and invasion by mir-23b via targeting of pyk2. PloS one. 7(6):e39818.

Long MW. 2001. Osteogenesis and bone-marrow-derived cells. Blood cells, molecules & diseases. 27(3):677-690.

Lu IF, Hasio AC, Hu MC, Yang FM, Su HM. 2010. Docosahexaenoic acid induces proteasome-dependent degradation of estrogen receptor alpha and inhibits the downstream signaling target in mcf-7 breast cancer cells. The Journal of nutritional biochemistry. 21(6):512-517.

Maatta JA, Buki KG, Gu G, Alanne MH, Vaaraniemi J, Liljenback H, Poutanen M, Harkonen P, Vaananen K. 2013. Inactivation of estrogen receptor alpha in bone-forming cells induces bone loss in female mice. FASEB journal : official publication of the Federation of American Societies for Experimental Biology. 27(2):478-488.

Machwate M, Jullienne A, Moukhtar M, Marie PJ. 1995. Temporal variation of c-fos proto-oncogene expression during osteoblast differentiation and osteogenesis in developing rat bone. Journal of cellular biochemistry. 57(1):62-70.

MacNabb C, Patton D, Hayes JS. 2016. Sclerostin antibody therapy for the treatment of osteoporosis: Clinical prospects and challenges. Journal of osteoporosis. 2016:6217286.

Maillot G, Lacroix-Triki M, Pierredon S, Gratadou L, Schmidt S, Benes V, Roche H, Dalenc F, Auboeuf D, Millevoi S et al. 2009. Widespread estrogen-dependent repression of micrornas involved in breast tumor cell growth. Cancer research. 69(21):8332-8340.

Majeska RJ, Ryaby JT, Einhorn TA. 1994. Direct modulation of osteoblastic activity with estrogen. The Journal of bone and joint surgery American volume. 76(5):713-721.

Malkoch M, Vestberg R, Gupta N, Mespouille L, Dubois P, Mason AF, Hedrick JL, Liao Q, Frank CW, Kingsbury K et al. 2006. Synthesis of well-defined hydrogel networks using click chemistry. Chemical communications (Cambridge, England). (26):2774-2776.

Mandal CC, Das F, Ganapathy S, Harris SE, Choudhury GG, Ghosh-Choudhury N. 2016. Bone morphogenetic protein-2 (bmp-2) activates nfatc1 transcription factor via an autoregulatory loop involving smad/akt/ca2+ signaling. The Journal of biological chemistry. 291(3):1148-1161.

Marie PJ. 2008. Transcription factors controlling osteoblastogenesis. Archives of biochemistry and biophysics. 473(2):98-105.

Marino M, Galluzzo P, Ascenzi P. 2006. Estrogen signaling multiple pathways to impact gene transcription. Current genomics. 7(8):497-508.

Marzona L, Pavolini B. 2009. Play and players in bone fracture healing match. Clinical cases in mineral and bone metabolism : the official journal of the Italian Society of Osteoporosis, Mineral Metabolism, and Skeletal Diseases. 6(2):159-162.

Matsumori H, Hattori K, Ohgushi H, Dohi Y, Ueda Y, Shigematsu H, Satoh N, Yajima H, Takakura Y. 2009. Raloxifene: Its ossification-promoting effect on female mesenchymal stem cells. Journal of orthopaedic science : official journal of the Japanese Orthopaedic Association. 14(5):640-645.

Matsushita T, Chan YY, Kawanami A, Balmes G, Landreth GE, Murakami S. 2009. Extracellular signal-regulated kinase 1 (erk1) and erk2 play essential roles in osteoblast differentiation and in supporting osteoclastogenesis. Molecular and cellular biology. 29(21):5843-5857.

McCauley LK, Tozum TF, Kozloff KM, Koh-Paige AJ, Chen C, Demashkieh M, Cronovich H, Richard V, Keller ET, Rosol TJ et al. 2003. Transgenic models of metabolic bone disease: Impact of estrogen receptor deficiency on skeletal metabolism. Connective tissue research. 44 Suppl 1:250-263.

McClung MR, Lewiecki EM, Cohen SB, Bolognese MA, Woodson GC, Moffett AH, Peacock M, Miller PD, Lederman SN, Chesnut CH et al. 2006. Denosumab in postmenopausal women with low bone mineral density. The New England journal of medicine. 354(8):821-831.

McCullen SD, Zhu Y, Bernacki SH, Narayan RJ, Pourdeyhimi B, Gorga RE, Loboa EG. 2009. Electrospun composite poly(l-lactic acid)/tricalcium phosphate scaffolds induce proliferation and osteogenic differentiation of human adipose-derived stem cells. Biomedical materials (Bristol, England). 4(3):035002.

McKee MD, Nanci A. 1996. Osteopontin: An interfacial extracellular matrix protein in mineralized tissues. Connective tissue research. 35(1-4):197-205.

Mehta NM, Malootian A, Gilligan JP. 2003. Calcitonin for osteoporosis and bone pain. Current pharmaceutical design. 9(32):2659-2676.

Melville KM, Kelly NH, Khan SA, Schimenti JC, Ross FP, Main RP, van der Meulen MC. 2014. Female mice lacking estrogen receptor-alpha in osteoblasts have compromised bone mass and strength. Journal of bone and mineral research : the official journal of the American Society for Bone and Mineral Research. 29(2):370-379.

Mesfin A, Buchowski JM, Zebala LP, Bakhsh WR, Aronson AB, Fogelson JL, Hershman S, Kim HJ, Ahmad A, Bridwell KH. 2013. High-dose rhbmp-2 for adults: Major and minor complications: A study of 502 spine cases. The Journal of bone and joint surgery American volume. 95(17):1546-1553.

Mirza FS, Padhi ID, Raisz LG, Lorenzo JA. 2010. Serum sclerostin levels negatively correlate with parathyroid hormone levels and free estrogen index in postmenopausal women. The Journal of clinical endocrinology and metabolism. 95(4):1991-1997.

Moedano DE, Irigoyen ME, Borges-Yanez A, Flores-Sanchez I, Rotter RC. 2011. Osteoporosis, the risk of vertebral fracture, and periodontal disease in an elderly group in mexico city. Gerodontology. 28(1):19-27.

Moller P, Fall A, Chikkadi V, Derks D, Bonn D. 2009. An attempt to categorize yield stress fluid behaviour. Philosophical transactions Series A, Mathematical, physical, and engineering sciences. 367(1909):5139-5155.

Mont MA, Ragland PS, Biggins B, Friedlaender G, Patel T, Cook S, Etienne G, Shimmin A, Kildey R, Rueger DC et al. 2004. Use of bone morphogenetic proteins for musculoskeletal applications. An overview. The Journal of bone and joint surgery American volume. 86-A Suppl 2:41-55.

Mourino V, Boccaccini AR. 2010. Bone tissue engineering therapeutics: Controlled drug delivery in three-dimensional scaffolds. Journal of the Royal Society, Interface / the Royal Society. 7(43):209-227.

Moustafa A, Sugiyama T, Prasad J, Zaman G, Gross TS, Lanyon LE, Price JS. 2012. Mechanical loading-related changes in osteocyte sclerostin expression in mice are more closely associated with the subsequent osteogenic response than the peak strains engendered. Osteoporosis international : a journal established as result of cooperation between the European Foundation for Osteoporosis and the National Osteoporosis Foundation of the USA. 23(4):1225-1234.

Murata H, Kawamura M, Hamada T, Chimori H, Nikawa H. 2004. Physical properties and compatibility with dental stones of current alginate impression materials. Journal of oral rehabilitation. 31(11):1115-1122.

Nakahama K. 2010. Cellular communications in bone homeostasis and repair. Cellular and molecular life sciences : CMLS. 67(23):4001-4009.

Nakamura T, Imai Y, Matsumoto T, Sato S, Takeuchi K, Igarashi K, Harada Y, Azuma Y, Krust A, Yamamoto Y et al. 2007. Estrogen prevents bone loss

via estrogen receptor alpha and induction of fas ligand in osteoclasts. Cell. 130(5):811-823.

Narayanan D, M GG, H L, Koyakutty M, Nair S, Menon D. 2013. Poly-(ethylene glycol) modified gelatin nanoparticles for sustained delivery of the anti-inflammatory drug ibuprofen-sodium: An in vitro and in vivo analysis. Nanomedicine : nanotechnology, biology, and medicine. 9(6):818-828.

Nasu M, Sugimoto T, Kaji H, Chihara K. 2000. Estrogen modulates osteoblast proliferation and function regulated by parathyroid hormone in osteoblastic saos-2 cells: Role of insulin-like growth factor (igf)-i and igf-binding protein-5. The Journal of endocrinology. 167(2):305-313.

Nawaz Z, Lonard DM, Dennis AP, Smith CL, O'Malley BW. 1999. Proteasome-dependent degradation of the human estrogen receptor. Proceedings of the National Academy of Sciences of the United States of America. 96(5):1858-1862.

Nefussi JR, Brami G, Modrowski D, Oboeuf M, Forest N. 1997. Sequential expression of bone matrix proteins during rat calvaria osteoblast differentiation and bone nodule formation in vitro. The journal of histochemistry and cytochemistry : official journal of the Histochemistry Society. 45(4):493-503.

Nicks KM, Fujita K, Fraser D, McGregor U, Drake MT, McGee-Lawrence ME, Westendorf JJ, Monroe DG, Khosla S. 2015. Deletion of estrogen receptor beta in osteoprogenitor cells increases trabecular but not cortical bone mass in female mice. Journal of bone and mineral research : the official journal of the American Society for Bone and Mineral Research.

Noble BS. 2008. The osteocyte lineage. Archives of biochemistry and biophysics. 473(2):106-111.

Noda-Seino H, Sawada K, Hayakawa J, Ohyagi-Hara C, Mabuchi S, Takahashi K, Nishio Y, Sakata M, Kurachi H, Kimura T. 2013. Estradiol and raloxifene induce the proliferation of osteoblasts through g-protein-coupled receptor gpr30. Journal of endocrinological investigation. 36(1):21-27.

Novack DV. 2007. Estrogen and bone: Osteoclasts take center stage. Cell metabolism. 6(4):254-256.

Nudelman F, Pieterse K, George A, Bomans PH, Friedrich H, Brylka LJ, Hilbers PA, de With G, Sommerdijk NA. 2010. The role of collagen in bone apatite formation in the presence of hydroxyapatite nucleation inhibitors. Nat Mater. 9(12):1004-1009.

Okigaki M, Davis C, Falasca M, Harroch S, Felsenfeld DP, Sheetz MP, Schlessinger J. 2003. Pyk2 regulates multiple signaling events crucial for macrophage morphology and migration. Proceedings of the National Academy of Sciences of the United States of America. 100(19):10740-10745.

Oliver RC, Tervonen T. 1994. Diabetes--a risk factor for periodontitis in adults? Journal of periodontology. 65(5 Suppl):530-538.

Onoe Y, Miyaura C, Ohta H, Nozawa S, Suda T. 1997. Expression of estrogen receptor beta in rat bone. Endocrinology. 138(10):4509-4512.

Orwoll ES. 2003. Toward an expanded understanding of the role of the periosteum in skeletal health. Journal of bone and mineral research : the official journal of the American Society for Bone and Mineral Research. 18(6):949-954.

Oryan A, Alidadi S, Moshiri A, Maffulli N. 2014. Bone regenerative medicine: Classic options, novel strategies, and future directions. Journal of orthopaedic surgery and research. 9(1):18.

Oryan A, Monazzah S, Bigham-Sadegh A. 2015. Bone injury and fracture healing biology. Biomedical and environmental sciences : BES. 28(1):57-71.

Oursler MJ, Cortese C, Keeting P, Anderson MA, Bonde SK, Riggs BL, Spelsberg TC. 1991. Modulation of transforming growth factor-beta production in normal human osteoblast-like cells by 17 beta-estradiol and parathyroid hormone. Endocrinology. 129(6):3313-3320.

Parfitt AM. 2001. The bone remodeling compartment: A circulatory function for bone lining cells. Journal of bone and mineral research : the official journal of the American Society for Bone and Mineral Research. 16(9):1583-1585.

Parikka V, Peng Z, Hentunen T, Risteli J, Elo T, Vaananen HK, Harkonen P. 2005. Estrogen responsiveness of bone formation in vitro and altered bone phenotype in aged estrogen receptor-alpha-deficient male and female mice. European journal of endocrinology / European Federation of Endocrine Societies. 152(2):301-314.

Park JB. 2011. The use of hydrogels in bone-tissue engineering. Medicina oral, patologia oral y cirugia bucal. 16(1):e115-118.

Parlato M, Reichert S, Barney N, Murphy WL. 2014. Poly(ethylene glycol) hydrogels with adaptable mechanical and degradation properties for use in biomedical applications. Macromolecular bioscience. 14(5):687-698.

Patti A, Gennari L, Merlotti D, Dotta F, Nuti R. 2013. Endocrine actions of osteocalcin. International journal of endocrinology. 2013:846480.

Pazianas M, Abrahamsen B. 2016. Osteoporosis treatment: Bisphosphonates reign to continue for a few more years, at least? Annals of the New York Academy of Sciences.

Peppas NA, Huang Y, Torres-Lugo M, Ward JH, Zhang J. 2000. Physicochemical foundations and structural design of hydrogels in medicine and biology. Annual review of biomedical engineering. 2:9-29.

Pereira FM, Rodrigues VP, de Oliveira AE, Brito LM, Lopes FF. 2015. Association between periodontal changes and osteoporosis in postmenopausal women. Climacteric : the journal of the International Menopause Society. 18(2):311-315.

Petrel TA, Brueggemeier RW. 2003. Increased proteasome-dependent degradation of estrogen receptor-alpha by tgf-beta1 in breast cancer cell lines. Journal of cellular biochemistry. 88(1):181-190.

Pineda B, Hermenegildo C, Tarin JJ, Cano A, Garcia-Perez MA. 2012. Effects of administration of hormone therapy or raloxifene on the immune system and on biochemical markers of bone remodeling. Menopause (New York, NY). 19(3):319-327.

Pisani P, Renna MD, Conversano F, Casciaro E, Di Paola M, Quarta E, Muratore M, Casciaro S. 2016. Major osteoporotic fragility fractures: Risk factor updates and societal impact. World journal of orthopedics. 7(3):171-181.

Plant A, Tobias JH. 2001. Characterisation of the temporal sequence of osteoblast gene expression during estrogen-induced osteogenesis in female mice. Journal of cellular biochemistry. 82(4):683-691.

Proff P, Romer P. 2009. The molecular mechanism behind bone remodelling: A review. Clinical oral investigations. 13(4):355-362.

Ratko TA, Belinson SE, Samson DJ, Bonnell C, Ziegler KM, Aronson N. 2010. Bone morphogenetic protein: The state of the evidence of on-label and off-label use. Rockville MD.

Razzaque MS. 2011. Osteocalcin: A pivotal mediator or an innocent bystander in energy metabolism? Nephrology, dialysis, transplantation : official publication of the European Dialysis and Transplant Association - European Renal Association. 26(1):42-45.

Riancho JA, Hernandez JL. 2012. Pharmacogenomics of osteoporosis: A pathway approach. Pharmacogenomics. 13(7):815-829.

Rickard DJ, Hofbauer LC, Bonde SK, Gori F, Spelsberg TC, Riggs BL. 1998. Bone morphogenetic protein-6 production in human osteoblastic cell lines. Selective regulation by estrogen. The Journal of clinical investigation. 101(2):413-422.

Riggs BL, Hartmann LC. 2003. Selective estrogen-receptor modulators -- mechanisms of action and application to clinical practice. The New England journal of medicine. 348(7):618-629.

Roach HI. 1994. Why does bone matrix contain non-collagenous proteins? The possible roles of osteocalcin, osteonectin, osteopontin and bone sialoprotein in bone mineralisation and resorption. Cell biology international. 18(6):617-628.

Roberts WG, Ung E, Whalen P, Cooper B, Hulford C, Autry C, Richter D, Emerson E, Lin J, Kath J et al. 2008. Antitumor activity and pharmacology of a

selective focal adhesion kinase inhibitor, pf-562,271. Cancer research. 68(6):1935-1944.

Robinson JA, Harris SA, Riggs BL, Spelsberg TC. 1997. Estrogen regulation of human osteoblastic cell proliferation and differentiation. Endocrinology. 138(7):2919-2927.

Rodan GA, Noda M. 1991. Gene expression in osteoblastic cells. Critical reviews in eukaryotic gene expression. 1(2):85-98.

Rodgers MA, Brown JV, Heirs MK, Higgins JP, Mannion RJ, Simmonds MC, Stewart LA. 2013. Reporting of industry funded study outcome data: Comparison of confidential and published data on the safety and effectiveness of rhbmp-2 for spinal fusion. BMJ (Clinical research ed). 346:f3981.

Rodriguez-Carballo E, Gamez B, Ventura F. 2016. P38 mapk signaling in osteoblast differentiation. Frontiers in cell and developmental biology. 4:40.

Romagnoli C, D'Asta F, Brandi ML. 2013. Drug delivery using composite scaffolds in the context of bone tissue engineering. Clinical cases in mineral and bone metabolism : the official journal of the Italian Society of Osteoporosis, Mineral Metabolism, and Skeletal Diseases. 10(3):155-161.

Rosen CJ. 2005. Clinical practice. Postmenopausal osteoporosis. The New England journal of medicine. 353(6):595-603.

Rosen CJ, Bouxsein ML. 2006. Mechanisms of disease: Is osteoporosis the obesity of bone? Nature clinical practice Rheumatology. 2(1):35-43.

Ruggiero SL, Mehrotra B, Rosenberg TJ, Engroff SL. 2004. Osteonecrosis of the jaws associated with the use of bisphosphonates: A review of 63 cases. Journal of oral and maxillofacial surgery : official journal of the American Association of Oral and Maxillofacial Surgeons. 62(5):527-534.

Russell RG. 2015. Pharmacological diversity among drugs that inhibit bone resorption. Current opinion in pharmacology. 22:115-130.

Salasznyk RM, Klees RF, Boskey A, Plopper GE. 2007. Activation of fak is necessary for the osteogenic differentiation of human mesenchymal stem cells on laminin-5. Journal of cellular biochemistry. 100(2):499-514.

Sanchez M, Picard N, Sauve K, Tremblay A. 2013. Coordinate regulation of estrogen receptor beta degradation by mdm2 and creb-binding protein in response to growth signals. Oncogene. 32(1):117-126.

Santoro M, Tatara AM, Mikos AG. 2014. Gelatin carriers for drug and cell delivery in tissue engineering. Journal of controlled release : official journal of the Controlled Release Society. 190:210-218.

Seeherman H, Li R, Wozney J. 2003. A review of preclinical program development for evaluating injectable carriers for osteogenic factors. The Journal of bone and joint surgery American volume. 85-A Suppl 3:96-108.

Seeherman H, Wozney JM. 2005. Delivery of bone morphogenetic proteins for orthopedic tissue regeneration. Cytokine & growth factor reviews. 16(3):329-345.

Seibel MJ. 2005. Biochemical markers of bone turnover: Part i: Biochemistry and variability. The Clinical biochemist Reviews / Australian Association of Clinical Biochemists. 26(4):97-122.

Shi J, Xing MM, Zhong W. 2012. Development of hydrogels and biomimetic regulators as tissue engineering scaffolds. Membranes. 2(1):70-90.

Simmonds MC, Brown JV, Heirs MK, Higgins JP, Mannion RJ, Rodgers MA, Stewart LA. 2013. Safety and effectiveness of recombinant human bone morphogenetic protein-2 for spinal fusion: A meta-analysis of individual-participant data. Annals of internal medicine. 158(12):877-889.

Simoncini T, Genazzani AR. 2003. Non-genomic actions of sex steroid hormones. European journal of endocrinology / European Federation of Endocrine Societies. 148(3):281-292.

Simonet WS, Lacey DL, Dunstan CR, Kelley M, Chang MS, Luthy R, Nguyen HQ, Wooden S, Bennett L, Boone T et al. 1997. Osteoprotegerin: A novel secreted protein involved in the regulation of bone density. Cell. 89(2):309-319.

Sims NA, Clement-Lacroix P, Da Ponte F, Bouali Y, Binart N, Moriggl R, Goffin V, Coschigano K, Gaillard-Kelly M, Kopchick J et al. 2000. Bone homeostasis

in growth hormone receptor-null mice is restored by igf-i but independent of stat5. The Journal of clinical investigation. 106(9):1095-1103.

Sims NA, Dupont S, Krust A, Clement-Lacroix P, Minet D, Resche-Rigon M, Gaillard-Kelly M, Baron R. 2002. Deletion of estrogen receptors reveals a regulatory role for estrogen receptors-beta in bone remodeling in females but not in males. Bone. 30(1):18-25.

Sims NA, Martin TJ. 2014. Coupling the activities of bone formation and resorption: A multitude of signals within the basic multicellular unit. BoneKEy reports. 3:481.

Slootweg MC, Swolin D, Netelenbos JC, Isaksson OG, Ohlsson C. 1997. Estrogen enhances growth hormone receptor expression and growth hormone action in rat osteosarcoma cells and human osteoblast-like cells. The Journal of endocrinology. 155(1):159-164.

Soares CJ, Santana FR, Pereira JC, Araujo TS, Menezes MS. 2008. Influence of airborne-particle abrasion on mechanical properties and bond strength of carbon/epoxy and glass/bis-gma fiber-reinforced resin posts. The Journal of prosthetic dentistry. 99(6):444-454.

Somjen D, Katzburg S, Sharon O, Grafi-Cohen M, Knoll E, Stern N. 2011. The effects of estrogen receptors alpha- and beta-specific agonists and antagonists on cell proliferation and energy metabolism in human bone cell line. Journal of cellular biochemistry. 112(2):625-632.

Sonnet C, Simpson CL, Olabisi RM, Sullivan K, Lazard Z, Gugala Z, Peroni JF, Weh JM, Davis AR, West JL et al. 2013. Rapid healing of femoral defects in rats with low dose sustained bmp2 expression from pegda hydrogel microspheres. Journal of orthopaedic research : official publication of the Orthopaedic Research Society. 31(10):1597-1604.

Standal T, Borset M, Sundan A. 2004. Role of osteopontin in adhesion, migration, cell survival and bone remodeling. Experimental oncology. 26(3):179-184.

Stein GS, Lian JB, van Wijnen AJ, Stein JL, Montecino M, Javed A, Zaidi SK, Young DW, Choi JY, Pockwinse SM. 2004. Runx2 control of organization,

assembly and activity of the regulatory machinery for skeletal gene expression. Oncogene. 23(24):4315-4329.

Sutter M, Siepmann J, Hennink WE, Jiskoot W. 2007. Recombinant gelatin hydrogels for the sustained release of proteins. Journal of controlled release : official journal of the Controlled Release Society. 119(3):301-312.

Szulc P, Delmas PD. 2008. Biochemical markers of bone turnover: Potential use in the investigation and management of postmenopausal osteoporosis. Osteoporosis international : a journal established as result of cooperation between the European Foundation for Osteoporosis and the National Osteoporosis Foundation of the USA. 19(12):1683-1704.

Tan SD, de Vries TJ, Kuijpers-Jagtman AM, Semeins CM, Everts V, Klein-Nulend J. 2007. Osteocytes subjected to fluid flow inhibit osteoclast formation and bone resorption. Bone. 41(5):745-751.

Taranta A, Brama M, Teti A, De luca V, Scandurra R, Spera G, Agnusdei D, Termine JD, Migliaccio S. 2002. The selective estrogen receptor modulator raloxifene regulates osteoclast and osteoblast activity in vitro. Bone. 30(2):368-376.

Tateishi Y, Sonoo R, Sekiya Y, Sunahara N, Kawano M, Wayama M, Hirota R, Kawabe Y, Murayama A, Kato S et al. 2006. Turning off estrogen receptor beta-mediated transcription requires estrogen-dependent receptor proteolysis. Molecular and cellular biology. 26(21):7966-7976.

Tatsumi S, Ishii K, Amizuka N, Li M, Kobayashi T, Kohno K, Ito M, Takeshita S, Ikeda K. 2007. Targeted ablation of osteocytes induces osteoporosis with defective mechanotransduction. Cell metabolism. 5(6):464-475.

Tau KR, Hefferan TE, Waters KM, Robinson JA, Subramaniam M, Riggs BL, Spelsberg TC. 1998. Estrogen regulation of a transforming growth factor-beta inducible early gene that inhibits deoxyribonucleic acid synthesis in human osteoblasts. Endocrinology. 139(3):1346-1353.

Tee MK, Rogatsky I, Tzagarakis-Foster C, Cvoro A, An J, Christy RJ, Yamamoto KR, Leitman DC. 2004. Estradiol and selective estrogen receptor

modulators differentially regulate target genes with estrogen receptors alpha and beta. Molecular biology of the cell. 15(3):1262-1272.

Tian X, Jee WS, Li X, Paszty C, Ke HZ. 2011. Sclerostin antibody increases bone mass by stimulating bone formation and inhibiting bone resorption in a hindlimb-immobilization rat model. Bone. 48(2):197-201.

Tollemar V, Collier ZJ, Mohammed MK, Lee MJ, Ameer GA, Reid RR. 2016. Stem cells, growth factors and scaffolds in craniofacial regenerative medicine. Genes & Diseases. 3(1):56-71.

Totta P, Pesiri V, Marino M, Acconcia F. 2014. Lysosomal function is involved in 17beta-estradiol-induced estrogen receptor alpha degradation and cell proliferation. PloS one. 9(4):e94880.

Tronci G, Ajiro H, Russell SJ, Wood DJ, Akashi M. 2014. Tunable drug-loading capability of chitosan hydrogels with varied network architectures. Acta biomaterialia. 10(2):821-830.

Tse KW, Dang-Lawson M, Lee RL, Vong D, Bulic A, Buckbinder L, Gold MR. 2009. B cell receptor-induced phosphorylation of pyk2 and focal adhesion kinase involves integrins and the rap gtpases and is required for b cell spreading. The Journal of biological chemistry. 284(34):22865-22877.

Vaananen HK, Laitala-Leinonen T. 2008. Osteoclast lineage and function. Archives of biochemistry and biophysics. 473(2):132-138.

van Oers RF, Ruimerman R, Tanck E, Hilbers PA, Huiskes R. 2008. A unified theory for osteonal and hemi-osteonal remodeling. Bone. 42(2):250-259.

van Oers RF, van Rietbergen B, Ito K, Hilbers PA, Huiskes R. 2011. A sclerostin-based theory for strain-induced bone formation. Biomechanics and modeling in mechanobiology. 10(5):663-670.

Varela-Lopez A, Giampieri F, Bullon P, Battino M, Quiles JL. 2016. A systematic review on the implication of minerals in the onset, severity and treatment of periodontal disease. Molecules (Basel, Switzerland). 21(9).

Vasikaran S, Eastell R, Bruyere O, Foldes AJ, Garnero P, Griesmacher A, McClung M, Morris HA, Silverman S, Trenti T et al. 2011. Markers of bone turnover for the prediction of fracture risk and monitoring of osteoporosis

treatment: A need for international reference standards. Osteoporosis international : a journal established as result of cooperation between the European Foundation for Osteoporosis and the National Osteoporosis Foundation of the USA. 22(2):391-420.

Viguet-Carrin S, Garnero P, Delmas PD. 2006. The role of collagen in bone strength. Osteoporosis international : a journal established as result of cooperation between the European Foundation for Osteoporosis and the National Osteoporosis Foundation of the USA. 17(3):319-336.

Villafan-Bernal JR, Sanchez-Enriquez S, Munoz-Valle JF. 2011. Molecular modulation of osteocalcin and its relevance in diabetes (review). International journal of molecular medicine. 28(3):283-293.

Wagner EF. 2002. Functions of ap1 (fos/jun) in bone development. Annals of the rheumatic diseases. 61 Suppl 2:ii40-42.

Wakeling AE, Dukes M, Bowler J. 1991. A potent specific pure antiestrogen with clinical potential. Cancer research. 51(15):3867-3873.

Wang L, Liu S, Zhao Y, Liu D, Liu Y, Chen C, Karray S, Shi S, Jin Y. 2015. Osteoblast-induced osteoclast apoptosis by fas ligand/fas pathway is required for maintenance of bone mass. Cell death and differentiation. 22(10):1654-1664.

Wang Q, Xie Y, Du QS, Wu XJ, Feng X, Mei L, McDonald JM, Xiong WC. 2003. Regulation of the formation of osteoclastic actin rings by proline-rich tyrosine kinase 2 interacting with gelsolin. The Journal of cell biology. 160(4):565-575.

Wang X, Goh CH, Li B. 2007. P38 mitogen-activated protein kinase regulates osteoblast differentiation through osterix. Endocrinology. 148(4):1629-1637.

Whittier X, Saag KG. 2016. Glucocorticoid-induced osteoporosis. Rheumatic diseases clinics of North America. 42(1):177-189, x.

Windahl SH, Borjesson AE, Farman HH, Engdahl C, Moverare-Skrtic S, Sjogren K, Lagerquist MK, Kindblom JM, Koskela A, Tuukkanen J et al. 2013. Estrogen receptor-alpha in osteocytes is important for trabecular bone

formation in male mice. Proceedings of the National Academy of Sciences of the United States of America. 110(6):2294-2299.

Windahl SH, Vidal O, Andersson G, Gustafsson JA, Ohlsson C. 1999. Increased cortical bone mineral content but unchanged trabecular bone mineral density in female erbeta(-/-) mice. The Journal of clinical investigation. 104(7):895-901.

Wiren KM, Chapman Evans A, Zhang XW. 2002. Osteoblast differentiation influences androgen and estrogen receptor-alpha and -beta expression. The Journal of endocrinology. 175(3):683-694.

Woo BH, Fink BF, Page R, Schrier JA, Jo YW, Jiang G, DeLuca M, Vasconez HC, DeLuca PP. 2001. Enhancement of bone growth by sustained delivery of recombinant human bone morphogenetic protein-2 in a polymeric matrix. Pharmaceutical research. 18(12):1747-1753.

Xiong J, O'Brien CA. 2012. Osteocyte rankl: New insights into the control of bone remodeling. Journal of bone and mineral research : the official journal of the American Society for Bone and Mineral Research. 27(3):499-505.

Yang YH, Chen K, Li B, Chen JW, Zheng XF, Wang YR, Jiang SD, Jiang LS. 2013. Estradiol inhibits osteoblast apoptosis via promotion of autophagy through the er-erk-mtor pathway. Apoptosis : an international journal on programmed cell death. 18(11):1363-1375.

Yoshimoto H, Shin YM, Terai H, Vacanti JP. 2003. A biodegradable nanofiber scaffold by electrospinning and its potential for bone tissue engineering. Biomaterials. 24(12):2077-2082.

You L, Temiyasathit S, Lee P, Kim CH, Tummala P, Yao W, Kingery W, Malone AM, Kwon RY, Jacobs CR. 2008. Osteocytes as mechanosensors in the inhibition of bone resorption due to mechanical loading. Bone. 42(1):172-179.

Zaidi M. 2007. Skeletal remodeling in health and disease. Nature medicine. 13(7):791-801.

Zhou S, Turgeman G, Harris SE, Leitman DC, Komm BS, Bodine PV, Gazit D. 2003. Estrogens activate bone morphogenetic protein-2 gene transcription

in mouse mesenchymal stem cells. Molecular endocrinology (Baltimore, Md). 17(1):56-66.

Zhou S, Zilberman Y, Wassermann K, Bain SD, Sadovsky Y, Gazit D. 2001. Estrogen modulates estrogen receptor alpha and beta expression, osteogenic activity, and apoptosis in mesenchymal stem cells (mscs) of osteoporotic mice. Journal of cellular biochemistry Supplement. Suppl 36:144-155.

Zhou W, Slingerland JM. 2014. Links between oestrogen receptor activation and proteolysis: Relevance to hormone-regulated cancer therapy. Nature reviews Cancer. 14(1):26-38.

Zhu BT, Han GZ, Shim JY, Wen Y, Jiang XR. 2006. Quantitative structure-activity relationship of various endogenous estrogen metabolites for human estrogen receptor alpha and beta subtypes: Insights into the structural determinants favoring a differential subtype binding. Endocrinology. 147(9):4132-4150.

Zhu JX, Sasano Y, Takahashi I, Mizoguchi I, Kagayama M. 2001. Temporal and spatial gene expression of major bone extracellular matrix molecules during embryonic mandibular osteogenesis in rats. The Histochemical journal. 33(1):25-35.

Zomorodian E, Baghaban Eslaminejad M. 2012. Mesenchymal stem cells as a potent cell source for bone regeneration. Stem cells international.1-9.

CURRICULUM VITAE

Sumana Posritong

EDUCATION

Doctor of Philosophy (Ph.D. in Dental Science, 2017)

Indiana University, Indianapolis, IN, USA

Master of Science in Dentistry (M.S.D., Prosthodontics, 2012)

Indiana University, Indianapolis, IN, USA

Doctor of Dental Surgery (D.D.S., 1997)

Faculty of Dentistry, Khon Kaen University, Khon Kaen, Thailand

APPOINTMENTS

Academic

Instructor and dentist, (2003-2009)

Institute of Dentistry, Nonthaburi, Thailand

Bench instructor (2013-2015)

Indiana University School of Dentistry, Indianapolis, IN, USA

Other

Dentist (1997-2003), Chonburi, Thailand

PEER-REVIEWED PUBLICATIONS

1. Posritong S, Borges AL, Chu TM, Eckert GJ, Bottino MA, Bottino MC. The impact of hydrofluoric acid etching followed by unfilled resin on the biaxial strength of a glass-ceramic. Dental materials: official publication of the Academy of Dental Materials 2013, 29 (11), e281-90.
2. Eleniste PP, Patel V, Posritong S, Zero O, Largura H, Cheng YH, Himes ER, Hamilton M, Baughman J, Kacena MA, Bruzzaniti A. Pyk2 and Megakaryocytes Regulate Osteoblast Differentiation and Migration via

Distinct and Overlapping Mechanisms. J Cell Biochem 2016, Jun; 117 (6): 1396-406.

3. Borges AL, Posritong S, Campos F, Ozcan M, de Melo R, Bottino MC. Can cleaning regimens effectively eliminated saliva contamination from lithium disilicate ceramic surface? Eur J Prosthodont Restor Dent (accepted August 2016).

AWARDS AND HONORS

1. Thai Dental Board of General Dentistry (2003): Thai Dental Council, Bangkok, Thailand
2. Full-scholarship (2008): Royal Thai government, Bangkok, Thailand
3. Lester Furnas Scholarship Award (2010): Graduate prosthodontics program, Indiana University School of Dentistry, Indianapolis, IN, USA
4. The John F. Johnston Performance Award (Honorable Mention) (2011): Graduate prosthodontics program, Indiana University School of Dentistry, Indianapolis, IN, USA
5. The John F. Johnston Award for Academic Achievement and Technical, Clinical Excellence (2012): Graduate prosthodontics program, Indiana University School of Dentistry, Indianapolis, IN, USA
6. 2nd place Shofu PhD Student Research Award (2014): 22nd Annual Research Day, Indiana University School of Dentistry, Indianapolis, IN, USA
7. ASBMR young investigator travel grant (2015): ASBMR, Washington, DC, USA
8. IUPUI graduate office travel fellowship award (2015): IUPUI, Indianapolis, IN, USA

PUBLISHED ABSTRACTS (INTERNATIONAL)

1. Posritong S, Borges AL, Chu TG, Bottino MA, Bottino MC. Glass-ceramic Flexural Strength after Hydrofluoric acid and Unfilled resin Treatment. International Association of Dental Researches, Seattle, WA, USA, 2013.

2. Posritong S, Wayakanon K, Bruzzaniti A, Bottino MC. Scaffolds Properties for Periodontal Bone Tissue Regeneration-A Systemic Approach Tailoring. International Association of Dental Researches, Cape Town, South Africa 2014.
3. Posritong S, Eleniste P, Bruzzaniti A. Pyk2 Deletion Regulates Estrogen Signaling in Osteoblasts, Promoting Bone Formation. International Association of Dental Researches, Boston, MA, USA, 2015.
4. Posritong S, Eleniste P, Himes ER, Kacena MA, Bruzzaniti A. Pyk2-Deletion Enhances Bone Mass through Estrogen Signaling in Osteoblasts and Osteoclasts. ASBMR, 37th Annual Meeting, Seattle, WA, USA, 2015.
5. Posritong S, Largura HW, Himes ER, Kacena MA, Eleniste P, Bruzzaniti A. Pyk2-Deletion Potentiates Osteoblast Differentiation and Mineralization By Estrogen and Raloxifene. ASBMR, 38th Annual Meeting, Atlanta, GA, USA, 2016.

PUBLISHED ABSTRACTS (LOCAL)

1. Posritong S, Bottino MC. Micro-morphological Changes of a Glass-ceramic–Effects of Hydrofluoric Acid Etching. 20th annual Research Day, Indiana University School of Dentistry, Indianapolis, IN, USA, 2012.
2. Posritong S, Sundeep A, Vang M, Eleniste P, Wheaton B, Bruzzaniti A. The Role of Presenilin-1 on Osteoclast Differentiation. 21st annual Research Day, Indiana University School of Dentistry, Indianapolis, IN, USA, 2013.
3. Posritong S, Eleniste P, Wayakanon K, Bruzzaniti A. Expression and Function of Tyrosine Kinase Pyk2 on Osteoblast Differentiation. 22nd annual Research Day, Indiana University School of Dentistry, Indianapolis, IN, USA, 2014.
4. Posritong S, Eleniste P, Bruzzaniti A. Pyk2-Deletion Enhances Bone Formation Through Estrogen Signaling in Osteoblasts. 23rd Annual Research Day, Indiana University School of Dentistry, Indianapolis, IN, USA, 2015.

5. Posritong S, Eleniste P, Himes ER, Kacena MA, Bruzzaniti A. Pyk2-Deletion Potentiates Osteoblast Differentiation and Mineralization by Estrogen and Raloxifene. 24th Annual IUSD Research Day, Indiana University School of Dentistry, Indianapolis, IN, USA, 2016.
6. Posritong S, Largura HW, Himes ER, Kacena MA, Eleniste P, Bruzzaniti A. Pyk2-Deletion Potentiates Osteoblast Differentiation and Mineralization by Estrogen and Raloxifene. 1st Musculoskeletal Symposium, Indianapolis, IN, USA, 2016.